

CLOSED-FORM DESCRIPTION OF POLARIZATION IN  
ELASTIC AND INELASTIC SCATTERING OF  
LIGHT AND HEAVY IONS

by

T.F. HILL

Thesis submitted for the degree of Doctor of Philosophy  
in the Faculty of Science, University of Cape Town

November 1977

Promoter : Professor W.E. Frahn

The copyright of this thesis vests in the author. No quotation from it or information derived from it is to be published without full acknowledgement of the source. The thesis is to be used for private study or non-commercial research purposes only.

Published by the University of Cape Town (UCT) in terms of the non-exclusive license granted to UCT by the author.

## ACKNOWLEDGEMENTS

I wish to express my sincere appreciation to the following:

Professor W.E. Frahn for suggesting the topic of this thesis and for his guidance and encouragement;

Professor D. Fick, Heidelberg, and Dr. J.B.A. England, Birmingham, for kindly providing listings of their experimental data prior to publication;

Dr. S.K. Kauffmann for helpful discussions;

The South African Council for Scientific and Industrial Research for the award of a bursary;

The University of Cape Town for the award of the Jamison Scholarship;

My parents for their support and encouragement;

Miss L. Jennings for typing the manuscript.

## CONTENTS

	Page
1. INTRODUCTION .....	1
2. SPIN FORMALISM FOR ELASTIC SCATTERING .....	3
3. SPIN FORMALISM FOR INELASTIC SCATTERING .....	19
4. CLOSED-FORM EXPRESSIONS - ELASTIC SCATTERING .....	32
5. CLOSED-FORM EXPRESSIONS - INELASTIC SCATTERING ...	48
6. PARAMETRIC MODEL OF THE SCATTERING FUNCTION .....	61
6.1 Elastic scattering function .....	61
6.2 Elastic scattering amplitudes - illuminated region .....	64
6.3 Elastic scattering amplitudes - shadow region .....	67
6.4 Inelastic scattering amplitudes .....	77
7. ANALYSIS OF EXPERIMENTAL DATA .....	80
7.1 Analysis of elastic scattering data .....	80
7.2 Analysis of inelastic scattering data .....	94
8. SUMMARY .....	100
APPENDIX I .....	101
APPENDIX II .....	104
APPENDIX III .....	106
APPENDIX IV .....	108
APPENDIX V .....	110
APPENDIX VI .....	113
REFERENCES .....	117

## 1. INTRODUCTION

The optical model provides a fully quantal description of heavy ion elastic scattering and, in conjunction with distorted-wave theory, of inelastic scattering as well. In this approach the scattering matrix (S-matrix) appears as an intermediate step in the calculation of the scattering amplitudes.

In the study of elastic and inelastic scattering of heavy ions at energies well above the Coulomb barrier, strong absorption prevails and results in the angular momentum dependence of the relevant part of the S-matrix taking on a simple form. This allows for an alternative approach which takes as its starting point the S-matrix rather than the optical potential. For example we refer to the "sharp cutoff model" of Blair<sup>1)</sup> and the "strong absorption model" of Frahn and Venter<sup>2)</sup>.

Along these lines Frahn and Venter<sup>3)</sup> developed a closed formalism for the elastic scattering and polarization of light and heavy ions of spin  $\frac{1}{2}$ , and analyzed data of proton scattering at high energies ( $> 100$  MeV). Frahn and Wiechers<sup>4)</sup> applied the theory to study data on elastic scattering of polarized  $^3\text{He}$  ions.

Subsequently Hahne<sup>5)</sup> extended these methods to include the elastic scattering and polarization of spin-1 particles and, on the basis of DWBA, to inelastic scattering and polarization of spin- $\frac{1}{2}$  particles.

The present work is an extension of this formalism to vector and tensor polarization in elastic and inelastic scattering of spin- $s$  particles. Moreover, it uses the improved formalism developed by Frahn<sup>6,7,8)</sup> for the study of elastic and inelastic scattering of heavy ions with zero spin. With regard to inelastic scattering, this implies for instance that Coulomb excitation is included in the theory. This work also uses a modification, due to Kauffmann<sup>9)</sup>, of Frahn's formalism, whereby the effects of much stronger real nuclear phase shifts may be included.

In sections 2 and 3 we present the spin formalism for elastic scattering and, on the basis of DWBA, for inelastic scattering respectively. The general expressions for the scattering amplitudes are then simplified under the conditions of strong absorption. In sections 4 and 5 we derive closed-form analytical expressions for the scattering amplitudes for elastic and inelastic scattering respectively, and hence for the corresponding differential cross sections and the vector and tensor polarization components. In section 6 we evaluate the elastic and inelastic scattering amplitudes explicitly for a specific model of the elastic scattering function. In section 7 we use the closed formalism to analyze the data of the M.P.I. Heidelberg group<sup>10,11)</sup> on elastic and inelastic scattering of polarized  ${}^6\text{Li}$  ions by several target nuclei, as well as the data of the Birmingham group<sup>12)</sup> on elastic scattering of polarized  ${}^3\text{He}$  ions.

## 2. SPIN FORMALISM FOR ELASTIC SCATTERING

In this section we consider the non-relativistic elastic scattering of spin- $s$  projectiles by spin-0 targets. Although our approach takes as its starting point the partial-wave expansion of the scattering amplitudes, the form of this expansion, and the form of the S-matrix appearing in it, are governed by the type of spin-orbit coupling one would use in an optical model analysis.

We start by considering an optical potential of the form

$$U(r) = U_c(r) + \underline{\underline{l}} \cdot \underline{\underline{s}} U_s(r) , \quad (2.1)$$

where  $U_c(r)$  includes the Coulomb potential and the real and imaginary parts of the central nuclear potentials, while  $U_s(r)$  gives the  $r$ -dependence of the vector spin-orbit coupling term and may be complex. The reasons for leaving out tensor coupling terms (of rank  $\geq 2$ ) from the right hand side of eq. (2.1) are given below.

We assume that the non-central terms in the optical potential are sufficiently weak so that we need only consider their first order effects. (This is a basic assumption of section 3 and it is justified by the results shown in section 6.) In appendix I it is shown, by means of an argument based on DWBA, that to first order in the non-central part of the optical potential, the polarization terms of a given rank are due only to the coupling terms of the same rank in the optical

potential. This implies that there is no point in including a spin-orbit coupling term of rank  $k$  unless we have evidence of polarization of rank  $k$ .

Of the data analyzed in section 4, the only tensor polarization data available is that on the elastic scattering of  ${}^6\vec{\text{Li}} + {}^{58}\text{Ni}$  at 22.8 MeV, and this data is consistent with zero tensor polarization. This justifies our use of the form of the optical potential given by eq. (2.1).

We start by considering the relative motion, without scattering, in the centre of mass system, of a projectile of spin  $s$ ,  $z$  component of spin  $\nu$  and a target of zero spin. This is represented by the plane wave

$$\Psi_0(\underline{k}, s, \nu; \underline{r}) = |s\nu\rangle \left\{ \frac{4\pi}{kr} \sum_{\ell m} i^\ell u_\ell(kr) Y_{\ell m}(\hat{\underline{r}}) Y_{\ell m}^*(\hat{\underline{k}}) \right\} \quad (2.2)$$

$$= \frac{4\pi}{kr} \sum_{j m \ell} u_\ell(kr) Y_{j m}^M(\hat{\underline{r}}) Y_j^M(\ell, s, \nu; \hat{\underline{k}}) , \quad (2.3)$$

where

$$u_\ell(z) = z j_\ell(z) , \quad (2.4)$$

$$Y_{j m}^M(\hat{\underline{r}}) = \sum_{m\nu} \langle \ell s m \nu | j M \rangle Y_{\ell m}(\hat{\underline{r}}) |s\nu\rangle , \quad (2.5)$$

$$Y_j^M(\ell, s, \nu; \hat{\underline{k}}) = \sum_m \langle \ell s m \nu | j M \rangle i^{-\ell} Y_{\ell m}(\hat{\underline{k}}) . \quad (2.6)$$

Defining

$$\underline{j} = \underline{\ell} + \underline{s} , \quad j_z = \ell_z + s_z , \quad (2.7)$$

where  $\underline{l}$  and  $\underline{s}$  are the operators for the orbital angular momentum and spin of the projectile respectively, we see from eq. (2.5) that

$$\underline{j}^2 \mathcal{Y}_{j\ell s}^M = j(j+1) \mathcal{Y}_{j\ell s}^M, \quad j_z \mathcal{Y}_{j\ell s}^M = M \mathcal{Y}_{j\ell s}^M, \quad (2.8)$$

$$\underline{\ell}^2 \mathcal{Y}_{j\ell s}^M = \ell(\ell+1) \mathcal{Y}_{j\ell s}^M, \quad \underline{s}^2 \mathcal{Y}_{j\ell s}^M = s(s+1) \mathcal{Y}_{j\ell s}^M. \quad (2.9)$$

The operators  $\underline{j}^2$ ,  $j_z$ ,  $\underline{\ell}^2$  and  $\underline{s}^2$  commute with  $\underline{l} \cdot \underline{s}$  and hence with the optical potential  $U(r)$  given by eq. (2.1), so that the quantum numbers  $j$ ,  $M$ ,  $\ell$  and  $s$  are conserved in the scattering. This implies that the partial-wave expansion for the scattering wave functions takes the form, analogous to eq. (2.3),

$$\Psi^{(\pm)}(k, s, \nu; r) = \frac{4\pi}{kr} \sum_{jM\ell} \psi_{j\ell}^{(\pm)}(k, r) \mathcal{Y}_{j\ell s}^M(\hat{r}) \mathcal{Y}_j^M(\ell, s, \nu; \hat{k}) \quad (2.10)$$

The superscripts (+) and (-) denote the solutions with outgoing and incoming wave boundary conditions respectively.

Substituting eq. (2.10) into the Schrödinger equation

$$\left[ -\frac{\hbar^2}{2\mu} \frac{1}{r} \frac{d^2}{dr^2} r + \frac{\underline{\ell}^2}{2\mu r^2} + U_c(r) + \underline{\ell} \cdot \underline{s} U_s(r) - \frac{\hbar^2 k^2}{2\mu} \right] \Psi^{(\pm)} = 0 \quad (2.11)$$

and using

$$\underline{\ell} \cdot \underline{s} = \frac{1}{2} [\underline{j}^2 - \underline{\ell}^2 - \underline{s}^2], \quad (2.12)$$

gives

$$\sum_{jM\ell} \left\{ -\frac{d^2}{dr^2} + \frac{\ell(\ell+1)}{\hbar^2 r^2} + \frac{2\mu}{\hbar^2} V_{j\ell}(r) - k^2 \right\} \psi_{j\ell}^{(\pm)}(k, r) \mathcal{Y}_{j\ell s}^M(\hat{r}) \mathcal{Y}_j^M(\ell, s, \nu; \hat{k}) = 0, \quad (2.13)$$

where

$$V_{j\ell}(r) = U_c(r) + \frac{1}{2} [i(i+1) - \ell(\ell+1) - s(s+1)] U_s(r). \quad (2.14)$$

Because of the completeness and orthogonality of the functions  $\mathcal{Y}_{j\ell s}^M(\hat{r})$  and  $\mathcal{Y}_j^M(\ell, s, \nu; \hat{k})$  in  $\underline{r}$ -space and  $\underline{k}$ -space respectively, eq. (2.13) is equivalent to the set of equations

$$\left[ -\frac{d^2}{dr^2} + \frac{\ell(\ell+1)}{\hbar^2 r^2} + \frac{2\mu}{\hbar^2} V_{j\ell}(r) - k^2 \right] \psi_{j\ell}^{(\pm)}(k, r) = 0. \quad (2.15)$$

According to eqs. (2.15), each radial wave function  $\psi_{j\ell}^{(\pm)}(k, r)$  is generated by the potential  $V_{j\ell}(r)$ , so for each value of  $j$ , we may apply the theory for scattering by a spin-independent potential. We thus have the asymptotic forms

$$\psi_{j\ell}^{(\pm)}(k, r) \underset{\infty}{\sim} \frac{r}{2} \exp(\pm i \frac{1}{2} \pi) \quad (2.16)$$

$$\times \exp[\pm i \sigma_\ell(k)] \left\{ \exp[\mp i p_\ell(k, r)] - \eta_{j\ell}(k) \exp[\pm i 2 \delta_{j\ell}^{(N)}(k) \pm i p_\ell(k, r)] \right\},$$

where

$$p_\ell(k, r) = kr - n \ln(2kr) - \frac{\ell\pi}{2} + \sigma_\ell(k) \quad (2.17)$$

and where  $\sigma_\ell(k)$ ,  $\delta_{j\ell}^{(N)}(k)$  and  $\eta_{j\ell}(k)$  denote respectively the point-charge Coulomb scattering phase shift, the real nuclear

phase shift<sup>†</sup> and the reflection coefficient for the partial wave  $(j, \ell)$ . The elastic scattering matrix may now be written as

$$S_{j\ell}(k) = \eta_{j\ell}(k) \exp[i2(\sigma_{\ell}(k) + \delta_{j\ell}^{(N)}(k))] = S_{j\ell}^{(N)}(k) \exp[i2\sigma_{\ell}(k)] \quad (2.18)$$

and is related to the functions  $V_{j\ell}(r)$  and  $\psi_{j\ell}^{(+)}(k, r)$  by

$$S_{j\ell}(k) = 1 - \frac{i4\mu}{\hbar^2 k} \int_0^{\infty} dr U_{\ell}(kr) V_{j\ell}(r) \psi_{j\ell}^{(+)}(k, r), \quad (2.19)$$

which follows immediately from the corresponding formula for the elastic scattering matrix for particles of zero spin (c.f. eq. (2.11) of ref. 13).

The elastic scattering amplitude is given by<sup>††</sup>

$$A(\hat{k}_f, \nu_f, \hat{k}_i, \nu_i) = - \frac{\mu}{2\pi\hbar^2} \int d\hat{r}' d\hat{r} \Psi_0^{\dagger}(k_f, s, \nu_f; \hat{r}') \langle \hat{r}' | U(r) | \hat{r} \rangle \Psi^{(+)}(k_i, s, \nu_i; \hat{r}) \quad (2.20)$$

$$= - \frac{\mu}{2\pi\hbar^2} \int_0^{\infty} dr r^2 \int d\hat{r} \Psi_0^{\dagger}(k_f, s, \nu_f; \hat{r}) U(r) \Psi^{(+)}(k_i, s, \nu_i; \hat{r}), \quad (2.21)$$

where the subscripts  $i$  and  $f$  refer to the incident and scattered waves respectively. Substituting eqs. (2.1), (2.3) and (2.10) into eq. (2.21) and using eqs. (2.12) and (2.14),

---

† By "real nuclear phase shift" we mean  $\delta_{j\ell}(k) - \sigma_{\ell}(k)$  where  $\delta_{j\ell}(k)$  is the total real phase shift for the partial wave  $(j, \ell)$ .

†† See eq. (10.12) of ref. 14).

we obtain

$$A(\hat{k}_f, \nu_f, \hat{k}_i, \nu_i) = -\frac{8\pi\mu}{\hbar^2 k^2} \sum_{j_f M_f \ell_f} \sum_{j_i M_i \ell_i} \left[ \int_0^\infty dr u_\ell(kr) V_{j\ell}(r) \psi_{j\ell}^{(+)}(kr) \right] \\ \times \left[ \int d\hat{r} y_{j_f \ell_f s}^{M_f \dagger}(\hat{r}) y_{j_i \ell_i s}^{M_i}(\hat{r}) \right] y_{j_f}^{M_f}(\ell_f, s, \nu_f; \hat{k}_f) y_{j_i}^{M_i*}(\ell_i, s, \nu_i; \hat{k}_i) \quad (2.22)$$

Now

$$\int d\hat{r} y_{j_f \ell_f s}^{M_f \dagger}(\hat{r}) y_{j_i \ell_i s}^{M_i}(\hat{r}) = \delta_{j_f j_i} \delta_{\ell_f \ell_i} \delta_{M_f M_i} \quad (2.23)$$

so that eqs. (2.19) and (2.22) give the result

$$A(\hat{k}_f, \nu_f, \hat{k}_i, \nu_i) = \frac{4\pi}{2ik} \sum_{jM\ell} y_j^M(\ell, s, \nu_f; \hat{k}_f) a_{j\ell}(k) y_j^{M*}(\ell, s, \nu_i; \hat{k}_i) \quad (2.24)$$

where

$$a_{j\ell}(k) = S_{j\ell}(k) - 1 \quad (2.25)$$

If the reference axes are chosen so that

$$\hat{z} = \hat{k}_i \quad , \quad \hat{y} = \widehat{k_i \times k_f} \quad (2.26)$$

then using eq. (2.6), eq. (2.24) becomes

$$A(\nu_f, \nu_i; \theta) = \frac{(4\pi)^{\frac{1}{2}}}{2ik} \sum_{j\ell} \langle \ell s \nu_i - \nu_f \nu_f | j \nu_i \rangle \langle \ell s 0 \nu_i | j \nu_i \rangle (2\ell+1)^{\frac{1}{2}} \\ \times a_{j\ell}(k) Y_{\ell \nu_i - \nu_f}(\theta, 0) \quad (2.27)$$

where

$$\sin(\theta) = \left| \hat{k}_i \times \hat{k}_f \right| . \quad (2.28)$$

For  $\theta \neq 0$  we may replace  $a_{j\ell}(k)$  by  $S_{j\ell}(k)$  since the difference contributes only to forward scattering ( $\theta = 0$ ).

We now proceed under the conditions of strong absorption, namely that  $\eta_{j\ell}(k)$  varies smoothly with  $\ell$  from small values to unity within a transition region of width  $\Delta$  around the value  $\ell = L$  defined by  $\eta_{j\ell_0}(k) = \frac{1}{2}$ , and that  $\Delta \ll L$ . We also assume that  $s \ll L$  so that  $|v_i - v_f| \ll \ell_0$ . This implies that the right hand side of eq. (2.30) is dominated by those terms for which  $\ell \gg 1$  and  $j \ll s$ , so that we may use the following approximations<sup>15)</sup>:

$$\langle \ell s v_i - v_f v_f | j v_i \rangle \approx d_{v_f j - \ell}^s \left( \frac{1}{2} \pi \right) , \quad (2.29)$$

$$\langle \ell s 0 v_i | j v_i \rangle \approx d_{v_i j - \ell}^s \left( \frac{1}{2} \pi \right) , \quad (2.30)$$

where  $d_{mm}^s(\alpha)$  is the reduced rotation matrix element. The errors in the approximations (2.29-30) are of order  $(v_i - v_f)/j$  (or  $v_f/j$ ) and  $j^{-1}$  respectively. We also use the asymptotic expression

$$Y_{\ell-m}(\theta, 0) \approx \frac{e^{i\frac{1}{2}\pi m}}{2\pi(\sin\theta)^{\frac{1}{2}}} \left\{ \exp\left[ i\left(\ell + \frac{1}{2}\right)\theta - i\frac{1}{4}\pi - im\pi \right] + \exp\left[ -i\left(\ell + \frac{1}{2}\right)\theta + i\frac{1}{4}\pi \right] \right\}, \quad (2.31)$$

which holds for  $|m|/\ell \lesssim \theta \lesssim \pi - |m|/\ell$ . Eq. (2.27) then becomes

$$A(\nu_f, \nu_i; \theta) = \frac{1}{2ik(\pi \sin \theta)^{\frac{1}{2}}} \sum_{j \geq l} (2l+1)^{\frac{1}{2}} d_{\nu_f, j-l}^S(\frac{1}{2}\pi) d_{\nu_i, j-l}^S(\frac{1}{2}\pi) S_{j,l}(k) \\ \times \left\{ \exp\left[i\left(\lambda\theta - \frac{1}{4}\pi - \frac{1}{2}\pi\nu_f + \frac{1}{2}\pi\nu_i\right)\right] + \exp\left[-i\left(\lambda\theta - \frac{1}{4}\pi - \frac{1}{2}\pi\nu_f + \frac{1}{2}\pi\nu_i\right)\right] \right\}, \quad (2.32)$$

where  $\lambda = l + \frac{1}{2}$ .

We now define

$$f_{\tau}^{(\pm)}(\theta) = \frac{1}{2ik(\pi \sin \theta)^{\frac{1}{2}}} \sum_{\ell} (2\ell+1)^{\frac{1}{2}} S_{\ell+\tau, \ell}(k) \exp[\mp i(\lambda\theta - \frac{1}{4}\pi)], \quad (2.33)$$

where  $\tau = j - l$ , so that eq. (2.32) may be written in the form

$$A(\nu_f, \nu_i; \theta) = \sum_{\tau} d_{\nu_f, \tau}^S(\frac{1}{2}\pi) d_{\nu_i, \tau}^S(\frac{1}{2}\pi) \\ \left\{ f_{\tau}^{(+)}(\theta) \exp\left[i\frac{1}{2}\pi(\nu_f - \nu_i)\right] + f_{\tau}^{(-)}(\theta) \exp\left[-i\frac{1}{2}\pi(\nu_f - \nu_i)\right] \right\}. \quad (2.34)$$

The functions  $f_{\tau}^{(\pm)}(\theta)$  are analogous to the elastic scattering amplitudes  $f_{\pm}(\theta)$  of ref.<sup>6)</sup> and the amplitudes  $f^{(\pm)}(\theta)$  of ref.<sup>8)</sup> for spin-0 particles, and they are evaluated using similar methods.

It is convenient to rotate the reference axes defined by eqs. (2.26) to the new system  $(\bar{x}, \bar{y}, \bar{z})$  defined by

$$\hat{\bar{x}} = \hat{k}_i, \quad \hat{\bar{z}} = \widehat{k_i \times k_f}. \quad (2.35)$$

With respect to the new axes, the scattering amplitude is given by

$$\bar{A}(\bar{\nu}_f, \bar{\nu}_i; \theta) = \sum_{\nu_f, \nu_i} d_{\bar{\nu}_f, \nu_f}^S(\frac{1}{2}\pi) e^{-i\frac{1}{2}\pi\nu_f} A(\nu_f, \nu_i; \theta) e^{i\frac{1}{2}\pi\nu_i} d_{\nu_i, \bar{\nu}_i}^S(-\frac{1}{2}\pi). \quad (2.36)$$

Substituting eq. (2.34) into eq. (2.36) gives

$$\bar{A}(\bar{\nu}_f, \bar{\nu}_i; \theta) = \sum_{\nu_f \nu_i \tau} d_{\bar{\nu}_f \nu_f}^S(\frac{1}{2}\pi) d_{\nu_f \tau}^S(\frac{1}{2}\pi) d_{\nu_i \tau}^S(\frac{1}{2}\pi) d_{\nu_i \bar{\nu}_i}^S(-\frac{1}{2}\pi) \\ \times \left\{ f_{\tau}^{(+)}(\theta) + f_{\tau}^{(-)}(\theta) \exp[i\pi(\nu_i - \nu_f)] \right\} . \quad (2.37)$$

Now

$$\sum_{\nu_f} d_{\bar{\nu}_f \nu_f}^S(\frac{1}{2}\pi) d_{\nu_f \tau}^S(\frac{1}{2}\pi) = (-1)^{S-\tau} \delta_{\bar{\nu}_f - \tau} , \quad (2.38)$$

$$\sum_{\nu_i} d_{\nu_i \tau}^S(\frac{1}{2}\pi) d_{\nu_i \bar{\nu}_i}^S(-\frac{1}{2}\pi) = (-1)^{S-\tau} \delta_{\bar{\nu}_i - \tau} , \quad (2.39)$$

$$\sum_{\nu_f} d_{\bar{\nu}_f \nu_f}^S(\frac{1}{2}\pi) d_{\nu_f \tau}^S(\frac{1}{2}\pi) e^{-i\pi\nu_f} = \delta_{\bar{\nu}_f \tau} e^{-i\pi\tau} , \quad (2.40)$$

$$\sum_{\nu_i} d_{\nu_i \tau}^S(\frac{1}{2}\pi) d_{\nu_i \bar{\nu}_i}^S(-\frac{1}{2}\pi) e^{i\pi\nu_i} = \delta_{\bar{\nu}_i \tau} e^{i\pi\tau} , \quad (2.41)$$

so that eq. (2.37) reduces to the form

$$A(\nu_f, \nu_i; \theta) = \left[ f_{-\nu_i}^{(+)}(\theta) + f_{\nu_i}^{(-)}(\theta) \right] \delta_{\nu_f \nu_i} , \quad (2.42)$$

where we have dropped the bar notation on the understanding that the reference axes from now on are those defined by eqs. (2.35).

Since the elastic scattering amplitude given by eq. (2.42) is diagonal in the spin components, this implies that in this co-ordinate system no angular momentum is exchanged between the z-component of the projectile spin and the z-component of orbital angular momentum. The only effect of

the spin-orbit coupling is to scatter each z-component  $v_i$  of the spin in a different way.

According to eq. (2.33), the superscripts (+) and (-) denote, in a semiclassical description, the amplitudes for scattering from the near and far sides of the interaction region respectively. In view of this one can interpret the signs of the subscripts as they appear in eq. (2.42). According to our choice of co-ordinate system (2.35), the total angular momentum  $j$  of a projectile with z-component of spin  $v_i$  and orbital angular momentum  $l_i$  will be  $l_i - v_i$  or  $l_i + v_i$  depending on whether it is scattered from the near side or from the far side of the target nucleus respectively, hence the subscripts  $\mp v_i$  in the scattering amplitudes  $f_{\mp v_i}^{(\pm)}(\theta)$ .

It is convenient to define the operator  $Q(\theta)$  by

$$A(v_f, v_i; \theta) = \langle s v_f | Q(\theta) | s v_i \rangle . \quad (2.43)$$

Now the density operator for the spin of an unpolarized incident beam is given by

$$\rho_0 = \frac{1}{2s+1} \sum_{\tau} |s \tau\rangle \langle s \tau| , \quad (2.44)$$

therefore, from eq. (2.43), the density operator for the spin of the scattered wave is given by

$$\rho(\theta) = \frac{1}{2s+1} \sum_{\tau} Q(\theta) |s \tau\rangle \langle s \tau| Q^\dagger(\theta) \quad (2.45)$$

$$= \frac{1}{2s+1} Q(\theta) Q^\dagger(\theta) . \quad (2.46)$$

The matrix elements of  $\rho(\theta)$  are therefore given by

$$\rho_{\nu_f \nu_i}(\theta) = \frac{1}{2S+1} \sum_{\tau} A(\nu_f, \tau; \theta) A^*(\nu_i, \tau; \theta) \quad (2.47)$$

$$= \frac{1}{2S+1} \left| f_{-\nu_i}^{(+)}(\theta) + f_{\nu_i}^{(-)}(\theta) \right|^2 \delta_{\nu_f \nu_i} \quad (2.48)$$

The density matrix  $\rho_{\nu_f \nu_i}(\theta)$  may be expanded in terms of statistical tensors  $h_{\kappa q}(\theta)$  by

$$\rho_{\nu_f \nu_i}(\theta) = \frac{1}{2S+1} \sum_{\kappa q} (2\kappa+1)^{\frac{1}{2}} h_{\kappa q}(\theta) \langle s \kappa \nu_f q | s \nu_i \rangle, \quad (2.49)$$

or by inversion,

$$h_{\kappa q}(\theta) = (2\kappa+1)^{\frac{1}{2}} \sum_{\nu_f \nu_i} \rho_{\nu_f \nu_i}(\theta) \langle s \kappa \nu_f q | s \nu_i \rangle. \quad (2.50)$$

Substituting eq. (2.48) into (2.50) gives

$$h_{\kappa q}(\theta) = \frac{(2\kappa+1)^{\frac{1}{2}}}{2S+1} \left\{ \sum_{\tau} \left| f_{-\tau}^{(+)}(\theta) + f_{\tau}^{(-)}(\theta) \right|^2 \langle s \kappa \tau 0 | s \tau \rangle \right\} \delta_{q0}. \quad (2.51)$$

It is shown in appendix II that in the co-ordinate system (2.35), irrespective of the type of spin-orbit coupling present, and without any approximations,  $h_{\kappa q}(\theta) = 0$  for  $q$  odd. According to eq. (2.51)  $h_{\kappa q}(\theta) = 0$  for  $q \neq 0$ , so that our approximations have served to eliminate the components  $h_{\kappa q}(\theta)$  with  $q$  even and non-zero.

The statistical tensor  $h_{00}(\theta)$  gives the elastic scattering cross section since

$$h_{00}(\theta) = \frac{1}{2s+1} \sum_{\tau} |f_{-\tau}^{(+)}(\theta) + f_{\tau}^{(-)}(\theta)|^2 \quad (2.52)$$

$$= \frac{1}{2s+1} \text{tr}[a(\theta) a^{\dagger}(\theta)] \quad (2.53)$$

$$= \text{tr}[\rho(\theta)] = \sigma(\theta) \quad (2.54)$$

Using the formula

$$\langle s \mid \tau_0 \mid s \tau \rangle = \frac{\tau}{[s(s+1)]^{\frac{1}{2}}} \quad , \quad (2.55)$$

we have from eqs. (2.48) and (2.51)

$$h_{10}(\theta) = \frac{1}{2s+1} \left[ \frac{3}{s(s+1)} \right]^{\frac{1}{2}} \sum_{\tau} \tau |f_{-\tau}^{(+)}(\theta) + f_{\tau}^{(-)}(\theta)|^2 \quad (2.56)$$

$$= \text{tr}[\rho(\theta) \tau_{10}] \quad , \quad (2.57)$$

where

$$\tau_{10} = \left[ \frac{3}{s(s+1)} \right]^{\frac{1}{2}} s_z \quad . \quad (2.58)$$

Similarly, using the formula

$$\langle s \mid 2 \tau_0 \mid s \tau \rangle = \frac{3\tau^2 - s(s+1)}{[s(s+1)(2s+3)(2s-1)]^{\frac{1}{2}}} \quad , \quad (2.59)$$

we have

$$h_{20}(\theta) = \frac{1}{2s+1} \left[ \frac{5}{s(s+1)(2s+3)(2s-1)} \right]^{\frac{1}{2}} \sum_{\tau} [3\tau^2 - s(s+1)] |f_{-\tau}^{(+)}(\theta) + f_{\tau}^{(-)}(\theta)|^2 \quad (2.60)$$

$$= \text{tr}[\rho(\theta) \tau_{20}] \quad (2.61)$$

where

$$\tau_{20} = \left[ \frac{s}{s(s+1)(2s+3)(2s-1)} \right]^{\frac{1}{2}} [3s^2 - s(s+1)] . \quad (2.62)$$

For  $s = 1$  eqs. (2.58) and (2.62) agree with the definition of the spherical tensors  $\tau_{10}$  and  $\tau_{20}$  respectively, as given by the Madison Convention<sup>16)</sup> for spin-1 particles. In addition, for  $\kappa \neq 0$  and  $s = 1$ ,

$$t_{\kappa q}(\theta) = \frac{1}{s \sigma(\theta)} h_{\kappa q}(\theta) \quad (2.63)$$

gives the polarization components, as defined by the Madison Convention<sup>†</sup> for the scattering of an unpolarized beam of spin-1 particles.

From eqs. (2.46) and (2.57), and using the fact that  $Q(\theta)$  and  $\tau_{10}$  commute (since they are both diagonal), we have

$$t_{10}(\theta) = \frac{\text{tr}[A(\theta)A^\dagger(\theta)\tau_{10}]}{s \text{tr}[A(\theta)A^\dagger(\theta)]} \quad (2.64)$$

$$= \frac{\text{tr}[A(\theta)\tau_{10}A^\dagger(\theta)]}{s \text{tr}[A(\theta)A^\dagger(\theta)]} = T_{10}(\theta) , \quad (2.65)$$

where  $T_{10}(\theta)$  is the vector analyzing power in spherical tensor notation<sup>16)</sup>. Similarly, one can show that

$$t_{20}(\theta) = T_{20}(\theta) , \quad (2.66)$$

---

<sup>†</sup> Note that our choice of co-ordinate system (eqs. (2.39)) is different from the standard co-ordinate system laid down by the Madison Convention.

where  $T_{20}(\theta)$  is the tensor analyzing power of rank 2 <sup>16</sup>).

The formalism of this section deals explicitly with unpolarized beams, but eqs. (2.65) and (2.66) show that the formalism applies directly to the case of polarized incident beams as well. In section 7 we analyze differential cross section and vector analyzing power data of elastic scattering of vector-polarized incident particles. As a check we relate our functions  $\sigma(\theta)$  and  $t_{10}(\theta)$ , given by eqs. (2.54) and (2.63) respectively, to the experimental quantities.

Referring to the co-ordinate system (2.35), consider the vector polarization of the incident beam to be  $P_z \hat{z}$ . The density operator for the spin of the incident beam is then given by

$$\rho_i = \frac{1}{2s+1} \left[ I + \frac{3P_z}{s+1} S_z \right] , \quad (2.67)$$

where  $I$  is the identity operator and  $s_z$  is the operator for the z-component of the spin of the projectile. For a fully vector-polarized incident beam, we have

$$P_z = \frac{s+1}{3s} . \quad (2.68)$$

The density operator for the spin of the scattered particles is given by

$$\rho_f(\theta) = Q(\theta) \rho_i Q^\dagger(\theta) , \quad (2.69)$$

where  $Q(\theta)$  is defined by eq. (2.43), therefore the differential

cross section for scattering to the left is given by

$$\sigma^{(L)}(\theta) = \text{tr}[\rho_f(\theta)] \quad (2.70)$$

$$= \frac{1}{2s+1} \left\{ \text{tr}[A(\theta)A^\dagger(\theta)] + \frac{3P_z}{s+1} \text{tr}[A(\theta)s_z A^\dagger(\theta)] \right\} \quad (2.71)$$

The differential cross section  $\sigma^{(R)}(\theta)$ , for scattering to the right, is obtained by changing the sign of the second term on the right hand side of eq. (2.71).

We therefore have for the experimentally observed (average) elastic scattering cross section,

$$\frac{1}{2} [\sigma^{(L)}(\theta) + \sigma^{(R)}(\theta)] = \frac{1}{2s+1} \text{tr}[A(\theta)A^\dagger(\theta)] = \sigma(\theta) \quad , \quad (2.72)$$

where  $\sigma(\theta)$  is given by eqs. (2.52-54), and, using eqs. (2.58) and (2.65), we also have the experimentally observed left-right asymmetry given by

$$\frac{\sigma^{(L)}(\theta) - \sigma^{(R)}(\theta)}{2\sigma(\theta)} = \frac{3sP_z}{s+1} \left\{ \frac{\text{tr}[A(\theta)s_z A^\dagger(\theta)]}{s \text{tr}[A(\theta)A^\dagger(\theta)]} \right\} \quad (2.73)$$

$$= \frac{3sP_z}{s+1} A_z(\theta) \quad , \quad (2.74)$$

where  $A_z(\theta)$  is the vector analyzing power in Cartesian tensor notation<sup>16)</sup>. From eqs. (2.58) and (2.65) we see that

$$A_z(\theta) = \left[ \frac{1}{3}s(s+1) \right]^{\frac{1}{2}} t_{10}(\theta) \quad (2.75)$$

According to eqs. (2.68) and (2.74), the left-right asymmetry

for a fully vector-polarized incident beam is given by  $A_z(\theta)$ .

Using eqs. (2.56) and (2.63), this gives

$$A_z(\theta) = \frac{1}{5(2s+1)\sigma(\theta)} \sum_{\tau} \tau |f_{-\tau}^{(+)}(\theta) + f_{\tau}^{(-)}(\theta)|^2. \quad (2.76)$$

### 3. SPIN FORMALISM FOR INELASTIC SCATTERING

The transition amplitude for inelastic scattering of a spin- $s$  projectile by a spin-0 target with excitation of a low-lying collective (rotational or vibrational) state of multipolarity  $(L, M)$  is given in first order distorted-wave theory<sup>17)</sup> by

$$T_{LM} \nu_f \nu_i = \int d^3r \Psi_f^{(-)\dagger}(k_f, s, \nu_f; r) \langle LM | V(r, \xi_t, \xi_p) | 00 \rangle \Psi_i^{(+)}(k_i, s, \nu_i; r) \quad (3.1)$$

where the elastic scattering wave functions  $\Psi_{i,f}^{(\pm)}$  are given by eq. (2.10), except that the subscripts  $i$  and  $f$  refer to the entrance and exit channels respectively,  $V(r, \xi_t, \xi_p)$  is the interaction operator for inelastic scattering,  $\xi_t$  and  $\xi_p$  are the internal co-ordinates of the target and projectile respectively and  $\nu$  is the  $z$ -component of the spin of the projectile.

In the spirit of the optical model approach to elastic scattering, one may regard inelastic scattering to low-lying collective states as being induced by non-spherical deformations of the optical potential<sup>18)</sup>. This approach leads us to consider the following form for the interaction operator:

$$V(r, \xi_t, \xi_p) = \sum_{L'M'} \left\{ \left[ \alpha_{L'M'}^{(N)}(\xi_t) V^{(N)}(r) + \alpha_{L'M'}^{(C)}(\xi_t) V_L^{(C)}(r) \right] Y_{L'M'}^*(\hat{r}) + \alpha_{L'M'}^{(N)}(\xi_t) \frac{1}{2} V_S(r) \left[ Y_{L'M'}^*(\hat{r}) \hat{L} \cdot \hat{S} + \hat{L} \cdot \hat{S} Y_{L'M'}^*(\hat{r}) \right] \right\}, \quad (3.2)$$

where  $\alpha_{LM}^{(N)}(\xi_t)$  and  $\alpha_{LM}^{(C)}(\xi_t)$  are the deformation parameters<sup>18)</sup> for the deformation, of multipolarity (L,M), of the nuclear and Coulomb potentials respectively,

$$V^{(N)}(r) = R_0 \frac{\partial U_c^{(N)}(r)}{\partial R} = -R_0 \frac{\partial U_c^{(N)}(r)}{\partial r}, \quad (3.3)$$

$$V_s(r) = R_0 \frac{\partial U_s(r)}{\partial R} = -R_0 \frac{\partial U_s(r)}{\partial r} \quad (3.4)$$

$$V_L^{(C)}(r) = \frac{3e^2 Z_1 Z_2}{2L+1} \begin{cases} \frac{r^L}{R_C^{L+1}} & r \leq R_C \\ \frac{R_C^L}{r^{L+1}} & r \geq R_C \end{cases}, \quad (3.5)$$

and  $R_0$  and  $R_C$  are the nuclear radius and the Coulomb charge radius respectively. Referring to the optical potential (2.1),  $U_c^{(N)}(r)$  is the nuclear part of  $U_c(r)$ . In eqs. (3.3) and (3.4) we have assumed that  $U_c^{(N)}(r)$  and  $U_s(r)$  are functions of  $(r - R_0)$ . For the terms in eq. (3.2) describing the deformation of the central parts of the optical potential, we refer to ref.<sup>18)</sup>, while for the terms describing the deformation of the spin-orbit potential, we refer to ref.<sup>19)</sup>.

Using the Wigner-Eckart theorem<sup>17)</sup>, we have

$$\langle LM | \alpha_{LM'}(\xi_t) | 00 \rangle = \frac{1}{(2L+1)^{\frac{1}{2}}} \langle L || \alpha_L(\xi_t) || 0 \rangle \langle 0 L' 0 M' | LM \rangle \quad (3.6)$$

$$= \frac{1}{(2L+1)^{\frac{1}{2}}} \langle L || \alpha_L(\xi_t) || 0 \rangle \delta_{LL'} \delta_{MM'}. \quad (3.7)$$

It is convenient to define the nuclear and Coulomb deformation parameters  $\beta_L^{(N)}$  and  $\beta_L^{(C)}$  respectively, and the corresponding

deformation lengths  $\delta_L^{(N)}$  and  $\delta_L^{(C)}$  by

$$\beta_L^{(N)} = \langle L || \alpha_L^{(N)}(\xi_t) || 0 \rangle = \frac{\delta_L^{(N)}}{R_0}, \quad (3.8)$$

$$\beta_L^{(C)} = \langle L || \alpha_L^{(C)}(\xi_t) || 0 \rangle = \frac{\delta_L^{(C)}}{R_C}. \quad (3.9)$$

Combining eqs. (3.2-9) we obtain

$$\langle LM | V(r, \xi_t, \xi_p) | 00 \rangle = C_{LM}(r) + S_{LM}(r), \quad (3.10)$$

where

$$C_{LM}(r) = \frac{1}{(2L+1)^{\frac{1}{2}}} \left[ -\delta_L^{(N)} \frac{\partial U_C^{(N)}(r)}{\partial r} + \delta_L^{(C)} \frac{3z_1 z_2 e^2}{2L+1} \left\{ \begin{matrix} r^L \\ R_C^{L+2} \\ R_C^{L-1} \\ r^{L+1} \end{matrix} \right\} \right] Y_{LM}^*(\hat{r}) \quad (3.11)$$

and

$$S_{LM}(r) = -\frac{1}{2} \delta_L^{(N)} \frac{1}{(2L+1)^{\frac{1}{2}}} \frac{\partial U_S(r)}{\partial r} [Y_{LM}^*(\hat{r}) \underline{\ell} \cdot \underline{s} + \underline{\ell} \cdot \underline{s} Y_{LM}^*(\hat{r})]. \quad (3.12)$$

With reference to eq. (2.16), it is convenient to rewrite the radial wave functions appearing in eq. (2.10) as

$$\psi_{j\ell}^{(+)}(k, r) = e^{i\sigma_\ell(k)} f_{j\ell}(k, r), \quad (3.13)$$

$$\psi_{j\ell}^{(-)}(k, r) = e^{-i\sigma_\ell(k)} f_{j\ell}^*(k, r), \quad (3.14)$$

so that

$$\Psi_L^{(+)}(\underline{k}, s, \nu; r) = \frac{4\pi}{kr} \sum_{j\ell} e^{i\sigma_\ell^{(i)}(k)} f_{j\ell}^{(i)}(k, r) y_{j\ell s}^M(\hat{r}) y_j^{M*}(\ell, s, \nu; \hat{k}), \quad (3.15)$$

$$\Psi_f^{(-)}(\underline{k}, s, \nu; \underline{r}) = \frac{4\pi}{kr} \sum_{jM\ell} e^{-i\sigma_\ell^{(f)}(k)} f_{j\ell}^{(f)*}(k, r) Y_{j\ell s}^M(\hat{r}) Y_j^{M*}(\ell, s, \nu; \hat{k}). \quad (3.16)$$

If we write the variables  $\underline{k}$ ,  $k$ ,  $\nu$ ,  $j$ ,  $M$  and  $\ell$  in eqs. (3.15) and (3.16) with the subscripts  $i$  and  $f$  respectively, and use eqs. (2.8), (2.9) and (2.12), we can then make the replacement

$$\frac{1}{k^2} [Y_{LM}^*(\hat{r}) \underline{\ell} \cdot \underline{s} + \underline{\ell} \cdot \underline{s} Y_{LM}^*(\hat{r})] \rightarrow \frac{1}{2} [j_f(j_f+1) + j_i(j_i+1) - \ell_f(\ell_f+1) - \ell_i(\ell_i+1) - 2s(s+1)] Y_{LM}^*(\hat{r}) \quad (3.17)$$

when we substitute eqs. (3.10-12), (3.15) and (3.16) into eq. (3.1). It is convenient to define the functions

$$C_L^{(C)}(r) = \delta_L^{(C)} \frac{3z_1 z_2 e^2}{2L+1} \begin{cases} \frac{r^L}{R_C^{L+2}} & r \leq R_C \\ \frac{R_C^{L-1}}{r^{L+1}} & r \geq R_C \end{cases}, \quad (3.18)$$

$$C_{L j_f \ell_f j_i \ell_i}^{(N)}(r) = -\frac{1}{2} \delta_L^{(N)} \frac{\partial}{\partial r} [V_{j_f \ell_f}^{(N)}(r) + V_{j_i \ell_i}^{(N)}(r)] \quad (3.19)$$

where

$$V_{j\ell}^{(N)}(r) = U_c^{(N)}(r) + \frac{1}{2} U_s(r) [j(j+1) - \ell(\ell+1) - s(s+1)] \quad (3.20)$$

denotes the nuclear part of the potential  $V_{j\ell}(r)$  given by eq. (2.14). We define the radial integrals

$$R_{j_f l_f j_i l_i}^{(C)L}(k_f, k_i) = \frac{4\pi}{k_f k_i} \int_0^\infty dr f_{j_f l_f}^{(F)}(k_f, r) C_L^{(C)}(r) f_{j_i l_i}^{(i)}(k_i, r), \quad (3.21)$$

$$R_{j_f l_f j_i l_i}^{(N)L}(k_f, k_i) = \frac{4\pi}{k_f k_i} \int_0^\infty dr f_{j_f l_f}^{(F)}(k_f, r) C_L^{(N)}(r) f_{j_i l_i}^{(i)}(k_i, r), \quad (3.22)$$

where the superscripts (C) and (N) refer to Coulomb and nuclear excitation respectively.

Writing

$$R_{j_f l_f j_i l_i}^L = R_{j_f l_f j_i l_i}^{(C)L} + R_{j_f l_f j_i l_i}^{(N)L}, \quad (3.23)$$

eq. (3.1) becomes

$$T_{LM\nu_f\nu_i} = \frac{4\pi}{(2L+1)^{\frac{1}{2}}} \sum_{j_f l_f M_f} \sum_{j_i l_i M_i} \exp\{i[\sigma_{l_f}(k_f) + \sigma_{l_i}(k_i)]\} R_{j_f l_f j_i l_i}^L(k_f, k_i) \\ Y_{j_f}^{M_f}(l_f, s, \nu_f; \hat{k}_f) Y_{j_i}^{M_i^*}(l_i, s, \nu_i; \hat{k}_i) \int d\hat{\Omega} Y_{j_f l_f}^{M_f \dagger}(\hat{\Omega}) Y_{LM}^*(\hat{\Omega}) Y_{j_i l_i}^{M_i}(\hat{\Omega}). \quad (3.24)$$

With the reference axes (2.26), we have from eq. (2.6)

$$Y_{j_i}^{M_i}(l_i, s, \nu_i; \hat{k}_i) = \langle l_i s 0 \nu_i | j_i M_i \rangle i^{-l_i} \left( \frac{2l_i+1}{4\pi} \right)^{\frac{1}{2}}, \quad (3.25)$$

$$Y_{j_f}^{M_f}(l_f, s, \nu_f; \hat{k}_f) = \sum_{m_f} \langle l_f s m_f \nu_f | j_f M_f \rangle i^{-l_f} Y_{l_f m_f}(\theta, 0), \quad (3.26)$$

where

$$\sin(\theta) = \left| \hat{k}_i \times \hat{k}_f \right| . \quad (3.27)$$

We now introduce the conditions of strong absorption in the elastic channels. This refers to the  $\ell$ -dependence of the reflection coefficients  $\eta_{j\ell}^{(i,f)}(k)$  and is discussed in section 2. Under these conditions the radial integrals (3.21) and (3.22) are approximately zero for  $\ell_i \lesssim \ell_0^{(i)}$  and  $\ell_f \lesssim \ell_0^{(f)}$ , where  $\ell_0^{(i)}$  and  $\ell_0^{(f)}$  are the critical  $\ell$ -values in the entrance and exit channels respectively. This is also due to phase averaging in the rapidly oscillating integrands in eqs. (3.21) and (3.22). We refer to ref.<sup>18)</sup> for a more detailed discussion of this phenomenon. The right hand side of eq. (3.24) is therefore dominated by those terms for which  $\ell_0^{(i,f)} \gg 1$ . As in the case of elastic scattering, it is further assumed that  $s \ll \ell_0^{(i,f)}$ . In appendix III the angular integral is evaluated to give, to a good approximation,

$$\int d\hat{x} Y_{j_f \ell_f}^{M_f \dagger}(\hat{x}) Y_{LM}^*(r) Y_{j_i \ell_i}^{M_i}(\hat{x}) = \frac{1}{(4\pi)^{\frac{1}{2}}} \delta_{M_f M_i - M} \delta_{\tau_f \tau_i} \frac{\hat{\ell}_f \hat{\ell}_i}{\hat{\ell}_i} d_{0 \ell_i - \ell_f}^L(\frac{1}{2}\pi) d_{M \ell_i - \ell_f}^L(\frac{1}{2}\pi) , \quad (3.28)$$

where

$$\tau = j - \ell , \quad \hat{x} \equiv (2x + 1)^{\frac{1}{2}} . \quad (3.29)$$

Substituting eqs. (3.25), (3.26) and (3.28) into eq. (3.24) gives

$$T_{LM\nu_f\nu_i} = \sum_{\ell_f \ell_i \tau} i^{\ell_i - \ell_f} (2\ell_f + 1)^{\frac{1}{2}} \exp\{i[\sigma_{\ell_f}(k_f) + \sigma_{\ell_i}(k_i)]\} R_{j_f \ell_f j_i \ell_i}^L(k_f, k_i) \\ \times \langle \ell_i s_0 \nu_i | j_i \nu_i \rangle \langle \ell_f s - m \nu_f | j_f \nu_f - m \rangle d_{0 \ell_i - \ell_f}^L(\frac{1}{2}\pi) d_{M \ell_i - \ell_f}^L(\frac{1}{2}\pi) Y_{\ell_f - m}^L(\theta, 0), \quad (3.30)$$

where

$$j_f = \ell_f + \tau, \quad j_i = \ell_i + \tau, \quad m = M - \nu_i + \nu_f. \quad (3.31)$$

Since  $\nu_f$ ,  $\nu_i$  and  $m$  are each an order of magnitude less than  $j_f$ ,  $j_i$ ,  $\ell_f$  and  $\ell_i$ , we may use the approximations (2.29-31) in eq. (3.30). Replacing  $m$  by  $(M - \nu_i + \nu_f)$ , we obtain

$$T_{LM\nu_f\nu_i} = \frac{1}{2\pi(\sin\theta)^{\frac{1}{2}}} \sum_{\ell_f \ell_i \tau} i^{\ell_i - \ell_f} (2\ell_f + 1)^{\frac{1}{2}} \exp\{i[\sigma_{\ell_f}(k_f) + \sigma_{\ell_i}(k_i)]\} \\ \times R_{j_f \ell_f j_i \ell_i}^L(k_f, k_i) \left[ \exp\{i[\lambda_f \theta - \frac{1}{4}\pi - \frac{1}{2}\pi(M - \nu_i + \nu_f)]\} \right. \\ \left. + \exp\{-i[\lambda_f \theta - \frac{1}{4}\pi - \frac{1}{2}\pi(M - \nu_i + \nu_f)]\} \right] d_{\nu_i \tau}^S(\frac{1}{2}\pi) d_{\nu_f \tau}^S(\frac{1}{2}\pi) d_{0\kappa}^L(\frac{1}{2}\pi) d_{M\kappa}^L(\frac{1}{2}\pi), \quad (3.32)$$

where

$$\lambda_f = \ell_f + \frac{1}{2}, \quad \kappa = \ell_i - \ell_f. \quad (3.33)$$

If we define

$$\begin{aligned} \mathcal{H}_{L\kappa\tau}(\pm\theta) &= \frac{1}{2\pi(\sin\theta)^{\frac{1}{2}}} \sum_{\ell_f} (2\ell_f+1)^{\frac{1}{2}} \\ &\times \exp\{i[\sigma_{\ell_f}(k_f) + \sigma_{\ell_i}(k_i) \pm \lambda_f\theta]\} R_{j_f\ell_f j_i\ell_i}^L(k_f, k_i), \end{aligned} \quad (3.34)$$

where  $j_f$  and  $j_i$  are given by eqs. (3.31), eq. (3.32) becomes

$$\begin{aligned} T_{LM\nu_f\nu_i} &= \sum_{\kappa\tau} i^\kappa \left\{ \exp[-i\frac{1}{2}\pi(\frac{1}{2}+M-\nu_i+\nu_f)] \mathcal{H}_{L\kappa\tau}(\theta) \right. \\ &+ \left. \exp[i\frac{1}{2}\pi(\frac{1}{2}+M-\nu_i+\nu_f)] \mathcal{H}_{L\kappa\tau}(-\theta) \right\} d_{\nu_i\tau}^S(\frac{1}{2}\pi) d_{\nu_f\tau}^S(\frac{1}{2}\pi) d_{0\kappa}^L(\frac{1}{2}\pi) d_{M\kappa}^L(\frac{1}{2}\pi). \end{aligned} \quad (3.35)$$

We now transform to the co-ordinate system (2.35).

With respect to the new axes, the inelastic scattering amplitude is given by

$$\bar{T}_{L\bar{M}\bar{\nu}_f\bar{\nu}_i} = \sum_{M\nu_f\nu_i} i^{\nu_i-\nu_f-M} d_{\bar{\nu}_f\nu_f}^S(\frac{1}{2}\pi) d_{\bar{M}M}^L(\frac{1}{2}\pi) T_{LM\nu_f\nu_i} d_{\nu_i\bar{\nu}_i}^S(-\frac{1}{2}\pi). \quad (3.36)$$

Using eqs. (2.38-41) and (3.35) and the relations

$$\sum_M d_{\bar{M}M}^L(\frac{1}{2}\pi) d_{M\kappa}^L(\frac{1}{2}\pi) = (-1)^{L-\kappa} \delta_{\bar{M}-\kappa}, \quad (3.37)$$

$$\sum_M (-1)^M d_{\bar{M}M}^L(\frac{1}{2}\pi) d_{M\kappa}^L(\frac{1}{2}\pi) = (-1)^{\bar{M}} \delta_{\bar{M}\kappa}, \quad (3.38)$$

eq. (3.36) becomes

$$\begin{aligned} \bar{T}_{L\bar{M}\bar{\nu}_f\bar{\nu}_i} &= \sum_{\kappa} i^\kappa d_{0\kappa}^L(\frac{1}{2}\pi) \left\{ (-1)^{\bar{M}} e^{-i\frac{1}{4}\pi} \mathcal{H}_{L\kappa\bar{\nu}_i}(\theta) \delta_{\kappa\bar{M}} \right. \\ &+ \left. (-1)^{L-\kappa} e^{i\frac{1}{4}\pi} \mathcal{H}_{L\kappa-\bar{\nu}_i}(-\theta) \delta_{\kappa-\bar{M}} \right\} \delta_{\bar{\nu}_f\bar{\nu}_i} \end{aligned} \quad (3.39)$$

$$= d_{0M}^L(\frac{1}{2}\pi) i^{\bar{M}} \left\{ (-1)^{\bar{M}} e^{-i\frac{1}{4}\pi} \mathcal{H}_{L\bar{M}\bar{\nu}_i}(\theta) + e^{i\frac{1}{4}\pi} \mathcal{H}_{L-\bar{M}-\bar{\nu}_i}(-\theta) \right\} \delta_{\bar{\nu}_f \bar{\nu}_i}, \quad (3.40)$$

where we have used

$$(-1)^L d_{0-M}^L(\frac{1}{2}\pi) = d_{0M}^L(\frac{1}{2}\pi). \quad (3.41)$$

If we now define, using eq. (3.34),

$$T_{LM\tau}^{(\pm)}(\theta) = i^M d_{0M}^L(\frac{1}{2}\pi) e^{\pm i\frac{1}{4}\pi} \mathcal{H}_{L\mp M\mp\tau}(\mp\theta) \quad (3.42)$$

$$= \frac{i^M}{2\pi(\sin\theta)^{\frac{1}{2}}} d_{0M}^L(\frac{1}{2}\pi) \sum_{\ell_f} (2\ell_f+1)^{\frac{1}{2}}$$

$$\times \exp\left\{ i \left[ \sigma_{\ell_f}(k_f) + \sigma_{\ell_f\mp M}(k_i) \mp (\lambda_f \theta - \frac{1}{4}\pi) \right] \right\} R_{\ell_f\mp\tau \ell_f \ell_f\mp M\mp\tau}^L(k_f, k_i), \quad (3.43)$$

eq. (3.40) can be written in the form

$$T_{LM\nu_f\nu_i} = \left\{ T_{LM\nu_i}^{(+)}(\theta) + (-1)^M T_{LM\nu_i}^{(-)}(\theta) \right\} \delta_{\nu_f\nu_i}, \quad (3.44)$$

in analogy with eq. (2.42) for the elastic scattering amplitude. The amplitudes  $T_{LM\tau}^{(\pm)}(\theta)$  are analogous to the amplitudes  $T_{LM}^{(\pm)}(\theta)$  given by eq. (3.19) of ref. 7).

As in eq. (2.42), the superscripts (+) and (-) denote, in a semiclassical description, the inelastic scattering amplitudes for scattering from the near and far sides of the interaction region respectively. According to eq. (3.44), the inelastic scattering amplitude is diagonal in the z-components  $\nu$  of the projectile spin in the co-ordinate

system (2.35). As in the case of elastic scattering, this implies that there is no exchange of angular momentum between the z-component of the projectile spin and the z-component of the orbital angular momentum, but each component  $v_i$  still has a different amplitude for scattering into the angle  $\theta$ .

One may therefore interpret the subscripts of the matrix  $R_{j_f l_f j_i l_i}^L$  in eq. (3.43) as follows. The difference between the total angular momentum  $j$  and the orbital angular momentum  $l$  is either  $-v_i$  or  $v_i$  in both the entrance channel (i) and the exit channel (f) depending on whether the projectile is scattered from the near side or far side of the target respectively. Secondly, by conservation of angular momentum between the entrance and exit channels, we must have  $j_f - j_i = l_f - l_i = -M$  or  $M$  depending on whether the projectile is scattered from the near side or far side of the target respectively.

The total inelastic cross section for excitation of the target nucleus to the collective mode  $L$  by an unpolarized beam of projectiles is given by

$$\sigma_L(\theta) = \sum_M \sigma_{LM}(\theta) , \quad (3.45)$$

where  $\sigma_{LM}(\theta)$  is the differential cross section for excitation of the target nucleus to the collective state  $(L, M)$ , and is given by

$$(2s+1)\sigma_{LM}(\theta) = \left(\frac{\mu}{2\pi\hbar^2}\right)^2 \frac{k_f}{k_i} \sum_{\tau} |T_{LM\tau\tau}(\theta)|^2 = \sum_{\tau} |B_{LM\tau}|^2 , \quad (3.46)$$

where the amplitudes  $B_{LM\tau}$  are defined, for  $k_f = k_i$ , by

$$B_{LM\tau} = B_{LM\tau}^{(+)} + (-1)^M B_{LM\tau}^{(-)}, \quad (3.47)$$

$$B_{LM\tau}^{(\pm)} = \frac{\mu}{2\pi\hbar^2} T_{LM\tau}^{(\pm)}. \quad (3.48)$$

In analogy with eq. (2.48), we may now write the density matrix for the spin of the projectiles in the scattered wave as

$$\rho_{\nu_f \nu_i}^{LM}(\theta) = \frac{1}{2S+1} |B_{LM\nu_i}^{(+)} + (-1)^M B_{LM\nu_i}^{(-)}|^2 \delta_{\nu_f \nu_i} \quad (3.49)$$

and expand it in terms of statistical tensors  $h_{\kappa q}^{LM}(\theta)$  in the form

$$\rho_{\nu_f \nu_i}^{LM}(\theta) = \frac{1}{2S+1} \sum_{\kappa q} h_{\kappa q}^{LM}(\theta) (2\kappa+1)^{\frac{1}{2}} \langle S\kappa \nu_f q | S\nu_i \rangle. \quad (3.50)$$

Inverting eq. (3.50) gives

$$h_{\kappa q}^{LM}(\theta) = (2\kappa+1)^{\frac{1}{2}} \sum_{\nu_f \nu_i} \rho_{\nu_f \nu_i}^{LM}(\theta) \langle S\kappa \nu_f q | S\nu_i \rangle \quad (3.51)$$

$$= \frac{(2\kappa+1)^{\frac{1}{2}}}{2S+1} \left\{ \sum_{\tau} |B_{LM\tau}^{(+)} + (-1)^M B_{LM\tau}^{(-)}|^2 \langle S\kappa \tau 0 | S\tau \rangle \right\} \delta_{q0}. \quad (3.52)$$

This gives, for example,

$$h_{00}^{LM}(\theta) = \frac{1}{2S+1} \sum_{\tau} |B_{LM\tau}^{(+)} + (-1)^M B_{LM\tau}^{(-)}|^2 = \sigma_{LM}(\theta). \quad (3.53)$$

However, we shall only be dealing with the case in which the

polarization of the target nucleus is not observed. This implies that we must add the contributions from the different magnetic substates  $M$ .

In analogy with eq. (2.63), the components  $t_{\kappa q}^L(\theta)$  ( $\kappa \neq 0$ ) of the analyzing power of the reaction are given by

$$t_{\kappa q}^L(\theta) = \frac{1}{s \sigma_L(\theta)} h_{\kappa q}^L(\theta), \quad (3.54)$$

where  $\sigma_L(\theta)$  is given by eq. (3.45) and

$$h_{\kappa q}^L(\theta) = \sum_M h_{\kappa q}^{LM}(\theta). \quad (3.55)$$

The interpretation of the components  $t_{\kappa q}$  and  $h_{\kappa q}$  for elastic scattering, given in section 2, applies directly to the components  $t_{\kappa q}^L$  and  $h_{\kappa q}^L$  for inelastic scattering. In section 7 we analyze data on inelastic scattering of polarized projectiles. By comparison with eq. (2.72), we have the average inelastic scattering cross section

$$\frac{1}{2} [\sigma_L^{(L)}(\theta) + \sigma_L^{(R)}(\theta)] = \sigma_L(\theta) \quad (3.56)$$

where  $\sigma_L(\theta)$  is given by eq. (3.45). Similarly, by comparison with eq. (2.75), the vector analyzing power in Cartesian notation is given by

$$A_z^L(\theta) = \left[ \frac{1}{3} s(s+1) \right]^{\frac{1}{2}} t_{10}^L(\theta). \quad (3.57)$$

Using eqs. (2.55), (3.52) and (3.54), this gives

$$A_z^L(\theta) = \frac{1}{s(2s+1)\sigma_L(\theta)} \sum_{M,\tau} \tau |B_{LM\tau}^{(+)} + (-1)^M B_{LM\tau}^{(-)}|^2, \quad (3.58)$$

and, following the discussion in section 2 on asymmetry in the elastic scattering cross section,  $A_z^L(\theta)$  gives the asymmetry in the inelastic scattering cross section  $\sigma_L(\theta)$  for a fully vector-polarized incident beam.

#### 4. CLOSED-FORM EXPRESSIONS - ELASTIC SCATTERING

In this section we derive closed-form analytical expressions for the elastic scattering amplitudes  $f_{\tau}^{(\pm)}(\theta)$  (eq. (2.33)) that appear in the expressions for the elastic scattering cross section  $\sigma(\theta)$  (eqs. (2.52-54)) and the vector analyzing power  $A_z(\theta)$  (eq. (2.76)).

To obtain eq. (2.32) we have already used the following conditions on the S-matrix  $S_{j\ell}(k)$ :

- I. The reflection coefficient  $\eta_{j\ell}$  varies smoothly with  $\ell$  from small values to unity within a transition region of "width"  $\Delta$  centred on some "critical  $\ell$ -value"  $\ell_0$ .
- II.  $\ell_0 \gg \Delta$ ,  $\ell_0 \gg 1$ ,  $\ell_0 \gg s$ .

To these we add the following condition:

- III. The nuclear phase shift  $\delta_{j\ell}^{(N)}$  varies smoothly with  $\ell$  and decreases to zero in the region  $\ell \gtrsim \ell_0$  over a transition region of "width"  $\Delta$ .

Conditions I-III are characteristic of heavy ion scattering well above the Coulomb barrier where we have strong absorption.

Under the above conditions we may make the approximation (c.f. refs.<sup>6,8</sup>) to eq. (2.33)

$$f_{\tau}^{(\pm)}(\theta) = -\frac{i}{k} \frac{1}{(2\pi \sin \theta)^{\frac{1}{2}}} \int_{\frac{1}{2}}^{\infty} d\lambda \lambda^{\frac{1}{2}} S_{\tau}(\lambda) e^{\mp i(\lambda\theta - \frac{1}{4}\pi)}, \quad (4.1)$$

where  $S_\tau(\lambda)$  is a continuously differentiable function of  $\lambda = \ell + \frac{1}{2}$  and interpolates the S-matrix  $S_{\ell+\tau\ell}$ , i.e. for all positive integral values of  $\ell$ ,

$$S_\tau(\ell + \frac{1}{2}) = S_{\ell+\tau\ell} \quad (4.2)$$

We now turn to the  $\tau$ -dependence of the scattering function  $S_\tau(\lambda)$ . Return to eq. (2.15) and consider the high-energy approximation to the S-matrix  $S_{j\ell}$  generated by the potential  $V_{j\ell}(r)$ , regarding it as a central potential dependent on the impact parameter  $b = (\ell + \frac{1}{2})/k$  and  $j$ . This gives (c.f. eq. (7.39) of ref.<sup>18</sup>)

$$S_{j\ell}(k) = \exp\left\{-i \frac{\mu}{\hbar^2 k} \int_{-\infty}^{\infty} dz V_{j\ell}(\underline{b} + \hat{k}z)\right\}, \quad (4.3)$$

where  $\underline{b}$  is the point on the (straight line) trajectory nearest to the origin, and  $\hat{k}$  is the direction of the trajectory. Referring to eq. (2.14), we now assume that  $|U_s(r)| \ll |U_c(r)|$  so that  $\underline{b}$  may be taken to be independent of  $j$ . Equation (4.3) then becomes

$$S_{j\ell}(k) = \exp\left\{-i \frac{2\mu}{\hbar^2 k} \int_b^{\infty} dr \frac{r V_{j\ell}(r)}{(r^2 - b^2)^{\frac{1}{2}}}\right\}. \quad (4.4)$$

According to eq. (4.3) or eq. (4.4), the phase shifts (real or imaginary), due to the different terms in the potential  $V_{j\ell}(r)$ , are additive. In this approximation therefore, we could write

$$S_{j\ell} = \eta_\ell \exp\left\{i2[\sigma_\ell + \delta_\ell^{(N)} + \delta_{j\ell}^{(N)}(\text{s.o.})]\right\}, \quad (4.5)$$

where, by eqs. (2.14) and (4.4),

$$\delta_{j\ell}^{(N)}(s.o.) = -\frac{\mu}{2\hbar^2 k} [j(j+1) - \ell(\ell+1) - s(s+1)] \int_b^\infty dr \frac{r U_s(r)}{(r^2 - b^2)^{\frac{1}{2}}} . \quad (4.6)$$

Writing  $j = \ell + \tau$ , we have

$$\frac{1}{2} [j(j+1) - \ell(\ell+1) - s(s+1)] = \tau(\ell + \frac{1}{2}) - \frac{1}{2} \tau^2 - \frac{1}{2} s(s+1) . \quad (4.7)$$

According to condition I we are only concerned with  $\ell$  values  $\gtrsim L$ , so by condition II we may approximate the right hand side of eq. (4.7) by  $\tau\lambda$ . The high-energy approximation to the elastic scattering function  $S_\tau(\lambda)$  therefore becomes

$$S_\tau(\lambda) = S_c(\lambda) e^{i2\delta_s(\lambda)} , \quad (4.8)$$

where the "central" part  $S_c(\lambda)$  is given by

$$S_c(\lambda) = \exp \left\{ -i \frac{2\mu}{\hbar^2} \int_{\frac{\lambda}{k}}^\infty dr \frac{r U_c(r)}{(k^2 r^2 - \lambda^2)^{\frac{1}{2}}} \right\} \quad (4.9)$$

and the spin-orbit phase shift function  $\delta_s(\lambda)$  is given by

$$\delta_s(\lambda) = -\frac{\lambda\mu}{\hbar^2} \int_{\frac{\lambda}{k}}^\infty dr \frac{r U_s(r)}{(k^2 r^2 - \lambda^2)^{\frac{1}{2}}} . \quad (4.10)$$

In general the spin-orbit potential  $U_s(r)$  is complex<sup>†</sup> which implies that  $\delta_s(\lambda)$  is complex.

The main purpose of the above analysis was to obtain the

---

<sup>†</sup> The presence of an imaginary term in the spin-orbit potential is justified in section 4.4 of ref.<sup>13</sup>.

$\tau$ -dependence of the elastic scattering function  $S_\tau(\lambda)$ , as given by eq. (4.8), and we use this form irrespective of whether the high-energy approximation is valid or not. The parametric form of  $S_c(\lambda)$  that is used in section 6 is independent of eq. (4.9), although the parametric form of  $\delta_s(\lambda)$  is based on eq. (4.10).

It is convenient to write

$$S_c(\lambda) = \eta_c(\lambda) \exp\{i2[\sigma(\lambda) + \delta_c^{(N)}(\lambda)]\} = S_c^{(N)}(\lambda) \exp[i2\sigma(\lambda)] , \quad (4.11)$$

where  $\eta_c(\lambda) = |S_c(\lambda)|$ ,  $\sigma(\lambda)$  is the point-charge Coulomb scattering phase shift given by

$$2\sigma(\lambda) = \arg \left[ \frac{\Gamma(\ell + \frac{1}{2} + in)}{\Gamma(\ell + \frac{1}{2} - in)} \right] , \quad (4.12)$$

where  $n$  is the Sommerfeld parameter defined by

$$n = \frac{\mu z_1 z_2 e^2}{\hbar^2 k} , \quad (4.13)$$

and  $\delta_c^{(N)}(\lambda)$  is the real phase shift due to the nuclear part  $U_c^{(N)}(r)$  of the central potential  $U_c(r)$ . From eqs. (4.8) and (4.11), we have

$$S_\tau(\lambda) = \eta_c(\lambda) \exp\{i2[\sigma(\lambda) + \delta_c^{(N)}(\lambda) + \tau\delta_s(\lambda)]\} \quad (4.14)$$

$$= S_c^{(N)}(\lambda) \exp\{i2[\sigma(\lambda) + \tau\delta_s(\lambda)]\} . \quad (4.15)$$

On the basis of our previous assumption that

$|U_S(r)| \ll |U_C(r)|$ , we now assume that for all values of  $\lambda$ ,

$$\text{IV. } |2s \delta_S(\lambda)| \ll 1 .$$

The idea now is to evaluate the scattering amplitudes  $f_{\tau}^{(\pm)}(\theta)$  for any form of the elastic scattering function  $S_{\tau}(\lambda)$  obeying conditions I-IV. The methods used follow closely those used in the evaluation of the scattering amplitudes  $f_{\pm}(\theta)$  in ref.<sup>6)</sup> (or  $f^{(\pm)}(\theta)$  in ref.<sup>8)</sup>).

Combining eqs. (4.1) and (4.14) and expanding  $S_{\tau}(\lambda)$  in powers of  $\delta_S(\lambda)$ , we have

$$f_{\tau}^{(\pm)}(\theta) = -\frac{i}{k} \frac{1}{(2\pi \sin\theta)^{\frac{1}{2}}} \int_{\frac{1}{2}}^{\infty} d\lambda \lambda^{\frac{1}{2}} \eta_c(\lambda) \times \exp\left\{i\left[2\sigma(\lambda) + 2\delta_c^{(N)}(\lambda) \mp \lambda\theta \mp \frac{1}{4}\pi\right]\right\} \sum_{q=0}^{\infty} \frac{1}{q!} [i2\tau\delta_S(\lambda)]^q \quad (4.16)$$

$$\equiv \sum_{q=0}^{\infty} (\mp\tau)^q f_q^{(\pm)}(\theta) . \quad (4.17)$$

Equation (4.17) amounts to an expansion of the elastic scattering amplitudes  $f_{\tau}^{(\pm)}(\theta)$  to different orders in the spin-orbit coupling, similar to the expansion one would obtain by treating the spin-orbit coupling in DWBA.

On the basis of assumption IV,  $|f_{q+1}^{(\pm)}(\theta)|$  is an order of magnitude smaller than  $|f_q^{(\pm)}(\theta)|$  so that from eqs. (2.52) and (2.54), we have to first order,

$$\sigma(\theta) = \frac{1}{2s+1} \sum_{\tau} |f_0(\theta) + \tau f_1(\theta)|^2 \quad (4.18)$$

$$= |f_0(\theta)|^2 + \frac{1}{3} s(s+1) |f_1(\theta)|^2 , \quad (4.19)$$

where we have defined

$$f_q(\theta) = f_q^{(+)}(\theta) + f_q^{(-)}(\theta). \quad (4.20)$$

From eq. (2.76) we have, to first order for the vector analyzing power,

$$A_z(\theta) = \frac{1}{s(2s+1)\sigma(\theta)} \sum_{\tau} \tau |f_0(\theta) + \tau f_1(\theta)|^2 \quad (4.21)$$

$$= \frac{2}{3}(s+1) \frac{1}{\sigma(\theta)} \operatorname{Re} [f_0(\theta) f_1^*(\theta)]. \quad (4.22)$$

From eqs. (2.60), (2.63) and (2.66), we have to third order for the tensor analyzing power of rank 2,

$$T_{20}(\theta) = \frac{1}{s(s+1)\sigma(\theta)} \left[ \frac{5}{s(s+1)(2s+3)(2s-1)} \right]^{\frac{1}{2}} \times \sum_{\tau} \left\{ [3\tau^2 - s(s+1)] |f_0(\theta) + \tau f_1(\theta) + \tau^2 f_2(\theta)|^2 \right\} \quad (4.23)$$

$$= \frac{1}{15} \frac{1}{\sigma(\theta)} \left[ \frac{5}{s(s+1)(2s+3)(2s-1)} \right]^{\frac{1}{2}} \left\{ |f_1(\theta)|^2 + 2 \operatorname{Re} [f_0(\theta) f_2^*(\theta)] \right\} \quad (4.24)$$

According to eqs. (4.22) and (4.24),  $T_{20}(\theta)$  is an order of magnitude smaller than  $A_z(\theta)$  (or  $T_{10}(\theta)$ ). This agrees with the analysis in appendix I based on distorted-wave theory. We therefore evaluate only  $\sigma(\theta)$  and  $A_z(\theta)$ , for which we need the amplitudes  $f_0(\theta)$  and  $f_1(\theta)$ .

From eqs. (4.16) and (4.17) we have

$$f_0^{(\pm)}(\theta) = -\frac{i}{k} \frac{1}{(2\pi \sin\theta)^{\frac{1}{2}}} \int_{\frac{1}{2}}^{\infty} d\lambda \lambda^{\frac{1}{2}} \eta_c(\lambda) \exp\{i[2\delta_c^{(N)}(\lambda) + \varphi_{\pm}(\lambda, \theta)]\}, \quad (4.25)$$

$$f_i^{(\pm)}(\theta) = \mp \frac{2}{k(2\pi \sin \theta)^{\frac{1}{2}}} \int_{\frac{1}{2}}^{\infty} d\lambda \lambda^{\frac{1}{2}} \eta_c(\lambda) \delta_c^{(N)}(\lambda) \exp\{i[2\delta_c^{(N)}(\lambda) + \varphi_{\pm}(\lambda, \theta)]\}, \quad (4.26)$$

where we have defined

$$\varphi_{\pm}(\lambda, \theta) = 2\sigma(\lambda) \mp i(\lambda\theta - \frac{1}{4}\pi). \quad (4.27)$$

The amplitudes  $f_0^{(\pm)}(\theta)$  are identical to the elastic scattering amplitudes  $f_{\pm}(\theta)$  in ref. <sup>6)</sup> and  $f^{(\pm)}(\theta)$  in ref. <sup>8)</sup>.

From eqs. (4.14) and (4.15) we have by definition

$$S_c^{(N)}(\lambda) = \eta_c(\lambda) e^{i2\delta_c^{(N)}(\lambda)}. \quad (4.28)$$

We define

$$D_c^{(N)}(\lambda) = \frac{d}{d\lambda} S_c^{(N)}(\lambda) \quad (4.29)$$

in analogy with the "absorptive shape function" of refs. <sup>6, 8)</sup>, which is defined in the above notation as

$$D(\lambda) = \frac{d}{d\lambda} \eta_c(\lambda). \quad (4.30)$$

This modification of Frahn's formalism is due to Kauffmann<sup>9)</sup>. Its advantages are discussed after eq. (4.36).

We now define

$$\mathfrak{F}(\Delta z) = \int_{-\infty}^{\infty} d\lambda D_c^{(N)}(\lambda) \exp[i(\lambda - \lambda)z], \quad (4.31)$$

where

$$\Lambda = l_0 + \frac{1}{2} . \quad (4.32)$$

This is equivalent to

$$S_c^{(N)}(\lambda) = \frac{i}{2\pi} \lim_{\epsilon \rightarrow 0^+} \int_{-\infty}^{\infty} dz \frac{1}{z+i\epsilon} \exp[-i(\lambda-\Lambda)z] \mathcal{F}(\Delta z) . \quad (4.33)$$

Substituting eq. (4.33) into eq. (4.25), using eq. (4.28), gives

$$f_0^{(+)}(\theta) = \frac{i}{2\pi} \lim_{\epsilon \rightarrow 0^+} \int_{-\infty}^{\infty} dz \frac{\mathcal{F}(\Delta z)}{z+i\epsilon} e^{i\Lambda z} \left[ \frac{\sin(z+\theta)}{\sin(\theta)} \right]^{\frac{1}{2}} f_R(z+\theta) , \quad (4.34)$$

$$f_0^{(-)}(\theta) = \frac{1}{2\pi} \lim_{\epsilon \rightarrow 0^+} \int_{-\infty}^{\infty} dz \frac{\mathcal{F}(\Delta z)}{z+i\epsilon} e^{i\Lambda z} \left[ \frac{\sin(z-\theta)}{\sin(\theta)} \right]^{\frac{1}{2}} f_R(z-\theta) , \quad (4.35)$$

where

$$f_R(\theta) = -\frac{i}{k} \frac{1}{(2\pi \sin \theta)^{\frac{1}{2}}} \int_{\frac{1}{2}}^{\infty} d\lambda \lambda^{\frac{1}{2}} e^{i\varphi_+(\lambda, \theta)} \quad (4.36)$$

is the amplitude for Rutherford scattering.

The advantage of Kauffmann's modification is that the effect of the central nuclear potentials (real and imaginary) is contained in the function  $\mathcal{F}(\Delta z)$  while  $f_R(\theta)$  is now the amplitude for scattering by a Coulomb potential only. Since the stationary phase approximation to  $f_R(\theta)$  is used in refs.<sup>6,8)</sup>, one no longer has to assume monotonicity of the function†

$$\Theta_c(\lambda) = 2 \frac{d}{d\lambda} [\sigma(\lambda) + \delta_c^{(N)}(\lambda)] , \quad (4.37)$$

---

† The function  $\Theta_c(\lambda)$  is the total quantal deflection function in the absence of spin-orbit coupling.

since only the Coulomb phase shift  $\sigma(\lambda)$  appears in the phase of the integral in eq. (4.36) and the Rutherford deflection function  $2 d\sigma(\lambda)/d\lambda$  is monotone decreasing. This is important in the scattering of light and medium ions when the effect of the real nuclear potential is comparable to that of the Coulomb potential for those partial waves which are not strongly absorbed. In fitting the data in section 7, the quantal deflection function  $\Theta_C(\lambda)$  had a pronounced dip in some cases, corresponding to refraction caused by the real nuclear potential. For heavy ions the Coulomb potential tends to mask the effect of the real nuclear potential to the extent that the deflection function  $\Theta_C(\lambda)$  is monotone decreasing for  $\lambda \gtrsim \Lambda$ .

Because of conditions I and III,  $|\mathfrak{J}(\Delta z)|$  is a broad peak of width proportional to  $\Delta^{-1}$  and is therefore a slowly varying function compared with the rest of the integrand in the integrals in eqs. (4.34) and (4.35). These may be evaluated using the methods of ref.<sup>6)</sup> or ref.<sup>8)</sup>, giving, correct to order  $\Delta\Lambda^{-\frac{1}{2}}$ ,

$$f_0^{(+)}(\theta) = \left\{ f_R(\theta) - \mathfrak{J}[\Delta(\theta_R - \theta)] [f_R(\theta) - f_{SCO}^{(+)}(\theta)] \right\} \quad \theta \leq \theta_R, \quad (4.38)$$

$$f_0^{(+)}(\theta) = \mathfrak{J}[\Delta(\theta_R - \theta)] f_{SCO}^{(+)}(\theta) \quad \theta \geq \theta_R, \quad (4.39)$$

$$f_0^{(-)}(\theta) = \mathfrak{J}[\Delta(\theta_R + \theta)] f_{SCO}^{(-)}(\theta) \quad \forall \theta, \quad (4.40)$$

where  $\theta_R$  is the critical angle for Rutherford scattering, and is defined by

where

$$\Gamma_{\Sigma}(\theta_R - \theta) = \mp \gamma(\pm u_0) [1 + a_1(\theta_R - \theta)] - a_0, \quad (4.47)$$

$$\gamma(u_0) = \frac{1}{2} \operatorname{erfc}(u_0) \left[ \frac{2\pi}{-\Theta'_R(\lambda)} \right]^{\frac{1}{2}} \exp(i\frac{1}{4}\pi + u_0^2). \quad (4.48)$$

where

$$a_0 = -\frac{1}{2\lambda \Theta'_R(\lambda)} + \frac{\Theta''_R(\lambda)}{3[\Theta'_R(\lambda)]^2} + i\frac{1}{6} \frac{\Theta''_R(\lambda)}{[-\Theta'_R(\lambda)]^3} (\theta - \theta_R)^2, \quad (4.49)$$

$$a_1 = a_0 + \frac{1}{6} \frac{\Theta''_R(\lambda)}{[\Theta'_R(\lambda)]^2}, \quad (4.50)$$

$$u_0 = \frac{\theta - \theta_R}{[-2\Theta'_R(\lambda)]^{\frac{1}{2}}} e^{i\frac{1}{4}\pi}, \quad (4.51)$$

$$\operatorname{erfc}(u_0) = \frac{2}{\pi^{\frac{1}{2}}} \int_{u_0}^{\infty} dz e^{-z^2}. \quad (4.52)$$

The asymptotic form of  $\Gamma_{\Sigma}(\theta_R - \theta)$  is given by

$$\Gamma_{\Sigma}(\theta_R - \theta) = (\theta_R - \theta)^{-1} + o\{[\lambda(\theta_R - \theta)^2]^{-1}\}. \quad (4.53)$$

The errors in eqs. (4.44-46) are of order  $n^{-1}$ , where  $n$  is the Sommerfeld parameter (eq. (4.13)), over the whole angular range, or  $\Lambda^{-1}$  in the asymptotic regions defined by

$$\theta_R \mp \theta \gg |2\Theta'_R(\lambda)|^{\frac{1}{2}}. \quad (4.54)$$

In deriving eqs. (4.44-46), the stationary phase approximation to  $f_R(\theta)$  is used as an intermediate step.

This is given by

$$f_R(\theta) = -\frac{i}{k} \left( \frac{\lambda_\theta}{-\Theta'_R(\lambda_\theta) \sin \theta} \right)^{\frac{1}{2}} \exp\{i[2\sigma(\lambda_\theta) - \theta \lambda_\theta]\}, \quad (4.55)$$

where  $\lambda_\theta$  is the stationary phase point defined by

$$\theta = \Theta_R(\lambda_\theta). \quad (4.56)$$

Using

$$\Theta_R(\lambda) = 2 \arctan\left(\frac{n}{\lambda}\right) + O(\lambda^{-2}), \quad (4.57)$$

we have

$$\lambda_\theta \approx n \cot\left(\frac{1}{2}\theta\right), \quad (4.58)$$

$$\Theta'_R(\lambda) \approx \frac{-2n}{n^2 + \lambda^2}, \quad \Theta''_R(\lambda) \approx \frac{4n\lambda}{(n^2 + \lambda^2)^2}, \quad (4.59)$$

therefore

$$a_0 \approx \frac{\lambda}{3n} + \frac{n^2 + \lambda^2}{4n\lambda} \left\{ 1 + i \frac{\lambda^2}{3n} (\theta - \theta_R)^2 \right\}, \quad (4.60)$$

$$a_1 \approx a_0 + \frac{\lambda}{6n}, \quad (4.61)$$

$$u_0 \approx \left( \frac{n^2 + \lambda^2}{4n} \right)^{\frac{1}{2}} (\theta - \theta_R) e^{i\frac{1}{4}\pi}, \quad (4.62)$$

$$f_R(\theta) \approx -\frac{n}{2k} \frac{1}{(\sin \frac{1}{2}\theta)^2} \exp\{i[2\sigma(\lambda_\theta) - \theta n \cot(\frac{1}{2}\theta) + \frac{1}{2}\pi]\}. \quad (4.63)$$

We now turn to the functions  $f_1^{(\pm)}(\theta)$  defined by eq. (4.26).

Conditions I and III on the S-matrix  $S_{j\ell}$  and eq. (4.14) imply that the (complex) spin-orbit phase shift  $\delta_S(\lambda)$  decreases to zero in the region  $\lambda \gtrsim \Lambda$ . We denote the width of the transition region of  $\delta_S(\lambda)$  by  $\Delta_S$ . In subsection 6.1 we take  $\delta_S(\lambda)$  to be proportional to the derivative of a Woods-Saxon function of width  $\Delta_S \leq \Delta$  and critical  $\lambda$ -value  $\Lambda_S \leq \Lambda$ . This is shown in subsection 6.1 to be a reasonable parameterization, at least on the basis of the high-energy approximation (4.10) for  $\delta_S(\lambda)$  and with a Thomas-Fermi form for  $U_S(r)$ .

Using eq. (4.14) it is convenient to write

$$\eta_c(\lambda) \delta_S(\lambda) e^{i2\delta_c^{(N)}(\lambda)} = S_c^{(N)}(\lambda) \delta_S(\lambda). \quad (4.64)$$

The modulus of this term has the form of a narrow peak at some value  $\lambda = \bar{\Lambda}$  and "width"  $\leq \Delta$ . The amplitudes  $f_1^{(\pm)}(\theta)$  are therefore of diffractive origin. Since the main contribution to the integral in eq. (4.26) comes from the region around  $\lambda = \bar{\Lambda}$ , we evaluate this integral simply by expanding the phase  $\varphi_{\pm}(\lambda, \theta)$ , given by eq. (4.27), about the point  $\lambda = \bar{\Lambda}$  to first order in  $(\lambda - \bar{\Lambda})$ , and integrating.

To order  $(\lambda - \bar{\Lambda})^2$ , we have

$$\varphi_{\pm}(\lambda, \theta) = \varphi_{\pm}(\bar{\Lambda}, \theta) \mp (\bar{\Lambda}\theta - \frac{1}{4}\pi) + (\lambda - \bar{\Lambda})(\bar{\theta}_R \mp \theta), \quad (4.65)$$

where

$$\bar{\theta}_R \equiv \theta_R(\bar{\Lambda}), \quad (4.66)$$

so that, from eqs. (4.26) and (4.64), we have to order  $\bar{\Lambda}^{-1}$ ,

$$f_1^{(\pm)}(\theta) = \mp \frac{2}{k} \left( \frac{\bar{\lambda}}{2\pi \sin \theta} \right)^{\frac{1}{2}} G(\bar{\theta}_R \mp \theta) \exp[i\varphi_{\pm}(\bar{\lambda}, \theta)] , \quad (4.67)$$

where

$$G(z) = \int_{-\infty}^{\infty} d\lambda S_c^{(N)}(\lambda) \delta_s(\lambda) \exp[i(\lambda - \bar{\lambda})z] . \quad (4.68)$$

To summarize the results of this section, we have

$$\sigma(\theta) = \sigma_0(\theta) + \sigma_1(\theta) , \quad (4.69)$$

where

$$\sigma_0(\theta) = |f_0(\theta)|^2 \quad (4.70)$$

gives the differential cross section without spin-orbit coupling and

$$\sigma_1(\theta) = \frac{1}{3} s(s+1) |f_1(\theta)|^2 \quad (4.71)$$

gives the correction due to spin-orbit coupling;

$$A_z(\theta) = \frac{1}{\sigma(\theta)} \frac{2}{3} s(s+1) \operatorname{Re}[f_0(\theta) f_1^*(\theta)] , \quad (4.72)$$

where

$$f_0(\theta) = f_R(\theta) + \frac{\kappa(\theta)}{k} \left\{ \exp[i\varphi_+(\lambda, \theta)] \Gamma_{<}(\theta_R - \theta) \mathfrak{J}[\Delta(\theta_R - \theta)] \right. \\ \left. + \exp[i\varphi_-(\lambda, \theta)] \frac{1}{\theta_R + \theta} \mathfrak{J}[\Delta(\theta_R + \theta)] \right\} \quad \theta \leq \theta_R, \quad (4.73)$$

$$f_0(\theta) = \frac{\kappa(\theta)}{k} \left\{ \exp[i\varphi_+(\lambda, \theta)] \Gamma_{>}(\theta_R - \theta) \mathfrak{J}[\Delta(\theta_R - \theta)] \right. \\ \left. + \exp[i\varphi_-(\lambda, \theta)] \frac{1}{\theta_R + \theta} \mathfrak{J}[\Delta(\theta_R + \theta)] \right\} \quad \theta \geq \theta_R, \quad (4.74)$$

$$f_1(\theta) = -\frac{2\bar{\kappa}(\theta)}{k} \left\{ \exp[i\varphi_+(\bar{\lambda}, \theta)] G(\bar{\theta}_R - \theta) - \exp[i\varphi_-(\bar{\lambda}, \theta)] G(\bar{\theta}_R + \theta) \right\} \quad \forall \theta, \quad (4.75)$$

where

$$\kappa(\theta) = \left( \frac{\lambda}{2\pi \sin \theta} \right)^{\frac{1}{2}}, \quad \bar{\kappa}(\theta) = \left( \frac{\bar{\lambda}}{2\pi \sin \theta} \right)^{\frac{1}{2}}. \quad (4.76)$$

The phase functions  $\varphi_{\pm}$  (eq. (4.27)) are linear functions of  $\theta$  while the functions  $\Gamma_{\gtrless}$  (eq. (4.47)) have the simple asymptotic form given by eq. (4.53). The function  $\mathfrak{J}$ , defined by eq. (4.31), incorporates the effects of refraction, surface reflection and absorption due to the nuclear part  $U_c^{(N)}(r)$  of the central part  $U_c(r)$  of the optical potential (2.1). The function  $G$ , defined by eq. (4.68), includes in addition the effects of the spin-orbit part of the optical potential. Both functions  $\mathfrak{J}$  and  $G$  involve the Coulomb potential only through the critical angles  $\theta_R$  and  $\bar{\theta}_R$  which appear in the arguments  $\theta_R \pm \theta$  and  $\bar{\theta}_R \pm \theta$  respectively.

It can be seen from eqs. (4.73) and (4.74) that the functions  $\mathfrak{J}[\Delta(\theta_R \pm \theta)]$  to a large extent govern the structure of  $\sigma_0(\theta)$  since their relative magnitudes control the strength

of the oscillations coming from the phases  $\exp[i\psi_{\pm}(\Lambda, \theta)]$ , while their asymptotic behaviour governs the rate of fall-off of  $\sigma_0(\theta)$  at large angles. The functions  $G(\bar{\theta}_R \pm \theta)$  determine the angular dependence of  $\sigma_1(\theta)$  in a similar way.

A more detailed discussion of the differential cross section  $\sigma(\theta)$  and the vector analyzing power  $A_z(\theta)$  is given in section 6 when the functions  $\mathfrak{J}(\Delta z)$  and  $G(z)$  are evaluated explicitly for specific forms of  $S_c^{(N)}(\lambda)$  and  $\delta_s(\lambda)$ .

## 5. CLOSED FORM EXPRESSIONS - INELASTIC SCATTERING

In this section we derive closed-form analytical expressions for the inelastic scattering amplitudes  $B_{LM\tau}$  (eqs. (3.47) and (3.48)) that appear in the expressions for the inelastic cross section  $\sigma_L(\theta)$  (eqs. (3.45) and (3.46)) and the vector analyzing power  $A_Z^L(\theta)$  (eq. (3.58)).

The radial integrals  $R_{j_f \ell_f j_i \ell_i}^L(k_f, k_i)$  appearing on the right hand side of eq. (3.43) are given by eqs. (3.21-23). We approximate the radial integrals for Coulomb excitation (3.21) by means of the Sopkovich prescription<sup>20)</sup> which amounts to factoring out the nuclear distortion of the radial wave functions in the initial and final channels. This gives

$$R_{j_f \ell_f j_i \ell_i}^{(c)L}(k_f, k_i) \approx [S_{j_f \ell_f}^{(N)}(k_f)]^{\frac{1}{2}} R_{\ell_f \ell_i}^L(k_f, k_i) [S_{j_i \ell_i}^{(N)}(k_i)]^{\frac{1}{2}}, \quad (5.1)$$

where

$$R_{\ell_f \ell_i}^L(k_f, k_i) = \frac{4\pi}{k_f k_i} \int_0^\infty dr F_{\ell_f}(k_f; r) C_L^{(c)}(r) F_{\ell_i}(k_i; r) \quad (5.2)$$

are the radial integrals for Coulomb excitation formed with the regular Coulomb wave functions  $F_\ell(k; r)$  (ref.<sup>21)</sup>). As explained in section 3, the conditions of strong absorption in the entrance and exit channels imply that the radial integrals (3.21) and (3.22) need only be evaluated for large values of  $\ell_i$  and  $\ell_f$ . This implies that the interior part ( $r \leq R_c$ ) of the form factor  $C_L^{(c)}(r)$  (eq. (3.18)) is

unimportant since it has poor overlap with the radial wave functions  $F_{l_f}$  and  $F_{l_i}$  due to centrifugal repulsion. We may therefore write

$$R_{l_f l_i}^L(k_f, k_i) = \delta_L^{(C)} \frac{3Z_1 Z_2 e^2}{2L+1} R_C^{L-1} [S_{j_f l_f}^{(N)}(k_f) S_{j_i l_i}^{(N)}(k_i)]^{\frac{1}{2}} m_{l_f l_i}^L(k_f, k_i) \quad (5.3)$$

where

$$m_{l_f l_i}^L(k_f, k_i) = \frac{4\pi}{k_f k_i} \int_0^\infty dr F_{l_f}(k_f; r) r^{-(L+1)} F_{l_i}(k_i; r) \quad (5.4)$$

are standard integrals of Coulomb excitation theory<sup>22)</sup>. For the same reason these integrals may be evaluated using the WKB approximation, giving<sup>22)</sup>

$$m_{l_f l_i}^L(k_f, k_i) = \frac{\pi k^{L-2}}{n^L} I_{L-\kappa}(\vartheta, \xi), \quad (5.5)$$

where

$$k = \frac{1}{2}(k_i + k_f), \quad n = \frac{1}{2}(n_i + n_f), \quad n_{i,f} = \frac{\mu Z_1 Z_2 e^2}{\hbar^2 k_{i,f}} \quad (5.6)$$

$$\xi = n_f - n_i, \quad \vartheta = 2 \arctan\left(\frac{n}{l + \frac{1}{2}}\right), \quad (5.7)$$

$$\kappa = l_i - l_f, \quad l = \frac{1}{2}(l_i + l_f). \quad (5.8)$$

The Coulomb integrals  $I_{LM}(\vartheta, \xi)$  are defined and tabulated in ref.<sup>22)</sup>, but under the conditions  $\lambda \gg n$  and  $\vartheta \ll (2\xi)^{-1}$ , one can make the approximation (see eqs. (IIE.79) and (IIE.82) of ref.<sup>22)</sup>)

$$I_{LM}(\vartheta, \xi) = \frac{2\pi}{\Gamma[\frac{1}{2}(L+|M|)]} \frac{\xi^{\frac{1}{2}(L-M-1)}}{(\frac{2\lambda}{n})^{\frac{1}{2}(L+M+1)}} e^{-(\frac{1}{2}\pi + \frac{\lambda}{n})\xi}, \quad \vartheta = \frac{2n}{\lambda}. \quad (5.9)$$

The following considerations apply to the radial integrals for nuclear excitation:

It is possible to extend the Austern-Blair theory<sup>23</sup>, which deals with deformations of central potentials, to include deformations of a spin-orbit potential of the form  $U_s(r) \mathbf{l} \cdot \mathbf{s}$ . Referring to the elastic scattering formalism of section 2, it is possible to apply the Austern-Blair relations directly to each component  $j$  of the total angular momentum. This gives first of all the exact relation

$$e^{i2\sigma_\ell(k)} \int_0^\infty dr [f_{j\ell}(k, r)]^2 \frac{\partial V_{j\ell}(r)}{\partial R} = \frac{iE}{2k} \frac{\partial S_{j\ell}(k)}{\partial R}, \quad (5.10)$$

where  $R$  denotes any parameter of the potential  $V_{j\ell}(r)$  (eq. (2.14)) and  $S_{j\ell}(k)$  is the elastic S-matrix (eq. (2.18)). For our purposes the parameter  $R$  is the radius of the nuclear potentials appearing in  $V_{j\ell}(r)$ . For this reason we may replace  $V_{j\ell}(r)$  by  $V_{j\ell}^{(N)}(r)$  (eq. (3.20)) on the left hand side of eq. (5.10), and since the point-charge Coulomb scattering phase shifts  $\sigma_\ell(k)$  are independent of  $R$ , we may factor out the phase  $\exp[i2\sigma_\ell(k)]$ . Using eq. (2.18), this gives

$$\int_0^\infty dr [f_{j\ell}(k, r)]^2 \frac{\partial V_{j\ell}(r)}{\partial R} = \frac{iE}{2k} \frac{\partial S_{j\ell}^{(N)}(k)}{\partial R}. \quad (5.11)$$

It is assumed that the dependence of  $V_{j\ell}^{(N)}(r)$  on  $r$  and  $R$  involves only  $r$ - $R$  so that

$$\frac{\partial V_{j\ell}^{(N)}(r)}{\partial R} = - \frac{\partial V_{j\ell}^{(N)}(r)}{\partial r} . \quad (5.12)$$

It is also assumed that the  $\ell$ -dependence of  $S_{j\ell}^{(N)}$  involves only  $\ell - \ell_0$ , where  $\ell_0$  is the critical  $\ell$ -value of section 2, and that the semiclassical relation  $\ell_0 + \frac{1}{2} = kR$  holds, where  $k$  is the wavenumber. We therefore have

$$\frac{\partial S_{j\ell}^{(N)}}{\partial R} = \frac{\partial S_{j\ell}^{(N)}}{\partial \ell} \left( - \frac{\partial \ell_0}{\partial R} \right) = -k \frac{\partial S_{j\ell}^{(N)}}{\partial \ell} . \quad (5.13)$$

Combining eqs. (3.19), (3.22) and (5.11-13), we have

$$R_{j\ell j\ell}^{(N)L}(k, k) = -i \frac{\pi \hbar^2}{\mu} \delta_L^{(N)} \frac{\partial S_{j\ell}^{(N)}(k)}{\partial \ell} . \quad (5.14)$$

According to eqs. (3.34) and (3.31) we require the radial integrals (3.21) and (3.22) for which  $j_f - \ell_f = \tau = j_i - \ell_i$ . Equation (5.14) gives us an approximate formula for the radial integrals (3.22) in the limit  $\tau = 0$  and  $k_f = k_i$ .

As discussed in section 3, the radial integrals (3.23) are approximately zero for  $\ell_i \lesssim \ell_0^{(i)}$  and  $\ell_f \lesssim \ell_0^{(f)}$ . Furthermore, we consider only excitation of the target nucleus to collective states of low values of  $L$  and  $M$  (equal to 2, 4, ...) so that  $|\ell_0^{(f)} - \ell_0^{(i)}| \ll \ell_c$  where we define

$$\ell_c = \frac{1}{2} (\ell_0^{(f)} + \ell_0^{(i)}) . \quad (5.15)$$

Concerning the radial integrals (3.22), the overlap of the radial wave functions  $f_{j\ell}(k, r)$  and the functions  $C_{Lj_f \ell_f j_i \ell_i}^{(N)}$  for  $\ell_i$  and  $\ell_f$  greater than  $\ell_c$  is weak because of centrifugal

repulsion. The radial integrals (3.22) are therefore localized in orbital angular momentum space about the critical value  $l_c$ . We need only those radial integrals for which  $j_f - l_f = \tau = j_i - l_i$ , and these are localized in total angular momentum space about the value  $l_c + \tau$ .

On the strength of these considerations we make the approximation

$$R_{l_f + \tau, l_f, l_i + \tau, l_i}^{(N)L}(k_f, k_i) = -i \frac{\pi \hbar^2}{\mu} \delta_L^{(N)} \left[ \frac{\partial S_{l_f + \tau, l_f}^{(N)}(k_f)}{\partial l_f} \frac{\partial S_{l_i + \tau, l_i}^{(N)}(k_i)}{\partial l_i} \right]^{\frac{1}{2}} \quad (5.16)$$

which is equivalent to eq. (5.14) when  $l_f = l_i$  and  $k_f = k_i$ . With  $\tau = 0$  eq. (5.16) reduces to an approximation due to Hahne<sup>7,24)</sup> for the inelastic scattering of spin-0 projectiles.

We now evaluate the inelastic scattering amplitudes  $T_{LM\tau}^{(\pm)}(\theta)$  (eq. (3.42)) using methods similar to those used in ref.<sup>7)</sup> in the evaluation of the corresponding amplitudes  $T_{LM}^{(\pm)}(\theta)$ , and analogous to the methods used in section 4 for the elastic scattering amplitudes  $f_{\tau}^{(\pm)}(\theta)$ .

As we are dealing with inelastic heavy ion scattering near and above the Coulomb barrier and with excitation of low-lying collective states, we have  $k \approx k_i \approx k_f$ . We therefore replace  $k_i$  and  $k_f$  by  $k$  wherever they appear, except in the expression for the adiabaticity parameter  $\xi$  (eq. (5.7)). From eqs. (5.1), (5.3) and (5.5) we therefore have

$$R_{l_f + \tau, l_f, l_i + \tau, l_i}^{(C)L}(k_f, k_i) \approx \delta_L^{(C)} \frac{3}{2L+1} \left( \frac{k R_C}{n} \right)^{L-1} \frac{\pi \hbar^2}{\mu} \left[ S_{l_f + \tau, l_f}^{(N)}(k) S_{l_i + \tau, l_i}^{(N)}(k) \right]^{\frac{1}{2}} I_{L, l_f - l_i}(\vartheta, \xi). \quad (5.17)$$

Combining eqs. (3.23), (5.16) and (5.17), we make the following replacements in eq. (3.43),

$$R_{\ell_f \mp \tau \ell_f \ell_f \mp M \mp \tau \ell_f \mp M}^L(k_f, k_i) \rightarrow \frac{\pi k^2}{\mu} \left\{ \delta_L^C \frac{3}{2L+1} \left( \frac{k R_c}{n} \right)^{L-1} I_{L \pm M}(\vartheta, \xi) S_{\ell_f \mp \tau \ell}^{(N)}(k) - i \delta_L^{(N)} \frac{\partial S_{\ell_f \mp \tau \ell}(k)}{\partial \ell} \right\}, \quad (5.18)$$

$$\exp \left\{ i \left[ \sigma_{\ell_f}(k_f) + \sigma_{\ell_f \mp M}(k_i) \right] \right\} \rightarrow \exp \left[ i 2 \sigma_{\ell}(k) \right], \quad (5.19)$$

where  $\ell = \frac{1}{2}(\ell_i + \ell_f) = \ell_f \mp \frac{1}{2}M$  and  $S_{j\ell}^{(N)}(k)$  is now an average of the elastic scattering matrices for the entrance and exit channels.

We next replace the summation over  $\ell_f$  in eq. (3.43) by an integral over the continuous variable  $\lambda = \lambda_f \mp \frac{1}{2}M$  and make the replacements

$$\frac{\partial S_{\ell_f \mp \tau \ell}^{(N)}}{\partial \ell} \rightarrow \frac{\partial S_{\mp \tau}^{(N)}(\lambda)}{\partial \lambda}, \quad S_{\ell_f \mp \tau \ell}^{(N)} \rightarrow S_{\mp \tau}^{(N)}(\lambda), \quad e^{i 2 \sigma_{\ell}} \rightarrow e^{i 2 \sigma(\lambda)}, \quad (5.20)$$

in analogy with the interpolating functions of section 4.

Equation (3.43) then becomes

$$T_{LM\tau}^{(\pm)}(\theta) = \frac{k^2}{\mu(2s \sin \theta)^{\frac{1}{2}}} e^{i \frac{1}{2}M(\pi - \theta)} d_{0M}^L\left(\frac{1}{2}\pi\right) \int_0^{\infty} d\lambda \lambda^{\frac{1}{2}} b_{L \pm M \pm \tau}(\lambda) e^{i \varphi_{\pm}(\lambda, \theta)}, \quad (5.21)$$

where  $\varphi_{\pm}(\lambda, \theta)$  is given by eq. (4.27) and

$$b_{L \pm M \pm \tau}(\lambda) = N_{L \pm \tau}(\lambda) + C_{L \pm M \pm \tau}(\lambda), \quad (5.22)$$

where

$$N_{L\pm\tau}(\lambda) = -i\delta_L^{(N)} \frac{\partial S_{\mp\tau}^{(N)}(\lambda)}{\partial\lambda}, \quad (5.23)$$

$$C_{L\pm M\pm\tau}(\lambda) = \delta_L^{(C)} \frac{3}{2L+1} \left(\frac{kR_C}{n}\right)^{L-1} S_{\mp\tau}^{(N)}(\lambda) I_{L\pm M}(\vartheta, \xi) \quad (5.24)$$

refer to nuclear and Coulomb excitation respectively. By comparison with eq. (4.15) we write

$$S_{\tau}^{(N)}(\lambda) = \eta_c(\lambda) \exp\{i2[\delta_c^{(N)}(\lambda) + \tau\delta_s(\lambda)]\} = S_c^{(N)}(\lambda) \exp[i2\tau\delta_s(\lambda)]. \quad (5.25)$$

Because of assumption IV of section 4, we expand  $\exp[i2\tau\delta_s(\lambda)]$  only up to first order in  $\delta_s(\lambda)$ . This amounts to ignoring second-order projectile-spin-orbit coupling effects in the distorted waves. As for elastic scattering, this approximation is sufficient for calculating the differential cross section  $\sigma_L(\theta)$  and the vector analyzing power  $A_Z^L(\theta)$ . We can therefore write

$$N_{L\pm\tau}(\lambda) = N_L^{(C)}(\lambda) \mp \tau N_L^{(S)}(\lambda), \quad (5.26)$$

$$C_{L\pm M\pm\tau}(\lambda) = S_c^{(N)}(\lambda) C_{L\pm M}(\lambda) [1 \mp i2\tau\delta_s(\lambda)], \quad (5.27)$$

where

$$N_L^{(C)}(\lambda) = -i\delta_L^{(N)} \frac{\partial S_c^{(N)}(\lambda)}{\partial\lambda} = -i\delta_L^{(N)} D_c^{(N)}(\lambda), \quad (5.28)$$

$$N_L^{(s)}(\lambda) = 2 \delta_L^{(N)} \frac{\partial}{\partial \lambda} \left[ S_c^{(N)}(\lambda) \delta_s(\lambda) \right], \quad (5.29)$$

$$C_{L \pm M}(\lambda) = c_L I_{L \pm M}(\theta, \xi), \quad (5.30)$$

where  $D_c^{(N)}(\lambda)$  is defined by eq. (4.29) and

$$c_L = \delta_L^{(c)} \frac{3}{2L+1} \left( \frac{k R_c}{n} \right)^{L-1}. \quad (5.31)$$

It is convenient to work with the amplitudes  $B_{LM\tau}^{(\pm)}$  defined by eq. (3.48). From eq. (5.21) these are given by

$$B_{LM\tau}^{(\pm)} = \frac{y_{LM}(\theta)}{(2\pi \sin \theta)^{\frac{1}{2}}} \int_0^\infty d\lambda \lambda^{\frac{1}{2}} b_{L \pm M \pm \tau}(\lambda) e^{i\varphi_{\pm}(\lambda, \theta)}, \quad (5.32)$$

where

$$y_{LM}(\theta) = \frac{1}{(4\pi)^{\frac{1}{2}}} e^{i\frac{1}{2}M(\pi-\theta)} d_{0M}^L(\frac{1}{2}\pi) \quad (5.33)$$

$$= \frac{1}{(2L+1)^{\frac{1}{2}}} Y_{LM}(\frac{1}{2}\pi, 0) e^{i\frac{1}{2}M(\pi-\theta)}. \quad (5.34)$$

Substituting eqs. (5.22), (5.26) and (5.27) into eq. (5.32), we can write, in symbolic notation,

$$B_{LM\tau}^{(\pm)} = B_{LM}^{(c, \pm)}(N) + B_{LM}^{(c, \pm)}(cs) \pm \tau B_{LM}^{(s, \pm)}(N) \pm \tau B_{LM}^{(s, \pm)}(cs), \quad (5.35)$$

where

$$B_{LM}^{(c, \pm)}(N) = \frac{y_{LM}(\theta)}{(2\pi \sin \theta)^{\frac{1}{2}}} \int_0^\infty d\lambda \lambda^{\frac{1}{2}} N_L^{(c)}(\lambda) e^{i\varphi_{\pm}(\lambda, \theta)}, \quad (5.36)$$

$$B_{LM}^{(c,\pm)}(CS) = \frac{y_{LM}(\theta)}{(2\pi \sin\theta)^{\frac{1}{2}}} \int_0^\infty d\lambda \lambda^{\frac{1}{2}} C_{L\pm M}(\lambda) S_c^{(N)}(\lambda) e^{i\varphi_{\pm}(\lambda,\theta)}, \quad (5.37)$$

$$B_{LM}^{(s,\pm)}(N) = -\frac{y_{LM}(\theta)}{(2\pi \sin\theta)^{\frac{1}{2}}} \int_0^\infty d\lambda \lambda^{\frac{1}{2}} N_L^{(s)}(\lambda) e^{i\varphi_{\pm}(\lambda,\theta)}, \quad (5.38)$$

$$B_{LM}^{(s,\pm)}(CS) = -i2 \frac{y_{LM}(\theta)}{(2\pi \sin\theta)^{\frac{1}{2}}} \int_0^\infty d\lambda \lambda^{\frac{1}{2}} C_{L\pm M}(\lambda) \delta_s(\lambda) S_c^{(N)}(\lambda) e^{i\varphi_{\pm}(\lambda,\theta)}. \quad (5.39)$$

Equations (5.36-38) give the amplitudes for the central part of the nuclear excitation, Coulomb excitation and the first order spin orbit part of the nuclear excitation respectively. Equation (5.39) gives, to first order, the spin orbit correction to the amplitude for Coulomb excitation.

Because of conditions I-IV, given in section 4, on the functions  $S_c^{(N)}(\lambda)$  and  $\delta_s(\lambda)$ , the functions  $N_L^{(c)}(\lambda)$  and  $N_L^{(s)}(\lambda)$ , defined by eqs. (5.28) and (5.29), are sharply peaked in  $\lambda$ -space at the points  $\lambda = \Lambda$  and  $\lambda = \bar{\Lambda}$  respectively. The product  $C_{L\pm M}(\lambda) \delta_s(\lambda) S_c^{(N)}(\lambda)$  is also sharply peaked at  $\lambda = \bar{\Lambda}$  since the  $\lambda$ -dependence of the function  $I_{L\pm M}(\vartheta, \xi)$  is slow compared with that of  $S_c^{(N)}(\lambda)$  and  $\delta_s(\lambda)$ . We may therefore expand the phase function  $\varphi_{\pm}(\lambda, \theta)$  about  $\lambda = \Lambda$  to first order and integrate to get, from eq. (5.36),

$$B_{LM}^{(c,\pm)}(N) = -i \delta_L^{(N)} y_{LM}(\theta) \kappa(\theta) e^{i\varphi_{\pm}(\Lambda, \theta)} \mathfrak{F}[\Delta(\theta_R \mp \theta)], \quad (5.40)$$

where  $\kappa(\theta)$  is defined by eq. (4.76) and  $\mathfrak{F}(\Delta z)$  is defined by eq. (4.31).

From eq. (5.38), after expanding  $\varphi_{\pm}(\lambda, \theta)$  to first order

about  $\lambda = \bar{\lambda}$ , we obtain

$$B_{LM}^{(s,\pm)}(N) = -y_{LM}(\theta) \bar{\kappa}(\theta) e^{i\varphi_{\pm}(\bar{\lambda},\theta)} \int_{-\infty}^{\infty} d\lambda N_L^{(s)}(\lambda) e^{i(\lambda-\bar{\lambda})(\bar{\theta}_R \mp \theta)} \quad (5.41)$$

$$= i2 \delta_L^{(N)} y_{LM}(\theta) \bar{\kappa}(\theta) e^{i\varphi_{\pm}(\bar{\lambda},\theta)} (\bar{\theta}_R \mp \theta) \int_{-\infty}^{\infty} d\lambda S_c^{(N)}(\lambda) \delta_S(\lambda) e^{i(\lambda-\bar{\lambda})(\bar{\theta}_R \mp \theta)} \quad (5.42)$$

$$= i2 \delta_L^{(N)} y_{LM}(\theta) \bar{\kappa}(\theta) e^{i\varphi_{\pm}(\bar{\lambda},\theta)} (\bar{\theta}_R \mp \theta) G(\bar{\theta}_R \mp \theta) , \quad (5.43)$$

where  $\bar{\kappa}(\theta)$  and  $G(z)$  are defined by eqs. (4.76) and (4.68) respectively. Similarly, from eq. (5.39),

$$B_{LM}^{(s,\pm)}(cs) = -i2 y_{LM}(\theta) \bar{\kappa}(\theta) C_{L\pm M}(\bar{\lambda}) e^{i\varphi_{\pm}(\bar{\lambda},\theta)} G(\bar{\theta}_R \mp \theta) . \quad (5.44)$$

In order to evaluate the integral in eq. (5.37) for the near-side (+) amplitude, it is necessary to distinguish between the "illuminated" and "shadow" angular regions as follows:

$$B_{LM}^{(c,+)}(cs) = \begin{cases} B_{LM}^{(c,+)}(c) + B_{LM}^{(c,+)}(c[s-1]) & \theta \leq \theta_R \\ B_{LM}^{(c,+)}(cs) & \theta \geq \theta_R \end{cases} \quad (5.45)$$

where

$$B_{LM}^{(c,+)}(c) = \frac{y_{LM}(\theta)}{(2\pi \sin \theta)^{\frac{1}{2}}} \int_0^{\infty} d\lambda \lambda^{\frac{1}{2}} C_{LM}(\lambda) e^{i\varphi_+(\lambda,\theta)} , \quad (5.46)$$

$$B_{LM}^{(c,+)}(c[S-1]) = \frac{y_{LM}(\theta)}{(2\pi \sin \theta)^{\frac{1}{2}}} \int_0^{\infty} d\lambda \lambda^{\frac{1}{2}} C_{LM}(\lambda) [S_c^{(N)}(\lambda)-1] e^{i\varphi_+(\lambda,\theta)}. \quad (5.47)$$

The amplitudes  $B_{LM}^{(c,+)}(C)$ ,  $B_{LM}^{(c,+)}(C[S-1])$  and  $B_{LM}^{(c,\pm)}(CS)$  are similar to the amplitudes  $B_{LM}^{(+)}(E)$ ,  $B_{LM}^{(+)}(E[\eta-1])$  and  $B_{LM}^{(\pm)}(E\eta)$  respectively of ref. 7), except for the replacements

$$E_{L\pm M}(\lambda) \rightarrow C_{L\pm M}(\lambda), \quad \eta(\lambda) \rightarrow S_c^{(N)}(\lambda), \quad \phi_{\pm}(\lambda,\theta) \rightarrow \varphi_{\pm}(\lambda,\theta), \quad (5.48)$$

the last two of which are discussed in section 4.

By the methods of refs. 6, 7, 8) we obtain

$$B_{LM}^{(c,+)}(C) = ik y_{LM}(\theta) C_{LM}(\lambda_{\theta}) f_R(\theta), \quad (5.49)$$

where  $f_R(\theta)$  and  $\lambda_{\theta}$  are defined by eqs. (4.36) and (4.56) respectively;

$$B_{LM}^{(c,+)}(C[S-1]) = iy_{LM}(\theta) \kappa(\theta) C_{LM}(\lambda) G_{LM}(\theta_R - \theta) e^{i\varphi_+(\lambda,\theta)} \mathcal{J}[\Delta(\theta_R - \theta)] \quad \theta \leq \theta_R, \quad (5.50)$$

$$B_{LM}^{(c,+)}(CS) = iy_{LM}(\theta) \kappa(\theta) C_{LM}(\lambda) G_{LM}(\theta - \theta_R) e^{i\varphi_+(\lambda,\theta)} \mathcal{J}[\Delta(\theta_R - \theta)] \quad \theta \geq \theta_R, \quad (5.51)$$

$$B_{LM}^{(c,-)}(CS) = iy_{LM}(\theta) \kappa(\theta) C_{L-M}(\lambda) (\theta_R + \theta)^{-1} e^{i\varphi_-(\lambda,\theta)} \mathcal{J}[\Delta(\theta_R + \theta)], \quad (5.52)$$

where

$$G_{LM}(\pm x) = \mp \gamma(\pm u_0) [1 - x a_{LM}^{(1)}] - a_{LM}^{(0)}, \quad (5.53)$$

where

$$x = \theta - \theta_R, \quad u_0 = \frac{x e^{i\frac{1}{4}\pi}}{[-2\Theta_R^1(\lambda)]^{\frac{1}{2}}}, \quad (5.54)$$

$$a_{LM}^{(0)} = a_0 + e_{LM}, \quad a_{LM}^{(1)} = a_1 + e_{LM}, \quad (5.55)$$

with  $\gamma(u_0)$ ,  $a_0$  and  $a_1$  defined by eqs. (4.48), (4.49) and (4.50) respectively, and

$$e_{LM} = -\frac{1}{\Theta_R^1(\lambda)} \frac{C_{LM}^1(\lambda)}{C_{LM}(\lambda)}. \quad (5.56)$$

It can be shown<sup>7)</sup> that for large values of  $|x|$ ,

$$G_{LM}(|x|) \sim |x|^{-1}. \quad (5.57)$$

We summarize the results of this section as follows:

Using eqs. (3.47), (5.35) and (5.45) we write

$$B_{LM\gamma}(\theta) = B_{LM\gamma}^{(+)}(\theta) + (-1)^M B_{LM\gamma}^{(-)}(\theta) \quad (5.58)$$

$$= B_{LM}^{(c)}(\theta) + \gamma B_{LM}^{(s)}(\theta), \quad (5.59)$$

where

$$\begin{aligned} B_{LM}^{(c)}(\theta) = & B_{LM}^{(c,+)}(N) + B_{LM}^{(c,+)}(C) + B_{LM}^{(c,+)}(C[S-1]) \\ & + (-1)^M B_{LM}^{(c,-)}(N) + (-1)^M B_{LM}^{(c,-)}(CS) \quad \theta \leq \theta_R, \quad (5.60) \end{aligned}$$

$$B_{LM}^{(c)}(\theta) = B_{LM}^{(c,+)}(N) + B_{LM}^{(c,+)}(CS) + (-1)^M B_{LM}^{(c,-)}(N) + (-1)^M B_{LM}^{(c,-)}(CS) \quad \theta \geq \theta_R, \quad (5.61)$$

$$B_{LM}^{(s)}(\theta) = B_{LM}^{(s,+)}(N) + B_{LM}^{(s,+)}(CS) - (-i)^M B_{LM}^{(s,-)}(N) - (-i)^M B_{LM}^{(s,-)}(CS) \quad \forall \theta, \quad (5.62)$$

The amplitude  $B_{LM}^{(c)}(\theta)$  is the total inelastic scattering amplitude for spin-0 projectiles, while  $B_{LM}^{(s)}$  is the total first-order correction term due to spin-orbit coupling for the projectile spin.

From eqs. (3.45), (3.46) and (5.59) we now have for the total differential cross section for inelastic scattering of multipolarity  $L$ ,

$$\sigma_L(\theta) = \frac{1}{2s+1} \sum_{M,\tau} \left| B_{LM}^{(c)}(\theta) + \tau B_{LM}^{(s)}(\theta) \right|^2 \quad (5.63)$$

$$= \sum_M \left| B_{LM}^{(c)}(\theta) \right|^2 + \frac{1}{3} s(s+1) \sum_M \left| B_{LM}^{(s)}(\theta) \right|^2 \quad (5.64)$$

From eqs. (3.58) and (5.59) we have for the corresponding vector analyzing power,

$$A_{\tau}^L(\theta) = \frac{1}{s(2s+1)\sigma_L(\theta)} \sum_{M,\tau} \tau \left| B_{LM}^{(c)}(\theta) + \tau B_{LM}^{(s)}(\theta) \right|^2 \quad (5.65)$$

$$= \frac{2}{3}(s+1) \frac{1}{\sigma_L(\theta)} \sum_M \operatorname{Re} \left[ B_{LM}^{(c)}(\theta) B_{LM}^{(s)*}(\theta) \right] \quad (5.66)$$

## 6. PARAMETRIC MODEL OF THE SCATTERING FUNCTION

### 6.1 Elastic scattering function

In order to analyze experimental data using the results of sections 4 and 5, we have to evaluate the functions  $\mathcal{F}(\Delta z)$  (eq. (4.31)) and  $G(z)$  (eq. (4.68)) for a specific form of the scattering function  $S_\tau(\lambda)$ .

Recall from eqs. (4.14) and (4.15) that we write

$$S_\tau(\lambda) = \eta_c(\lambda) \exp\{i2[\sigma(\lambda) + \delta_c^{(N)}(\lambda) + \tau \delta_s(\lambda)]\} \quad (6.1)$$

$$= S_c^{(N)}(\lambda) \exp\{i2[\sigma(\lambda) + \tau \delta_s(\lambda)]\}, \quad (6.2)$$

where the function  $S_\tau(\lambda)$  interpolates the elastic S-matrix  $S_{j\ell}$  (eq. (4.2)). In view of conditions I and III given in section 4, it would be convenient to parameterize the functions  $\eta_c(\lambda)$  and  $\delta_c^{(N)}(\lambda)$  by

$$\eta_c(\lambda) = [1 + \exp(\frac{\Lambda - \lambda}{\Delta})]^{-1}, \quad 2\delta_c(\lambda) = \alpha [1 + \exp(\frac{\lambda - \Lambda}{\Delta})]^{-1}. \quad (6.3)$$

This parameterization is given by McIntyre et al.<sup>25)</sup> and for small values of  $\alpha$  it is equivalent to the Strong Absorption Model (SAM) of ref.<sup>2)</sup>.

From eq. (4.37) the quantal deflection function  $\Theta_c(\lambda)$  may be written as

$$\Theta_c(\lambda) = \Theta_R(\lambda) + \Theta_c^{(N)}(\lambda), \quad (6.4)$$

where

$$\Theta_R(\lambda) = 2 \frac{d\sigma(\lambda)}{d\lambda} \quad (6.5)$$

is the Rutherford deflection function, and from eq. (6.3),

$$\Theta_C^{(N)}(\lambda) = 2 \frac{d\delta_C^{(N)}(\lambda)}{d\lambda} = \alpha \frac{d}{d\lambda} \left\{ \left[ 1 + \exp\left(\frac{\lambda - \Lambda}{\Delta}\right) \right]^{-1} \right\} \quad (6.6)$$

is the nuclear deflection function due to the central nuclear potentials. Thus for  $\alpha > 0$   $\Theta_C^{(N)}(\lambda)$  has a dip of "width"  $\Delta$  with a minimum value  $-\frac{1}{4}\alpha$  at the point  $\lambda = \Lambda$ . This corresponds to refraction due to a real, attractive nuclear potential. For  $\alpha < 0$   $\Theta_C^{(N)}(\lambda)$  has a peak which would correspond to dominant surface reflection. This may occur if the diffuseness of the real or imaginary part of the optical potential is very small compared with the local wave-number of the radial wave function at the nuclear surface.

In appendix IV it is shown that in the high-energy approximation (eqs. (4.9) and (4.10)) with a Woods-Saxon form for  $U_C(r)$  and a Thomas-Fermi form for  $U_S(r)$ , the parameterization (6.3) of  $\delta_C^{(N)}(\lambda)$  implies the following form for  $\delta_S(\lambda)$ :

$$\delta_S(\lambda) = 2\kappa\Delta_S \frac{\partial}{\partial\lambda} \left\{ \left[ 1 + \exp\left(\frac{\Lambda_S - \lambda}{\Delta_S}\right) \right]^{-1} \right\} . \quad (6.7)$$

We allow  $\delta_S(\lambda)$  to have a width  $\Delta_S$  and a critical  $\lambda$ -value  $\Lambda_S$  different from those of  $\delta_C^{(N)}(\lambda)$  and  $\eta_C(\lambda)$  since optical model calculations<sup>10, 26, 27, 28</sup>) indicate that the widths and radii

of the spin-orbit potential are less than those of the central potentials. We allow  $\kappa$  to be a complex constant since we expect the spin-orbit potential to modify the absorptive as well as the refractive effects of the central potentials. From condition IV of section 4 and eq. (6.7), we must have

$$|\kappa| \ll \frac{1}{S} . \quad (6.8)$$

In order to simplify the form of the function  $\mathfrak{J}(\Delta z)$  defined by eq. (4.31), we introduce the following parameterization<sup>13,29)</sup> of  $S_c^{(N)}(\lambda)$ , which is roughly equivalent to eqs. (6.3), namely

$$S_c^{(N)}(\lambda) = [1 + \exp(\frac{\Lambda - \lambda}{\Delta} - i\alpha)]^{-1} . \quad (6.9)$$

For small  $\alpha$  eq. (6.9) is equivalent to eqs. (6.3) and therefore also equivalent to the SAM and McIntyre forms. From eqs. (6.1), (6.2) and (6.9) we have in general

$$\eta_c(\lambda) = \left\{ 1 + 2(\cos \alpha) \exp(\frac{\Lambda - \lambda}{\Delta}) + \exp[2(\frac{\Lambda - \lambda}{\Delta})] \right\}^{-\frac{1}{2}} , \quad (6.10)$$

$$2\delta_c(\lambda) = \sin \alpha \left[ \cos \alpha + \exp(\frac{\lambda - \Lambda}{\Delta}) \right]^{-1} . \quad (6.11)$$

The functions  $\eta_c(\lambda)$  and  $\delta_c(\lambda)$  are monotonic for  $|\alpha| < \frac{1}{2}\pi$ . We restrict  $\alpha$  to the interval  $(-\frac{1}{2}\pi, \frac{1}{2}\pi)$ .

The function  $\mathfrak{J}(\Delta z)$  (eq. (4.31)) is evaluated in appendix V to give

$$\mathcal{J}(\Delta z) = \frac{\pi \Delta z}{\sinh(\pi \Delta z)} e^{\alpha \Delta z}. \quad (6.12)$$

Similarly, the function  $G(z)$  (eq. (4.68)) is evaluated in appendix VI.

The critical angle  $\theta_R$  is given by eqs. (4.41), from which it can be seen that  $\theta_R$  increases with increasing  $n/\Lambda$  and is therefore indicative of the strength of the Coulomb interaction. In the limit in which the Sommerfeld parameter  $n$  (eq. (4.13)) tends to zero for constant  $\Lambda$  (the  $\mathcal{N}$ -limit of ref. <sup>6)</sup>) we have therefore  $\theta_R \rightarrow 0$  and the "illuminated region" ( $\theta \leq \theta_R$ ) is unimportant. This corresponds either to the scattering of neutral particles or to the scattering of charged particles at higher energies. In contrast we have the  $\mathcal{C}$ -limit <sup>6)</sup> in which  $n \rightarrow \infty$  and  $\Lambda \rightarrow \infty$  with  $n/\Lambda$  (or  $\theta_R$ ) constant. This corresponds to the scattering of heavy ions at medium energies. In this case the illuminated region extends over an appreciable part of the angular distribution.

## 6.2 Elastic scattering amplitudes - illuminated region

Substituting eqs. (4.53) and (6.12) into eq. (4.73), we have

$$\begin{aligned} f_{\theta}(\theta) = f_R(\theta) + \frac{\pi \Delta}{k} \kappa(\theta) e^{\alpha \Delta \theta_R} \left\{ e^{i\varphi_+(\mathcal{L}, \theta)} \frac{e^{-\alpha \Delta \theta}}{\sinh[\pi \Delta (\theta_R - \theta)]} \right. \\ \left. + e^{i\varphi_-(\mathcal{L}, \theta)} \frac{e^{\alpha \Delta \theta}}{\sinh[\pi \Delta (\theta_R + \theta)]} \right\} \quad \theta_R - \theta \gg \mathcal{L}^{-1}. \quad (6.13) \end{aligned}$$

Since  $|\alpha| < \frac{1}{2} \pi$  we see that  $\theta_R$  and  $\Delta$  have the effect of damping the second term in the braces  $\{ \}$  relative to the first term

and causing the first term to become small as  $\theta \rightarrow 0$ . We therefore have approximately

$$f_0(\theta) \rightarrow f_R(\theta) \quad \text{i.e.} \quad \frac{\sigma_0(\theta)}{\sigma_R(\theta)} \rightarrow 1 \quad \text{as } \theta \rightarrow 0, \quad (6.14)$$

where  $\sigma_0(\theta)$  is defined by eq. (4.70).

Oscillatory structure in  $\sigma_0(\theta)$  comes from the interference between the first two terms on the right hand side of eq. (6.13) and these (Fresnel) oscillations are damped as  $\theta \rightarrow 0$  (see refs. <sup>6, 13</sup>). According to eq. (6.13) the parameter  $\alpha$  opposes or enhances the damping of the Fresnel oscillations towards smaller angles  $\theta$  depending on whether  $\alpha > 0$  (nuclear refraction) or  $\alpha < 0$  (predominance of surface reflection over nuclear refraction).

At the critical angle  $\theta_R$ , it can be shown<sup>6)</sup> that

$$\frac{\sigma_0(\theta_R)}{\sigma_R(\theta_R)} = \frac{1}{4} + O(\lambda^{-\frac{1}{2}}) \quad (6.15)$$

From eqs. (4.71), (4.75) and (VI.11), we see that the spin-orbit correction term  $\sigma_1(\theta)$  is largest in the vicinity of the angle  $\bar{\theta}_R$ , but  $\sigma_1(\theta_R) \ll \sigma_0(\theta_R)$  since  $|\kappa| \ll 1$ . Now  $\bar{\theta}_R \geq \theta_R$  since  $\bar{\Lambda} \gtrsim \Lambda$  so, in the illuminated region,  $\sigma_0(\theta) \rightarrow \sigma_R(\theta)$  as  $\theta \rightarrow 0$  while  $\sigma_1(\theta) \rightarrow 0$  thereby becoming even more insignificant. For the purposes of this discussion we therefore ignore  $\sigma_1(\theta)$  in the illuminated region.

Similarly, from eq. (4.72), one can see that  $A_z(\theta) = O(|\kappa|)$  and that  $A_z(\theta) \rightarrow 0$  as  $\theta \rightarrow 0$ . This is confirmed by the experimental data in which, in all cases, the vector analyzing

power  $A_z(\theta)$  is several orders of magnitude less than unity in this angular region. However, there is some oscillatory structure and this is discussed below.

Since the illuminated region is of particular interest when the Coulomb interaction is strong, we consider the case when  $\theta_R$  is large enough so that, for  $0 < \theta \lesssim \theta_R$ ,

$$\mathcal{J}[\Delta(\theta_R - \theta)] \gg \mathcal{J}[\Delta(\theta_R + \theta)], \quad G[\Delta(\bar{\theta}_R - \theta)] \gg G[\Delta(\theta_R + \theta)]. \quad (6.16)$$

We further approximate  $f_0(\theta)$  in the angular region  $\theta_R - \theta \gg \Lambda^{-1}$  by  $f_R(\theta)$ . From eqs. (4.72) and (4.67) we therefore have approximately

$$A_z(\theta) = -\frac{1}{\sigma_R(\theta)} \frac{4}{3}(s+1) \frac{\bar{k}(\theta)}{k} \operatorname{Re} \left\{ f_R(\theta) e^{-i\varphi_+(\bar{\lambda}, \theta)} G^*(\bar{\theta}_R - \theta) \right\}$$

$$0 < \theta \ll \theta_R - \Lambda^{-1}. \quad (6.17)$$

Using eq. (4.55), the Rutherford scattering amplitude can be written as (c.f. ref.<sup>8</sup>)

$$f_R(\theta) = -\frac{\lambda}{k(\sin \theta)^{\frac{1}{2}}} C_+(\theta, \theta_\Lambda) \exp \left\{ i \left[ \varphi_+(\lambda, \theta) + u^2 + \frac{1}{4}\pi \right] \right\}, \quad (6.18)$$

where

$$u = \frac{\theta - \theta_R}{[-2\Theta_R^1(\lambda)]^{\frac{1}{2}}}, \quad (6.19)$$

and where  $C_+(\theta, \theta_\Lambda)$  is defined in ref.<sup>8</sup>. Since  $C_+(\theta, \theta_\Lambda)$  is a slowly varying function of  $\theta$ , we replace it by its value at

$\theta = \theta_\Lambda$ , giving

$$C_+(\theta, \theta_\Lambda) \approx [-\Lambda \Theta'_R(\Lambda)]^{-\frac{1}{2}}. \quad (6.20)$$

Combining eqs. (6.17-20) and taking  $\varphi_+(\bar{\Lambda}, \theta) = \varphi_+(\Lambda, \theta)$ , since  $\bar{\Lambda} \approx \Lambda$ , we have

$$A_z(\theta) \approx \frac{1}{\sigma_R(\theta)} \frac{4}{3} (s+1) \frac{\bar{\kappa}(\theta)}{k[-\Lambda \Theta'_R(\Lambda)]^{\frac{1}{2}}} \frac{\Lambda}{k(\sin \theta)^{\frac{1}{2}}} \\ \times \left\{ \text{Re} \left[ G^*(\theta_R - \theta) \exp(iu^2 + i\frac{1}{4}\pi) \right] \right\} \quad 0 < \theta \ll \theta_R - \Lambda^{-1}. \quad (6.21)$$

The term in braces { }, because of the exponent of argument  $i(u^2 + \frac{1}{4}\pi)$ , gives oscillations of Fresnel type similar to those that appear in the differential cross section. (This has already been shown for spin- $\frac{1}{2}$  particles<sup>3</sup>.)

### 6.3 Elastic scattering amplitudes - shadow region

Substituting eqs. (4.53) and (4.74) into eq. (4.70), we have

$$\sigma_0(\theta) = \frac{\kappa^2(\theta)}{k^2} \left| \left\{ \frac{\mathfrak{F}[\Delta(\theta_R - \theta)]}{\theta_R - \theta} e^{i\varphi_+(\Lambda, \theta)} + \frac{\mathfrak{F}[\Delta(\theta_R + \theta)]}{\theta_R + \theta} e^{i\varphi_-(\Lambda, \theta)} \right\} \right|^2 \quad \theta - \theta_R \gg \Lambda^{-1} \quad (6.22)$$

Substituting eq. (6.12) into (6.22) gives

$$\sigma_0(\theta) = \left( \frac{\pi \Delta}{k} \right)^2 \kappa^2(\theta) e^{2\alpha \Delta \theta_R} \left| \left\{ \frac{e^{-\alpha \Delta \theta}}{\sinh[\pi \Delta(\theta - \theta_R)]} e^{i\varphi_+(\Lambda, \theta)} - \frac{e^{\alpha \Delta \theta}}{\sinh[\pi \Delta(\theta + \theta_R)]} e^{i\varphi_-(\Lambda, \theta)} \right\} \right|^2 \quad \theta - \theta_R \gg \Lambda^{-1}. \quad (6.23)$$

For  $\pi\Delta |\theta - \theta_R| > 1$  eq. (6.23) gives

$$\sigma_0(\theta) \approx \left(\frac{\pi\Delta}{k}\right)^2 \kappa^2(\theta) e^{2\alpha\Delta\theta_R} e^{-2\pi\Delta\theta}$$

$$\left| \left\{ e^{\Delta(\pi\theta_R - \alpha\theta)} e^{i\varphi_+(\lambda, \theta)} - e^{-\Delta(\pi\theta_R - \alpha\theta)} e^{i\varphi_-(\lambda, \theta)} \right\} \right|^2 \quad \theta - \theta_R \gg \lambda^{-1}. \quad (6.24)$$

From eqs. (4.71) and (4.75) we have

$$\sigma_1(\theta) = \frac{4}{3} s(s+1) \left(\frac{\bar{\kappa}(\theta)}{k}\right)^2 \left| \left\{ G(\bar{\theta}_R - \theta) e^{i\varphi_+(\bar{\lambda}, \theta)} - G(\bar{\theta}_R + \theta) e^{i\varphi_-(\lambda, \theta)} \right\} \right|^2, \quad (6.25)$$

and from eqs. (4.72), (4.74) and (4.75),

$$A_z(\theta) = \frac{1}{\sigma(\theta)} \frac{4}{3} (s+1) \frac{\kappa(\theta) \bar{\kappa}(\theta)}{k^2}$$

$$\text{Re} \left\{ \left[ \frac{\mathcal{J}_+}{\theta - \theta_R} e^{i\varphi_+} - \frac{\mathcal{J}_-}{\theta + \theta_R} e^{i\varphi_-} \right] \left[ e^{i\bar{\varphi}_+} G_+ - e^{i\bar{\varphi}_-} G_- \right]^* \right\}, \quad (6.26)$$

where we have used the abbreviations

$$\mathcal{J}_\pm = \mathcal{J}[\Lambda(\theta_R \mp \theta)], \quad G_\pm = G(\bar{\theta}_R \mp \theta), \quad (6.27)$$

$$\varphi_\pm = \varphi_\pm(\lambda, \theta), \quad \bar{\varphi}_\pm = \varphi_\pm(\bar{\lambda}, \theta). \quad (6.28)$$

To simplify the discussion of  $\sigma_0(\theta)$ , we take only the term, in the expression (VI.11) for  $G(z)$ , that dominates at large values of  $|z|$ . From the asymptotic forms (VI.16) and (VI.17) we have, provided  $\Delta_S < \Delta$  or  $\alpha > 0$ ,

$$G(z) \sim 2\pi\kappa\Delta_S^2 z \frac{\exp[i(\lambda - \bar{\lambda} - \gamma\Delta_S)z \pm \pi\Delta_S z]}{1 + \exp\left[\frac{\gamma\Delta_S}{\Delta} + i\left(\pm\frac{\pi\Delta_S}{\Delta} - \alpha\right)\right]} \quad z \lesssim 0, \quad (6.29)$$

where

$$\gamma \equiv \frac{\lambda - \lambda_s}{\Delta_s} . \quad (6.30)$$

Equation (6.29) is only valid for integral values of  $\Delta/\Delta_s$ .

Using eq. (6.29), eq. (6.25) becomes

$$\sigma_1(\theta) = \frac{1}{3} s(s+1) |f_1(\theta)|^2 , \quad (6.31)$$

where

$$f_1(\theta) \sim - \frac{4\pi \kappa \Delta_s^2}{k} \bar{\kappa}(\theta) e^{-\pi \Delta_s \theta} \left\{ \begin{aligned} & (\bar{\theta}_R - \theta) \frac{\exp[-i(\lambda - \bar{\lambda} - \gamma \Delta_s)\theta + \pi \Delta_s \bar{\theta}_R + i\bar{\varphi}_+]}{1 + \exp\left[\frac{\gamma \Delta_s}{\Delta} + \left(\frac{\pi \Delta_s}{\Delta} - \alpha\right)\right]} \\ & - (\bar{\theta}_R + \theta) \frac{\exp[i(\lambda - \bar{\lambda} - \gamma \Delta_s)\theta - \pi \Delta_s \bar{\theta}_R + i\bar{\varphi}_-]}{1 + \exp\left[\frac{\gamma \Delta_s}{\Delta} - \left(\frac{\pi \Delta_s}{\Delta} + \alpha\right)\right]} \end{aligned} \right\} . \quad (6.32)$$

In eq. (6.32) we have dropped a constant overall phase factor and have used the abbreviations (6.28).

Concerning the differential cross section  $\sigma(\theta)$  and the vector analyzing power  $A_z(\theta)$ , we consider separately the following cases which are relevant to the analysis of the experimental data:

$$\text{case (a) : } e^{2\pi \Delta \theta_R} \gg 1 \quad \text{and} \quad e^{2\pi \Delta_s \bar{\theta}_R} \gg 1 \quad (6.33a)$$

$$\text{case (b) : } e^{2\pi \Delta \theta_R} \gg 1 \quad \text{and} \quad e^{2\pi \Delta_s \bar{\theta}_R} = o(1) \quad (6.33b)$$

$$\text{case (c) : } e^{2\pi \Delta \theta_R} = o(1) \quad \text{and} \quad e^{2\pi \Delta_s \bar{\theta}_R} = o(1) \quad (6.33c)$$

The features of the cross section ratio and the vector analyzing power that are characteristic of these three cases are discussed in more detail below and are illustrated in figs. 1 and 2. The curves are calculated using the formulae (4.69-75) with  $\mathcal{F}(\Delta z)$  and  $G(z)$  given by eqs. (V.9) and (VI.11) respectively and for various parameter values. Figures 1 and 2 are calculated assuming parameters characteristic of the Fresnel and Fraunhofer regions of elastic scattering respectively.

Case (a):

This corresponds to the  $C$ -limit of ref.<sup>6)</sup>. In this case the first term in braces { } in eqs. (6.23) or (6.24) dominates the second and  $\sigma_0(\theta)$  falls off, at sufficiently large angles, like  $\exp[-2(\pi + \alpha)\Delta\theta]$ .

Since  $|\kappa| \ll 1$ ,  $\sigma_1(\theta)$  is an order of magnitude less than  $\sigma_0(\theta)$  near the critical angle  $\theta_R$ . According to eqs. (6.31) and (6.32),  $\sigma_1(\theta)$  falls off at large angles like  $\exp(-2\pi\Delta_S\theta)$  so that if  $\Delta_S < \Delta$ ,  $\sigma_1(\theta)$  may become noticeable beyond some large angle, having the effect of decreasing the rate of fall-off of  $\sigma(\theta)$ . Up to this point, the ratio  $\sigma(\theta)/\sigma_R(\theta)$  has the characteristic form of a Fresnel diffraction pattern pattern<sup>6, 8, 13)</sup>.

If we take  $\sigma(\theta) \approx \sigma_0(\theta)$  and  $\Delta_S \approx \Delta$  in eq. (6.26) with  $\sigma_0(\theta)$ ,  $\mathcal{F}(\Delta z)$  and  $G(z)$  given by eqs. (6.24), (6.12) and (6.29) respectively, we get for the vector analyzing power

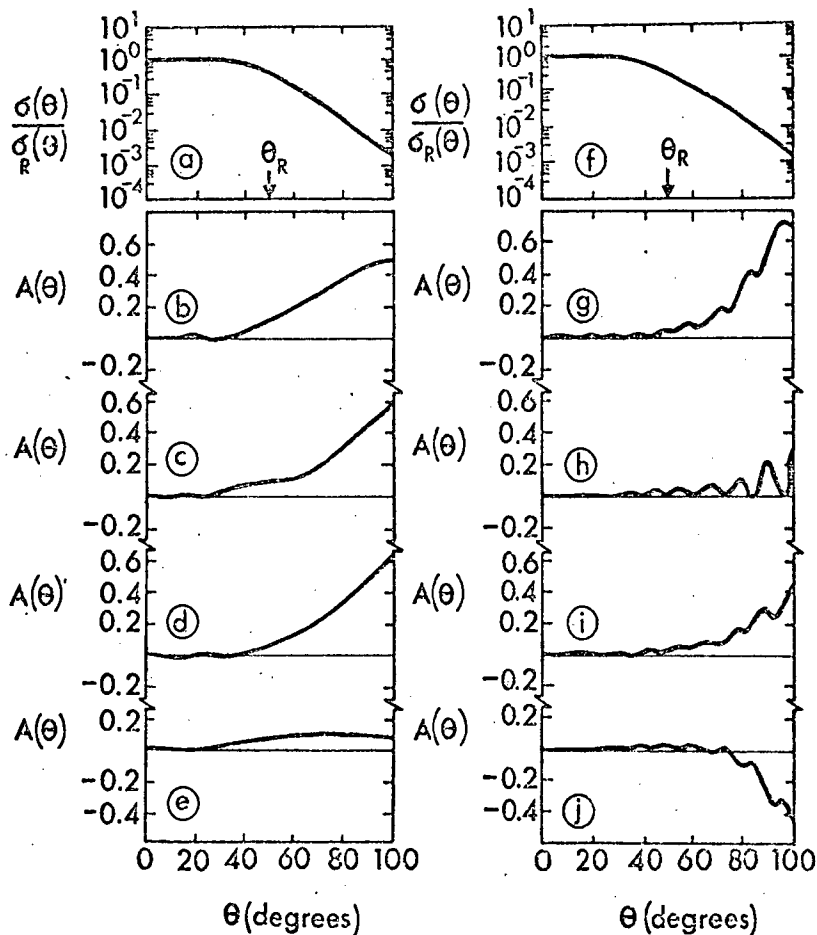


Fig. 1. Elastic scattering cross section ratio  $\sigma/\sigma_R$  and vector analyzing power  $A$  calculated from eqs. (4.69-75) using eqs. (6.12) and (VI.11) for various parameter values. Since  $\sigma/\sigma_R$  is similar for each case, it is shown only once at the top of each column. The common parameter values are  $\Lambda = 16.0$ ,  $\Delta = 1.5$  and  $\alpha = 0$ . The remaining parameters are tabulated below.

	(b)	(c)	(d)	(e)	(g)	(h)	(i)	(j)
$\Lambda_S$	16.0	16.0	14.5	14.5	16.0	16.0	14.5	14.5
$\kappa$	.2	.2i	.2	.2i	.2	.2i	.2	.2i
$\Delta_S$	1.5	1.5	1.5	1.5	.5	.5	.5	.5

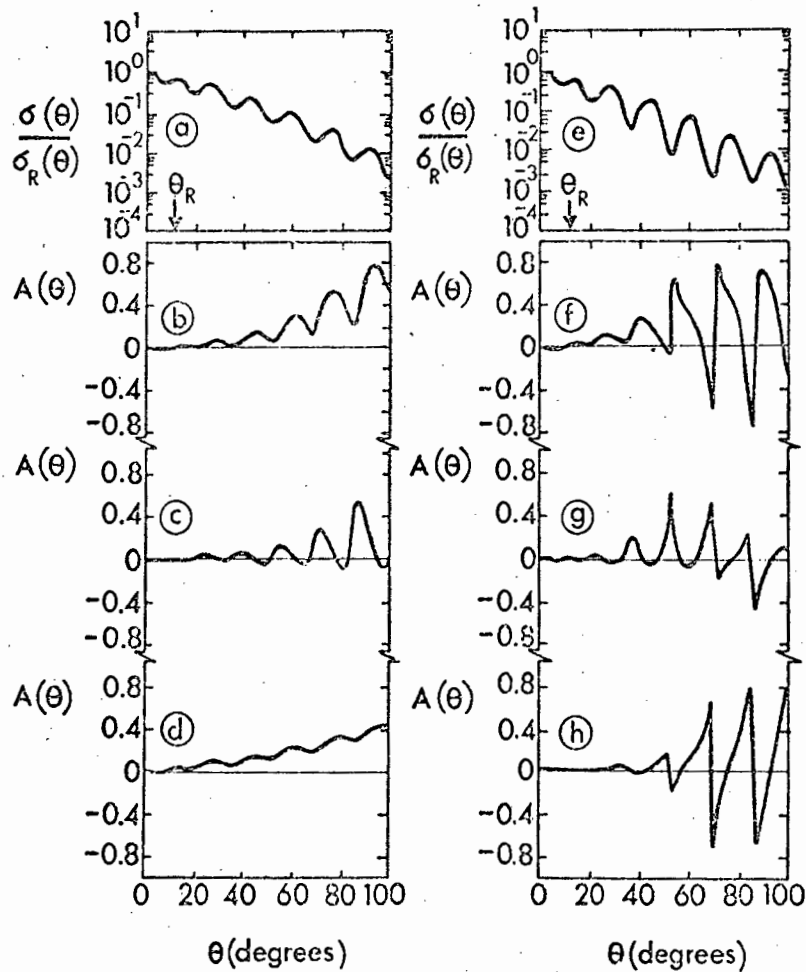


Fig. 2. Elastic scattering cross section ratio  $\sigma/\sigma_R$  and vector analyzing power  $A$  calculated from eqs. (4.69-75) using eqs. (6.12) and (VI.11) for various parameter values. Since  $\sigma/\sigma_R$  is similar for each of the cases (b)-(d) it is shown only once at the top of each column (similarly for cases (f)-(h)). The common parameter values are  $\Lambda = 11.0$  and  $\Delta = 1.0$ . The remaining parameters are tabulated below.

	(b)	(c)	(d)	(f)	(g)	(h)
$\alpha$	0	0	0	.5	.5	.5
$\Lambda_S$	11.0	11.0	10.0	11.0	11.0	10.0
$\Delta_S$	.5	.5	1.0	1.0	1.0	.5
$\kappa$	.1	.1i	.1	.1	.1i	.1

$$A_z(\theta) = \frac{4}{3}(s+1) \frac{\Delta_s^2}{\Delta} \left\{ \kappa_r + \kappa_i \tan \left[ \frac{1}{2} \left( \frac{\pi \Delta_s}{\Delta} - \alpha \right) \right] \right\} (\theta - \theta_R) \\ \times \exp \left\{ [(\pi + \alpha) \Delta - \pi \Delta_s] (\theta - \theta_R) \right\}, \quad (6.34)$$

where  $\kappa_r$  and  $\kappa_i$  are the real and imaginary parts of  $\kappa$  respectively. Equation (6.34) shows that beyond the critical angle  $\theta_R$ ,  $A_z(\theta)$  rises at least linearly with  $\theta$  and exponentially if  $\alpha > 0$  or  $\Delta_s < \Delta$ . This formula is valid only if  $\alpha > 0$  or  $\Delta_s < \Delta$  and only if  $\sigma_1(\theta) \ll \sigma_0(\theta)$ . Very large angles may therefore have to be excluded.

For  $\alpha = 0$ ,  $\Delta_s = \Delta$  and  $\Lambda_s = \Lambda$  we get, on substituting the exact expressions for  $\mathfrak{J}(\Delta z)$  (eq. (V.9)) and  $G(z)$  (eq. (VI.11)) into eq. (6.26),

$$A_z(\theta) = \frac{4}{3}(s+1) \Delta (\theta - \theta_R) [\kappa_r + \Delta \kappa_i (\theta - \theta_R)] \quad \theta - \theta_R \gg \Lambda^{-1}, \quad (6.35)$$

where we have approximated  $\sigma(\theta)$  by  $\sigma_0(\theta)$ .

These effects are illustrated in figs. 1(a-e) which show the vector analyzing power calculated assuming purely real and purely imaginary spin-orbit phase shifts, and for  $\Lambda_s = \Lambda$  and  $\Lambda_s < \Lambda$ .

Case (b):

This case is of interest when  $\Delta_s \bar{\theta}_R < \Delta \theta_R$  which implies that  $\Delta_s < \Delta$  since we expect to have  $\bar{\Lambda} \leq \Lambda$  i.e.  $\bar{\theta}_R \geq \theta_R$ . In this case  $\sigma_0(\theta)$  has the same form as in case (a), but in eq. (6.32) we see that the two terms in the braces  $\{ \cdot \}$  are of the

same order of magnitude. This implies that  $\sigma_1(\theta)$ , given by eq. (6.31), will show regular oscillations, of period  $\pi/(\Lambda - \gamma\Delta_S) = \pi/\Lambda_S$ , coming from the interference between the two components  $f_1^{(\pm)}(\theta)$  of  $f_1(\theta)$ . Similarly, from eq. (6.29) we see that the two terms  $G_{\pm} \exp(i\bar{\varphi}_{\pm})$  on the right hand side of eq. (6.26) will interfere to give similar oscillations in  $A_Z(\theta)$ . These are therefore also due to the interference between the components  $f_1^{(\pm)}(\theta)$ .

Recall from section 2 that the labels (+) and (-) refer respectively to the amplitudes for scattering from the near and far sides of the interaction region. We therefore conclude that in situations of type (b), the regular oscillations in  $\sigma_1(\theta)$  and  $A_Z(\theta)$ , in the shadow region, are of Fraunhofer type, and are due to the interference between the near- and far-side components of the spin-orbit correction term  $f_1(\theta)$  of the scattering amplitude.

As in case (a) the influence of  $\sigma_1(\theta)$  may only be noticeable at large angles and only if  $\Delta_S < \Delta$ . We consider in more detail the case in which  $\sigma_1(\theta) \ll \sigma_0(\theta)$ . The differential cross section  $\sigma(\theta)$  therefore has the same general form as in case (a), but from eqs. (6.24), (6.26) and (6.29), we obtain for the vector analyzing power,

$$A_Z(\theta) = \frac{4}{3}(s+1) \frac{\Delta_S^2}{\Delta} \exp[(\pi + \alpha)\Delta(\theta - \theta_R) - \pi\Delta_S\theta] \\ \times \left\{ (\theta - \theta_R) A e^{\pi\Delta_S\theta_R} - (\theta + \theta_R) e^{-\pi\Delta_S\theta_R} [B \sin(2\lambda\theta) + C \cos(2\lambda\theta)] \right\}, \quad (6.36)$$

where we have taken  $\Lambda_S \approx \Lambda$  and where

$$A = \kappa_r + \kappa_i \tan\left[\frac{1}{2}\left(\frac{\pi\Delta_s}{\Delta} - \alpha\right)\right], \quad B = \kappa_r - \kappa_i \tan\left[\frac{1}{2}\left(\frac{\pi\Delta_s}{\Delta} + \alpha\right)\right], \quad (6.37)$$

$$C = \kappa_i + \kappa_r \tan\left[\frac{1}{2}\left(\frac{\pi\Delta_s}{\Delta} + \alpha\right)\right],$$

where  $\kappa_r$  and  $\kappa_i$  are the real and imaginary parts of the spin-orbit coupling strength  $\kappa$  respectively. Equation (6.36) shows that  $A_z(\theta)$  is the same as in case (a) (eq. (6.34)), except for the two additional oscillatory terms of period  $\pi/\Lambda$ , which are damped relative to the non-oscillatory term by the factor  $[(\theta + \theta_R)/(\theta - \theta_R)] \exp(-2\pi\Delta_s \theta_R)$ .

These effects are illustrated in figs. 1(f-j). Over the angular range plotted, no oscillatory structure is visible in the differential cross section since  $\sigma_1(\theta) \ll \sigma_0(\theta)$ , but the Fraunhofer-type oscillations discussed above are seen in the vector analyzing power  $A_z(\theta)$ . For  $\theta < \theta_R$  one or more of the Fresnel-type oscillations discussed in subsection 6.2 are just visible in  $A_z(\theta)$ .

Figures 1(g) and 1(h) show the vector analyzing power calculated assuming purely real ( $\kappa_i = 0$ ) and purely imaginary ( $\kappa_r = 0$ ) spin-orbit phase shifts respectively. In agreement with the approximate formula (eqs. (6.36) and (6.37)), this affects the magnitude of the non-oscillatory term in eq. (6.36) while it mainly affects the phase of the oscillations coming from the second and third terms.

Case (c):

This corresponds to the  $\mathcal{R}$ -limit of ref.<sup>6</sup>). In this case we see the oscillations in  $\sigma_0(\theta)$  coming from the interference

between the two terms in the braces { } on the right hand side of eq. (6.24), since the factors  $\exp(\pm \pi \Delta \theta_R)$  are of the same order of magnitude, i.e. the Coulomb damping<sup>e)</sup> factor  $\exp(2\pi \Delta \theta_R)$  is small. The factors  $\exp(\mp \alpha \Delta \theta)$  in eq. (6.24) oppose or enhance<sup>†</sup> the Coulomb damping with increasing  $\theta$  depending on whether  $\alpha > 0$  (nuclear refraction) or  $\alpha < 0$  (predominance of surface reflection over nuclear refraction).

These effects are illustrated in fig. 2. A comparison of figs. 2(a) and 2(e) shows the effect of a positive value of  $\alpha$  when the Coulomb damping is still quite strong.

Figures 2(e-h) show the vector analyzing power to have a pronounced maximum or minimum wherever the differential cross section has a pronounced minimum. This can be seen from the formulae in the following special case:

For  $\Lambda_S = \Lambda$ ,  $\alpha = 0$ ,  $\Delta_S = \Delta$  and  $\theta_R = 0$ , we have from eq. (6.24)

$$\sigma_o(\theta) = 4 \left( \frac{\pi \Delta}{k} \right)^2 \kappa^2(\theta) e^{-2\pi \Delta \theta} \sin^2(\Lambda \theta - \frac{1}{4} \pi) \quad \theta \gg \Lambda^{-1}, \quad (6.38)$$

and from eqs. (6.26) and (VI.11),

$$A_z(\theta) = \frac{4}{3} (s+1) \kappa_r \Delta \theta [1 + \Delta \theta \cot(\Lambda \theta - \frac{1}{4} \pi)] \quad \theta \gg \Lambda^{-1} \quad (6.39)$$

where  $\kappa_r$  is the real part of  $\kappa$ .

Equations (6.38) and (6.39) agree with the general form

---

<sup>†</sup> We refer to ref.<sup>9)</sup> for a discussion of the influence of nuclear refraction and surface reflection on the differential cross section.

of  $\sigma(\theta)$  and  $A_z(\theta)$  illustrated in figs. 2(e) and 2(f) respectively, although in these plots the pronounced oscillations in  $\sigma(\theta)$  are due largely to the refractive parameter  $\alpha$  since the Coulomb damping factor  $\exp(2\pi\Delta\theta_R)$  is greater than unity. In agreement with fig. 2(g), eq. (6.39) shows that as  $\kappa_r \rightarrow 0$  the linear term in  $\theta$  vanishes and one is left only with the spikes of  $A_z(\theta)$  occurring at the zeros of  $\sigma(\theta)$ .

Figure 2(h) shows that having  $\Lambda_s < \Lambda$  may change the sign of the periodic part of  $A_z(\theta)$ .

#### 6.4 Inelastic scattering amplitudes

Due to the large number of terms comprising the inelastic scattering amplitude  $B_{LM\tau}(\theta)$  (eqs. (5.58-62)), we discuss the main features of  $\sigma_L(\theta)$  and  $A_z^L(\theta)$  in the asymptotic shadow region only, and under the condition that the nuclear excitation terms  $B_{LM}^{(c,+)}(N)$  and  $B_{LM}^{(s,+)}(N)$  dominate the Coulomb excitation terms  $B_{LM}^{(c,+)}(CS)$  and  $B_{LM}^{(s,+)}(CS)$  in this angular region. This condition applies in particular to the inelastic scattering data analyzed in section 7.

From eqs. (5.61), (5.62) and (5.64) we therefore have

$$\sigma_L(\theta) = \sigma_L^{(0)}(\theta) + \sigma_L^{(1)}(\theta) \quad \theta - \theta_R \gg \lambda^{-1}, \quad (6.40)$$

where

$$\sigma_L^{(0)}(\theta) = \sum_M \left| B_{LM}^{(c,+)}(N) + (-1)^M B_{LM}^{(c,-)}(N) \right|^2, \quad (6.41)$$

$$\sigma_L^{(1)}(\theta) = \frac{1}{3} s(s+1) \sum_M \left| B_{LM}^{(s,+)}(N) - (-1)^M B_{LM}^{(s,-)}(N) \right|^2, \quad (6.42)$$

while from eqs. (5.66), (5.61) and (5.62),

$$A_{\bar{z}}^L(\theta) = \frac{1}{\sigma_L(\theta)} \frac{2}{3} (s+1) \sum_M \left\{ \left[ B_{LM}^{(c,+)}(N) + (-1)^M B_{LM}^{(c,-)}(N) \right] \right. \\ \left. \times \left[ B_{LM}^{(s,+)}(N) - (-1)^M B_{LM}^{(s,-)}(N) \right]^* \right\}. \quad (6.43)$$

Substituting eqs. (5.34) and (5.40) into eq. (6.41) gives

$$\sigma_L^{(0)}(\theta) = \frac{1}{2L+1} \left[ \delta_L^{(N)} \kappa(\theta) \right]^2 \left[ \sum_M \left| \gamma_{LM}(\frac{1}{2}\pi, 0) \right|^2 \right] \\ \times \left| e^{i\varphi_+} \mathcal{J}_+ + (-1)^L e^{i\varphi_-} \mathcal{J}_- \right|^2 \quad \theta - \theta_R \gg \mathcal{L}^{-1}, \quad (6.44)$$

where we have used the abbreviations (6.27) and (6.28) and

where we have used the fact that  $\gamma_{LM}(\frac{1}{2}\pi, 0) = 0$  for  $L+M$  odd.

Substituting eqs. (5.34) and (5.43) into eq. (6.42) gives

$$\sigma_L^{(1)}(\theta) = \frac{4}{3} \frac{s(s+1)}{2L+1} \left[ \delta_L^{(N)} \bar{\kappa}(\theta) \right]^2 \left[ \sum_M \left| \gamma_{LM}(\frac{1}{2}\pi, 0) \right|^2 \right] \\ \times \left| e^{i\bar{\varphi}_+} (\bar{\theta}_R - \theta) \mathcal{G}_+ - (-1)^L e^{i\bar{\varphi}_-} (\bar{\theta}_R + \theta) \mathcal{G}_- \right|^2 \quad \theta - \theta_R \gg \mathcal{L}^{-1}. \quad (6.45)$$

Finally, from eqs. (6.43), (5.40) and (5.43), we have

$$A_{\bar{z}}^L(\theta) = \frac{1}{\sigma_L(\theta)} \frac{4}{3} \frac{s+1}{2L+1} \left[ \delta_L^{(N)} \right]^2 \kappa(\theta) \bar{\kappa}(\theta) \left[ \sum_M \left| \gamma_{LM}(\frac{1}{2}\pi, 0) \right|^2 \right] \\ \times \text{Re} \left\{ \left[ e^{i\varphi_+} \mathcal{J}_+ + (-1)^L e^{i\varphi_-} \mathcal{J}_- \right] \left[ e^{i\bar{\varphi}_+} (\theta - \bar{\theta}_R) \mathcal{G}_+ + (-1)^L e^{i\bar{\varphi}_-} (\bar{\theta}_R + \theta) \mathcal{G}_- \right]^* \right\} \\ \theta - \theta_R \gg \mathcal{L}^{-1}. \quad (6.46)$$

Equations (6.44), (6.45) and (6.46) bear a close resemblance to the expressions for the corresponding elastic scattering angular distributions  $\sigma_0(\theta)$  and  $\sigma_1(\theta)$  and the elastic vector analyzing power  $A_Z(\theta)$  given by eqs. (6.22), (6.25) and (6.26) respectively.

We compare these equations in the "neutral limit" (case (c) of subsection 6.3) since this is implied by the conditions of this section, namely that of dominance of the amplitudes for nuclear excitation over those for Coulomb excitation in the "shadow region". In this case the functions  $\sigma_L^{(0)}(\theta)$ ,  $\sigma_L^{(1)}(\theta)$  and  $A_Z^L(\theta)$  show the same general features as the functions  $\sigma_0(\theta)$ ,  $\sigma_1(\theta)$  and  $A_Z(\theta)$  respectively in the "shadow region", except that the factors  $(-1)^L$  in eqs. (6.44-46) cause the Fraunhofer oscillations to be in phase or out of phase with those of the corresponding expressions for elastic scattering, depending on whether  $L$  is odd or even respectively. For spin-0 projectiles this is the Blair phase rule<sup>7, 30</sup>). This relation has already been derived for spin- $\frac{1}{2}$  and spin-1 projectiles<sup>5</sup>).

Similarly, by comparing eqs. (3.52) and (2.51), the factor  $(-1)^M$  gives rise to the same phase rule for the tensor components of the analyzing powers for elastic and inelastic scattering.

## 7. ANALYSIS OF EXPERIMENTAL DATA

### 7.1 Analysis of elastic scattering data

At present the data that is available on polarization in elastic scattering of light ions other than nucleons and the deuteron is the data of the Birmingham group<sup>12)</sup> on the elastic scattering of polarized  $^3\text{He}$  ions, and the data of ref.<sup>31)</sup> on the scattering of polarized  $^3\text{H}$  ions. Recently it has also become possible to measure polarization in the elastic scattering of heavier ions. The Heidelberg group has determined the vector and tensor polarization of  $^6\text{Li}$  ions<sup>10,11,32)</sup> at 22.8 MeV, and has also provided preliminary data<sup>32)</sup> on the tensor analyzing power for the elastic scattering of  $^7\vec{\text{Li}} + ^{58}\text{Ni}$  at 23.2 MeV.

Of the light ion scattering data referred to above we have analyzed the cross section ratio and the vector analyzing power for the elastic scattering of  $^3\vec{\text{He}} + ^{26}\text{Mg}$  at 33.4 MeV<sup>†</sup>,  $^3\vec{\text{He}} + ^{27}\text{Al}$  at 29.6 MeV (cross section ratio<sup>††</sup>) and 33.1 MeV (analyzing power), and  $^3\text{He} + ^{58}\text{Ni}$  at 33.3 MeV. Of the data of the Birmingham group, it is only in the above cases that the number of partial waves involved is large enough for the conditions of our theory, given in section 4, to be applicable. In the case of the  $^3\text{He}$  data of ref.<sup>31)</sup>, there are too few partial waves involved since the energy is too low. Of the

---

† The differential cross section data is taken from ref.<sup>33)</sup>.

†† The differential cross section data is taken from ref.<sup>34)</sup>.

data of the Heidelberg group we have analyzed the cross section ratio<sup>†</sup> and the vector analyzing power for the elastic scattering of  ${}^6\vec{\text{Li}} + {}^{28}\text{Si}$  and  ${}^6\vec{\text{Li}} + {}^{58}\text{Ni}$  at 22.8 MeV, since these cases involve a sufficient number of partial waves for our theory to be applicable.

The results of our analysis are shown in figs. 3-7. The differential cross section  $\sigma(\theta)$  and the vector analyzing power  $A(\theta)$  are calculated from eqs. (4.69-72) using eqs. (4.73-75) and (4.63) with the functions  $\mathcal{J}(\Delta z)$  and  $G(z)$  given by eqs. (V.9) and (VI.11) respectively. The numerical values of the seven  $l$ -space parameters  $\Lambda$ ,  $\Delta$ ,  $\alpha$ ,  $\Lambda_S$ ,  $\Delta_S'$ ,  $\kappa_r$  and  $\kappa_i$  are listed in table 1. The parameters  $\kappa_r$  and  $\kappa_i$  are the real and imaginary parts of the spin-orbit coupling strength  $\kappa$  respectively.

The tensor analyzing power for the elastic scattering  ${}^6\vec{\text{Li}} + {}^{28}\text{Si}$  at 22.8 MeV has also been measured<sup>32)</sup> and was found to be consistent with zero. This is in agreement with our analysis of tensor polarization (which is based on the assumption of pure vector spin-orbit coupling) according to which the tensor analyzing power, given by eq. (4.24), is an order of magnitude smaller than the vector analyzing power. On the other hand, the data on the elastic scattering of  ${}^7\vec{\text{Li}} + {}^{58}\text{Ni}$  at 23.2 MeV shows the tensor analyzing power to be non-zero<sup>††</sup>. We have not analyzed this data since the data on

---

<sup>†</sup> The data of refs. <sup>10,11)</sup> on the cross section ratio for the elastic scattering of  ${}^6\vec{\text{Li}} + {}^{28}\text{Si}$  at 22.8 MeV is incorrectly normalized. The correctly normalized data is taken from ref. <sup>35)</sup>.

<sup>††</sup> It is possible that the tensor polarization in this case is due to the quadrupole moment of the  ${}^7\text{Li}$  nucleus which is an order of magnitude larger than that of the  ${}^6\text{Li}$  nucleus. The elastic scattering formalism of this thesis can easily be extended to investigate such an effect.

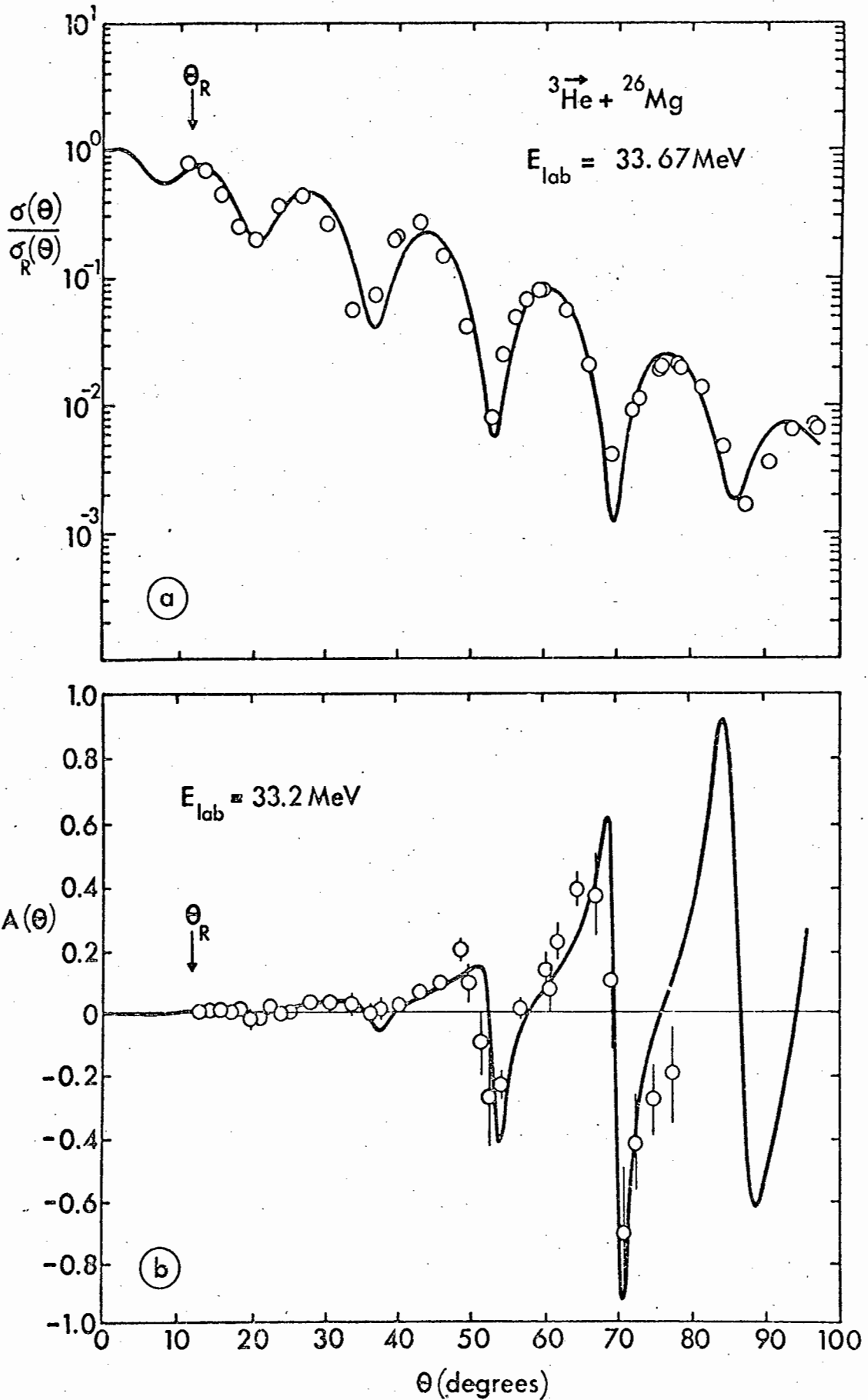


Fig. 3. Differential cross section (a) and analyzing power (b) for the elastic scattering of  ${}^3\text{He} + {}^{26}\text{Mg}$  at  $E_{\text{lab}} \approx 33.4 \text{ MeV}$ . The solid curves are calculated using the closed formalism with parameters given in Table 1. The data are from ref.<sup>33)</sup> (cross section) and ref.<sup>12)</sup> (analyzing power).

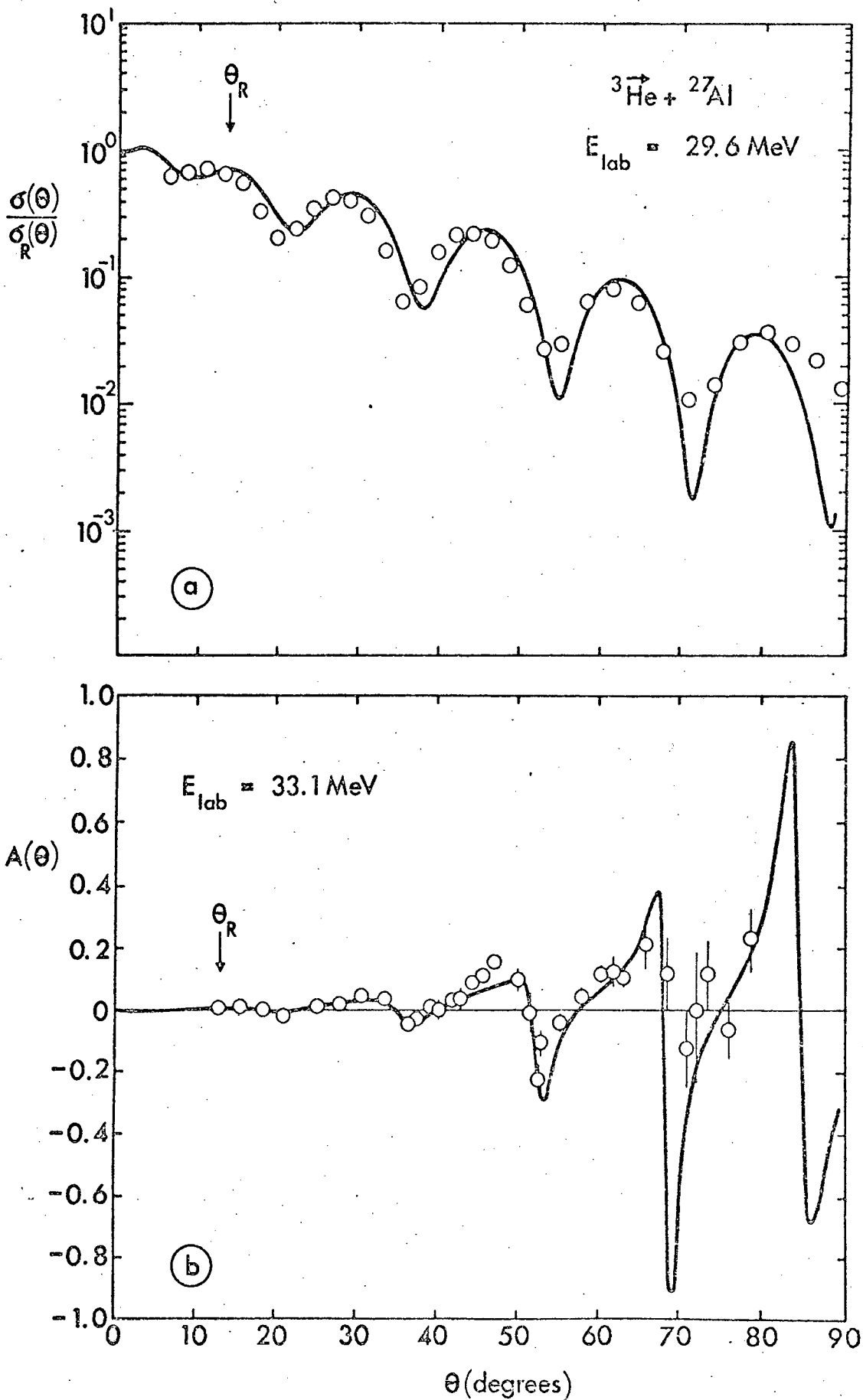


Fig. 4. Differential cross section (a) and analyzing power (b) for the elastic scattering of  ${}^3\vec{\text{He}} + {}^{27}\text{Al}$  at  $E_{\text{lab}} = 29.6 \text{ MeV}$  (cross section) and  $E_{\text{lab}} = 33.1 \text{ MeV}$  (analyzing power). The solid curves are calculated using the closed formalism with parameters given in Table 1. The data are from ref.<sup>34)</sup> (cross section) and ref.<sup>12)</sup> (analyzing power).

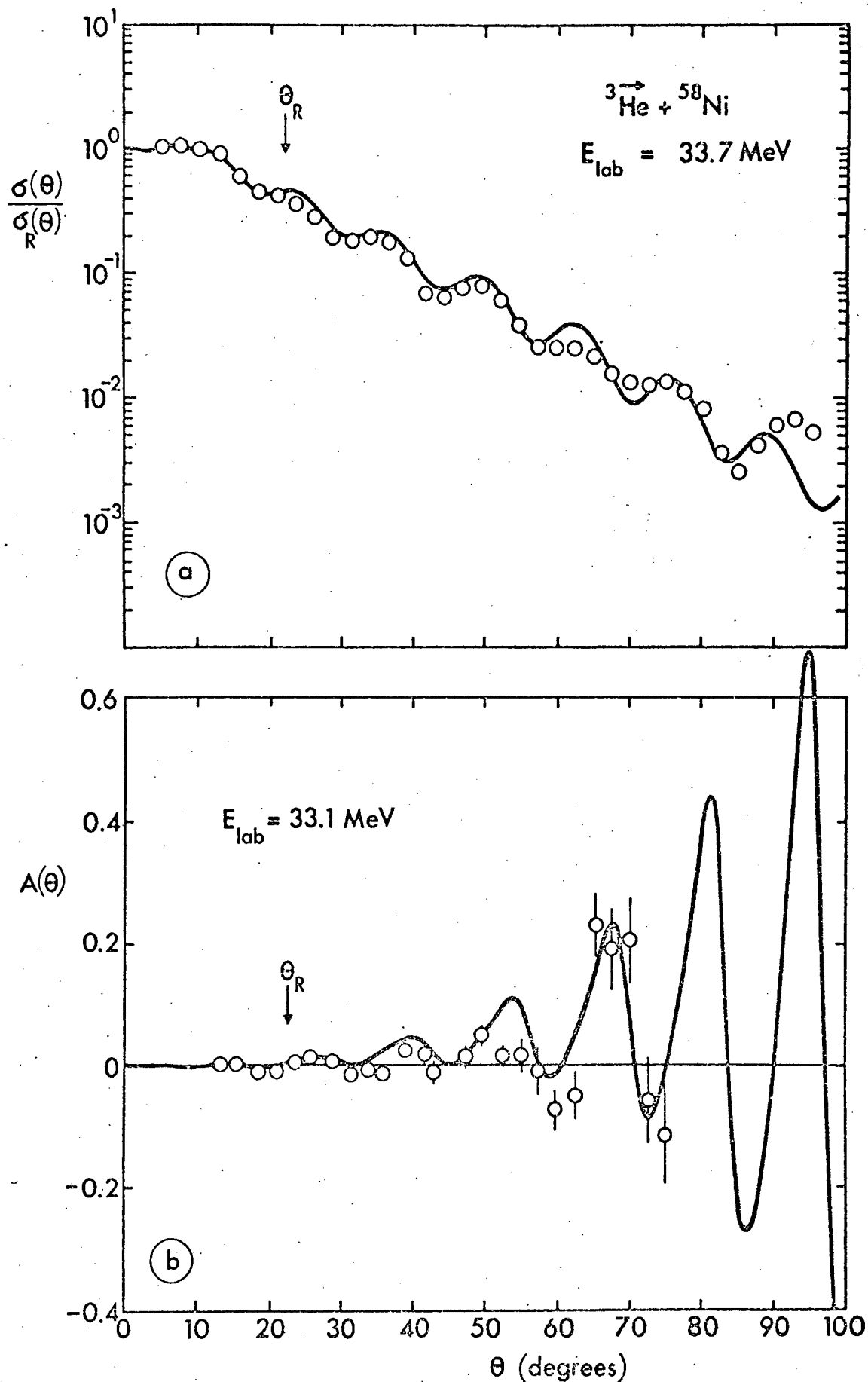


Fig. 5. Differential cross section (a) and analyzing power (b) for the elastic scattering of  ${}^3\text{He} + {}^{58}\text{Ni}$  at  $E_{\text{lab}} \approx 33.3 \text{ MeV}$ . The solid curves are calculated using the closed formalism with parameters given in Table 1. The data are from ref.<sup>12)</sup>.

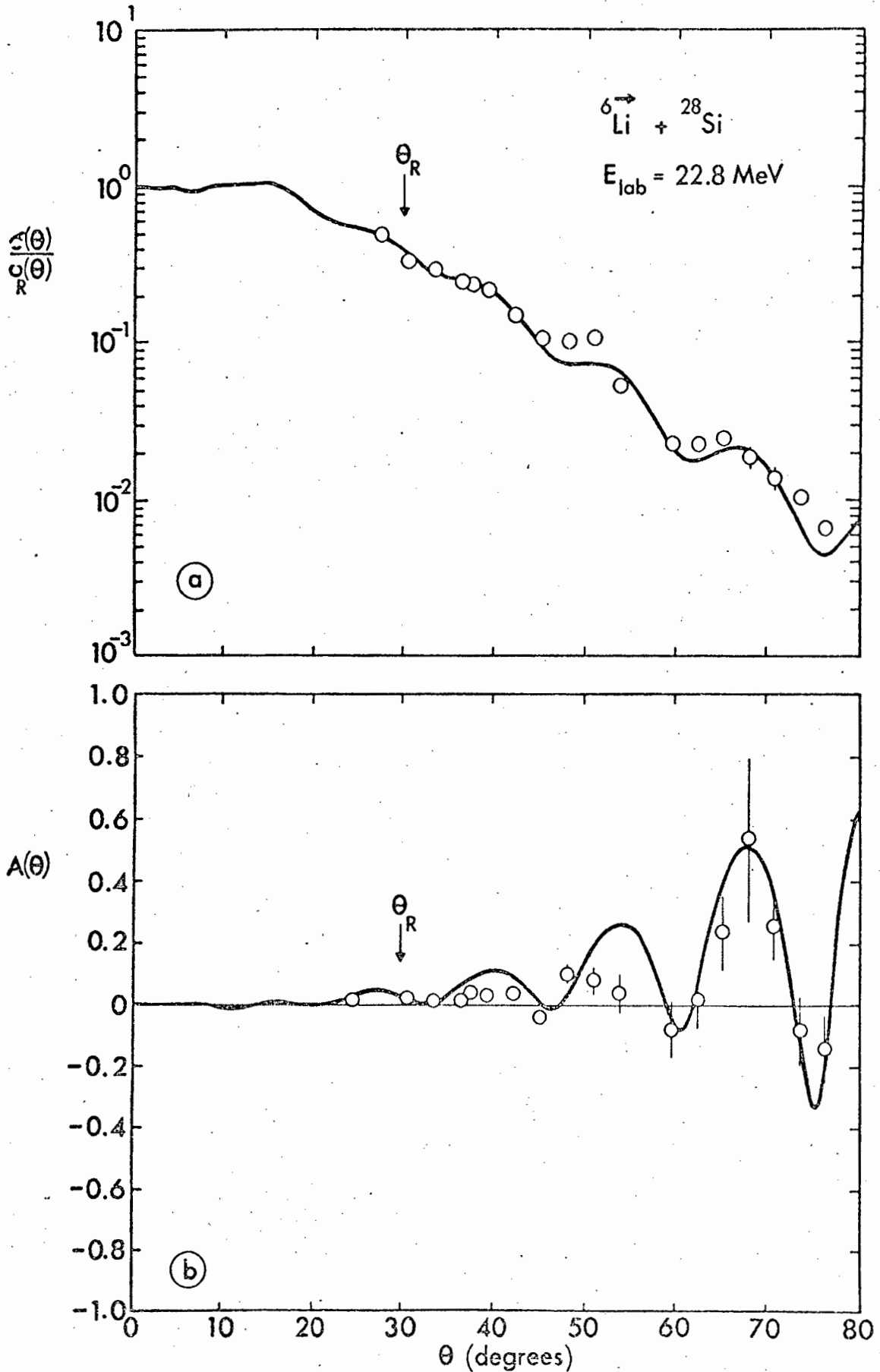


Fig. 6. Differential cross section (a) and vector analyzing power (b) for the elastic scattering of  ${}^6\text{Li} + {}^{28}\text{Si}$  at  $E_{\text{lab}} = 22.8 \text{ MeV}$ . The solid curves are calculated using the closed formalism with parameters given in Table 1. The data are from ref.<sup>11)</sup>.

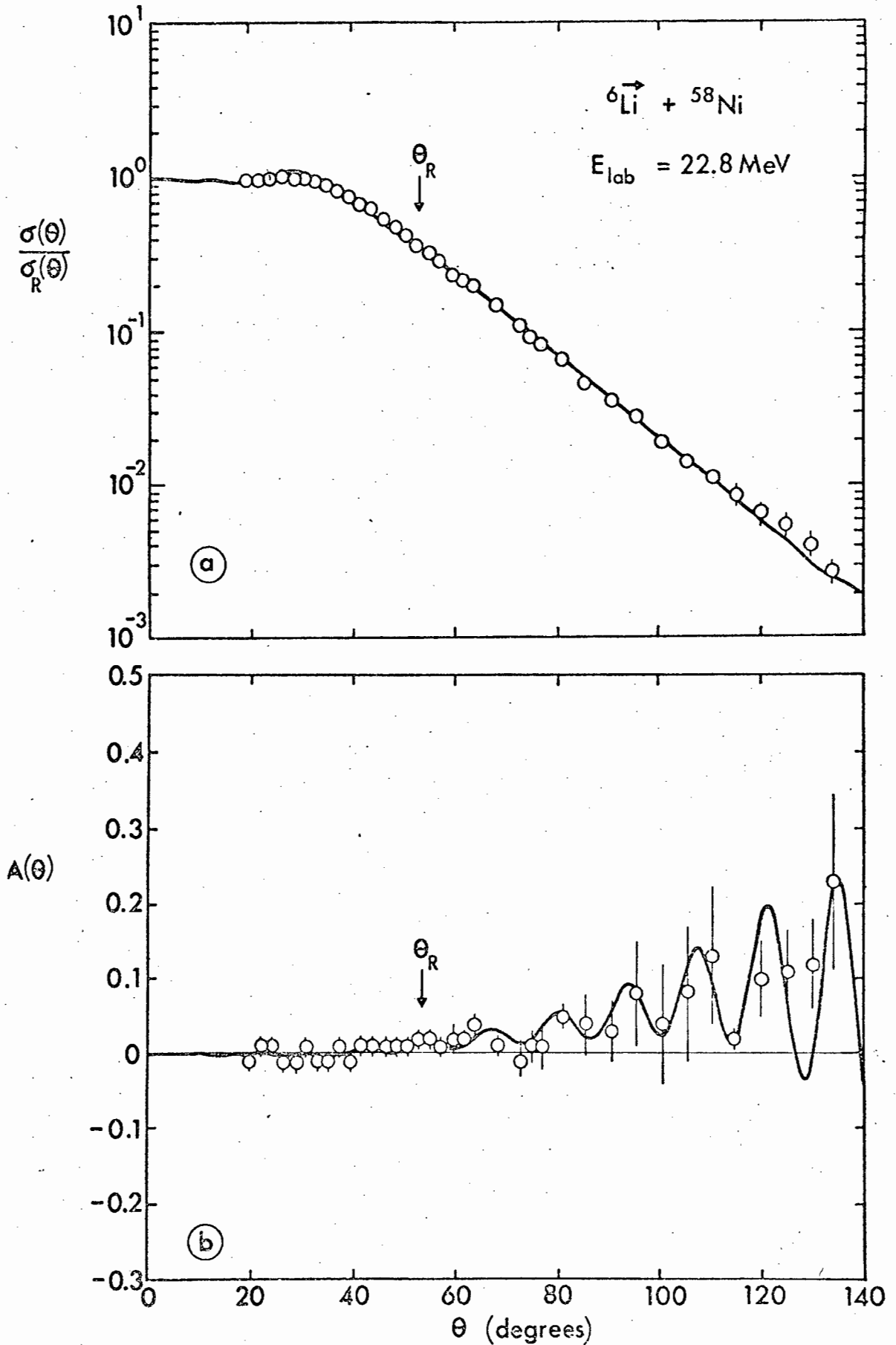


Fig. 7. Differential cross section (a) and vector analyzing power (b) for the elastic scattering of  ${}^6\text{Li} + {}^{58}\text{Ni}$  at  $E_{\text{lab}} = 22.8 \text{ MeV}$ . The solid curves are calculated using the closed formalism with parameters given in Table 1. The data are from ref.<sup>11)</sup>.

TABLE 1: Parameters of the analysis of the elastic scattering data.

Reaction	$E_{\text{lab}}$ (MeV)	n	$\theta_R$ (deg)	( $\ell$ -space parameters)							(geometrical parameters)		
				$\Lambda$	$\Delta$	$\alpha$	$\Lambda_s$	$\Delta_s$	$\kappa_r$	$\kappa_i$	$r_o$ (fm)	$r'_o$ (fm)	d (fm)
${}^3\text{He} + {}^{26}\text{Mg}$	33.4	1.14	11.8	11.0	1.05	0.5	9.69	0.52	0.145	0.080	1.41	2.09	0.53
${}^3\text{He} + {}^{27}\text{Al}$ (Cross Section)	29.6	1.31	14.0	10.7	0.93	0.5	9.32	0.46	0.155	0.085	1.46	2.17	0.50
${}^3\text{He} + {}^{27}\text{Al}$ (Analyzing Power)	33.1	1.24	12.6	11.2	0.93	0.5	9.82	0.46	0.175	0.095	1.43	2.12	0.47
${}^3\text{He} + {}^{58}\text{Ni}$	33.7	2.64	22.1	13.5	1.00	0.4	12.18	0.33	0.205	0.040	1.47	2.02	0.47
${}^6\text{Li} + {}^{28}\text{Si}$	22.8	3.40	29.8	12.8	1.10	0.75	12.06	0.37	0.380	0.120	1.62	2.60	0.50
${}^6\text{Li} + {}^{58}\text{Ni}$	22.8	6.81	53.2	13.6	0.88	0	12.56	0.29	0.165	0.035	1.67	2.45	0.34

the cross section ratio is not yet available.

It is convenient to reduce the  $\ell$ -space parameters  $\Lambda$  and  $\Delta$  to the geometrical parameters  $R_0$  and  $d$  using the semiclassical formulae

$$\Lambda = k R_0 \left[ 1 - \frac{2n}{k R_0} \right]^{\frac{1}{2}}, \quad \Delta = k d \frac{\left( 1 - \frac{n}{k R_0} \right)}{\left( 1 - \frac{2n}{k R_0} \right)^{\frac{1}{2}}}, \quad (7.1)$$

where  $n$  is the Sommerfeld parameter (eq. (4.13)) and  $k$  is the wave number for the relative motion. It is hoped that eqs. (7.1) give a good approximation to the energy dependence of  $\Lambda$  and  $\Delta$  respectively, in terms of the energy independent quantities  $R_0$  and  $d$ . The parameter  $R_0$  should be compared with the strong absorption radius, rather than with the Woods-Saxon radii of the optical potential, while the parameter  $d$  is a convenient geometrical diffuseness parameter. The radius parameters  $r_0$  and  $r'_0$  refer to the heavy and light ion options respectively and are calculated using the formulae

$$R_0 = r_0 (A_1^{\frac{1}{3}} + A_2^{\frac{1}{3}}) = r'_0 A_1^{\frac{1}{3}}, \quad (7.2)$$

where  $A_1$  and  $A_2$  are the atomic mass numbers of the target and projectile respectively. The numerical values of the parameters  $d$ ,  $r_0$  and  $r'_0$  are listed in table 1.

Recall that the data of the cross section ratio and the analyzing power for the elastic scattering of  ${}^3\text{He} + {}^{27}\text{Al}$  are at the energies 29.6 MeV and 33.1 MeV. Because of the comparatively large energy difference, our theoretical fits to the data at these two energies had to be done independently.

However, the close agreement between the two sets of geometrical parameters  $r_0$ ,  $r'_0$  and  $d$ , for the two different energies, is our justification for doing this.

The theoretical curves for  ${}^3\vec{\text{He}} + {}^{26}\text{Mg}$  and  ${}^3\vec{\text{He}} + {}^{27}\text{Al}$  shown in figs. 3 and 4 respectively are examples of case (c) (eq. (6.33c)), as can be shown from the parameter values of table 1. The cross section ratios of figs. 3 and 4 are typical of Fraunhofer diffraction scattering with weak Coulomb damping, as illustrated in fig. 2(e). The analyzing power in figs. 3 and 4 show the asymmetrical oscillations, characteristic of this type of diffraction scattering and which are illustrated in fig. 2(h).

By comparison, the theoretical curves for the cross section ratios for the elastic scattering of  ${}^3\vec{\text{He}} + {}^{58}\text{Ni}$  and  ${}^6\vec{\text{Li}} + {}^{28}\text{Si}$ , shown in figs. 5 and 6 respectively, are also examples of case (c) but with stronger Coulomb damping of the Fraunhofer oscillations. These curves are to be compared with fig. 2(a). The corresponding theoretical curves for the vector analyzing power, shown in figs. 5 and 6, show more symmetrical oscillations of Fraunhofer type as illustrated in figs. 2(b-d).

These features are explained in subsection 6.3 under case (c).

The theoretical fit for  ${}^6\vec{\text{Li}} + {}^{58}\text{Ni}$  shown in fig. 7 is an example of case (b) (eq. (6.33b)). The cross section ratio of fig. 7 is typical of Fresnel diffraction scattering. The corresponding vector analyzing power, shown in fig. 7, shows very small Fresnel-type oscillations at angles  $\theta \lesssim \theta_R$ , while

in the shadow region ( $\theta \geq \theta_R$ ) it shows Fraunhofer-type oscillations. These features are discussed in subsection 6.3 under case (b) and are illustrated in figs. 1(f-j).

The main conclusion of our analysis of elastic scattering is that the main features of the differential cross section and the vector analyzing power are characteristic of diffraction scattering which is the dominant mechanism involved. This was predicted in refs.<sup>3,4,5</sup>). More specifically, it was found that for the elastic scattering of  $^3\text{He}$  by  $^{26}\text{Mg}$ ,  $^{27}\text{Al}$  and  $^{58}\text{Ni}$ , at energies close to 33 MeV, and for the elastic scattering of  $^6\text{Li}$  by  $^{28}\text{Si}$  at 22.8 MeV, Fraunhofer diffraction scattering is the main mechanism involved, while for the elastic scattering of  $^6\text{Li}$  by  $^{58}\text{Ni}$  at 22.8 MeV, Fresnel diffraction scattering dominates.

In spite of the relatively few sets of data available, further general conclusions may be drawn from the parameter values listed in table 1.

For the lighter systems there is evidence of refraction ( $\alpha > 0$ ) due to an attractive nuclear potential. The only exception is the heaviest system  $^6\vec{\text{Li}} + ^{58}\text{Ni}$  which showed no evidence of nuclear refraction. There is no evidence of dominant surface reflection ( $\alpha < 0$ ).

The strength of the spin-orbit interaction is similar for  $^3\text{He}$  and  $^6\text{Li}$ . In all cases the spin-orbit coupling is seen to have a refractive ( $\kappa_r > 0$ ) as well as an absorptive ( $\kappa_i > 0$ ) part. The numerical values of the critical  $\lambda$ -value  $\Lambda_s$  and the diffuseness parameter  $\Delta_s$ , of the complex spin-orbit phase shift  $\delta_s(\lambda)$ , are consistently less than the

numerical values of the corresponding parameters  $\Lambda$  and  $\Delta$  of the elastic scattering function  $S_c^{(N)}(\lambda)$ .

There is a correspondence between the refractive and absorptive effects represented by the  $l$ -space parameters, and the effects of the real and imaginary optical potentials of the optical model. Optical model analyses have been carried out on most of the elastic scattering data that we have studied. It is therefore possible to compare some of the conclusions arrived at in the optical model studies with those of our  $l$ -space analysis.

We first consider the following optical model studies of the data on elastic scattering of polarized  ${}^3\text{He}$  ions:

M. Cohler et al.<sup>26)</sup> of the present data on the elastic scattering of  ${}^3\vec{\text{He}} + {}^{26}\text{Mg}$  at 33.4 MeV;

S. Roman<sup>28)</sup> of the earlier data on the elastic scattering of  ${}^3\vec{\text{He}} + {}^{26}\text{Mg}$  at 33.3 MeV and  ${}^3\vec{\text{He}} + {}^{27}\text{Al}$  at 33.3 MeV<sup>†</sup>;

S. Roman et al.<sup>27)</sup> of the data on the elastic scattering of  ${}^3\vec{\text{He}} + {}^{58}\text{Ni}$  at 33.3 MeV.

In all of the analyses referred to above, nine-parameter fits to the data were attempted using Woods-Saxon forms for the real and imaginary central nuclear potentials and a real Thomas-Fermi form for the spin-orbit potential. In all cases the diffuseness parameter of the spin-orbit potential turned out to be considerably less than the diffuseness

---

<sup>†</sup> No optical model analysis has been reported on the Birmingham data<sup>12)</sup> on the vector analyzing power in the elastic scattering of  ${}^3\vec{\text{He}} + {}^{27}\text{Al}$  at 33.1 MeV.

parameters of the central nuclear potentials (in some cases the ratio was less than  $\frac{1}{3}$ ). This agrees qualitatively with the finding of our  $\ell$ -space analysis that the diffuseness parameter  $\Delta_S$ , of the complex spin-orbit phase shift  $\delta_S(\lambda)$ , is consistently less than the diffuseness parameter  $\Delta$  of the elastic scattering function  $S_C^{(N)}(\lambda)$ .

In the above mentioned optical model analyses of the data on  ${}^3\vec{\text{He}} + {}^{26}\text{Mg}$  at 33.4 MeV and 33.3 MeV, the radius parameter of the spin-orbit potential turned out to be less than the radius parameters of the central potentials. This result may be compared qualitatively with the result of our analysis of the data on  ${}^3\vec{\text{He}} + {}^{26}\text{Mg}$  at 33.4 MeV in which the critical  $\lambda$ -value  $\Lambda_S$  of the complex spin-orbit phase shift  $\delta_S(\lambda)$  was found to be less than the critical  $\lambda$ -value  $\Lambda$  of the elastic scattering function  $S_C^{(N)}(\lambda)$ .

On the other hand in the above optical model analyses of the data on  ${}^3\vec{\text{He}} + {}^{27}\text{Al}$  at 33.3 MeV and 33.1 MeV and  ${}^3\vec{\text{He}} + {}^{58}\text{Ni}$  at 33.3 MeV, the radius parameter of the spin-orbit potential was found to be about the same as the radius parameter of the real central nuclear potential.

These comparisons are intended to be only qualitative since there is not a one-to-one correspondence between the radius and diffuseness parameters of the optical potential and the  $\ell$ -space parameters  $\Lambda$  and  $\Delta$  respectively. Furthermore, there are various ambiguities in determining the optical potential parameters in the optical model approach.

In each of the above-mentioned optical model analyses, except the analysis of the data on  ${}^3\vec{\text{He}} + {}^{27}\text{Al}$  at 33.3 MeV,

the analyzing power data could not be reproduced satisfactorily at small angles (say  $\lesssim 40^\circ$ ). Our fits to the  $^3\text{He}$  data in this angular range are qualitatively better. At larger angles our fits are of about the same quality as the best optical model fits to the data at these angles. In the case of the optical model analysis of the data on  $^3\vec{\text{He}} + ^{27}\text{Al}$  at 33.3 MeV, the data on the vector analyzing power, which does not extend beyond  $50^\circ$ , was reproduced very well, but only since the search was biased to fit this angular region. The corresponding fit to the data on the cross section ratio beyond about  $40^\circ$  was found to be unsatisfactory.

In the optical model study<sup>10)</sup> of the  $^6\text{Li}$  data of the Heidelberg group, the  $^6\text{Li}$  spin-orbit potential was calculated, by means of a folding model, from the deuteron-target spin-orbit potential. The data on the cross section ratio for the elastic scattering of  $^6\vec{\text{Li}} + ^{28}\text{Si}$  at 22.8 MeV was incorrectly normalized when the optical model analysis was done (see footnote † on page 81). The data on the cross section ratio for the elastic scattering of  $^6\vec{\text{Li}} + ^{58}\text{Ni}$  at 22.8 MeV was well reproduced, but the fit to the vector analyzing power data was unsatisfactory. Our fit to the cross section ratio (figure 7) is qualitatively the same, but our fit to the vector analyzing power (figure 7) is considerably better. Our fit to the (correctly normalized) data on  $^6\vec{\text{Li}} + ^{28}\text{Si}$  at 22.8 MeV is satisfactory.

The abovementioned optical model studies all involved nine-parameter fits to the data, while our  $\ell$ -space analysis involved seven parameters. The difference in the number of

parameters may be related to the well-known continuous ambiguities in the optical model parameters for a given fit to a set of experimental data, while for a given fit to the data in our  $\ell$ -space approach, the  $\ell$ -space parameters are determined uniquely.

The optical model studies referred to in this section all involved purely real spin-orbit potentials. We have already mentioned the fact that in our formalism, the  $\ell$ -space parameters  $\kappa_r$  and  $\kappa_i$  describe the effects of the spin-orbit potential referring to refraction ( $\kappa_r > 0$ ) and absorption ( $\kappa_i > 0$ ) respectively. Referring to the numerical values of  $\kappa_r$  and  $\kappa_i$  given in table 1, the ratio  $\kappa_i/\kappa_r$  is, in most cases large enough to suggest that the absorptive effect of the spin-orbit coupling, described by these parameters, could be reproduced in optical model calculations only if an imaginary term is included in the spin-orbit potential. The presence of an imaginary term in the spin-orbit potential is discussed in section 4.4 of ref.<sup>13</sup>).

## 7.2 Analysis of inelastic scattering data

The inelastic scattering formalism of section 5 is intended mainly for the analysis of future experimental data. However, there are at present a few sets of data available to which the theory is applicable. These are discussed below.

The Birmingham group<sup>12</sup>) has measured inelastic scattering of polarized  $^3\text{He}$  ions by various target nuclei. Of this data only the inelastic scattering of  $^3\text{He} + ^{26}\text{Mg}$  at 33.2 MeV, with excitation of the 1.809 MeV  $2^+$  state and the 2.938 MeV  $2^+$  state

of  $^{26}\text{Mg}$ , are suitable for analysis by our theory. However, in each case, the data on the vector analyzing power is not yet sufficiently conclusive (due to large experimental errors or irregular fluctuations), so that a detailed analysis cannot be made at this stage.

The Heidelberg group<sup>11)</sup> has measured inelastic scattering of vector polarized  $^6\text{Li}$  ions by various target nuclei. We have analyzed their data on the inelastic scattering of  $^6\text{Li} + ^{28}\text{Si}$  at 22.8 MeV with excitation of the 1.77 MeV  $2^+$  state of  $^{28}\text{Si}$ .

The results of our analysis are shown in fig. 8. The inelastic cross section  $\sigma_{2^+}(\theta)$  and the vector analyzing power  $A(\theta)$  are evaluated from eqs. (5.64) and (5.66) respectively, using eqs. (5.40), (5.43), (5.44), (5.49-52) and (5.60-62), with the functions  $\mathfrak{H}(\Delta z)$  and  $G(z)$  given by eqs. (V.9) and (VI.11) respectively. The Coulomb integrals  $I_{LM}(\vartheta, \xi)$  are evaluated using eq. (5.9). The numerical values of the seven  $\ell$ -space parameters  $\Lambda$ ,  $\Delta$ ,  $\alpha$ ,  $\Lambda_S$ ,  $\Delta_S$ ,  $\kappa_r$  and  $\kappa_i$ , that appear in the formulae, are given in table 2. For the Coulomb charge radius parameter  $r_c$ , we have used the standard value 1.25. Since the scattering function  $S_{\tau}^{(N)}(\lambda)$  of section 5 represents some average of the corresponding elastic scattering functions for the initial and final channels, which are at different energies, the numerical values of the seven  $\ell$ -space parameters given in table 2 are not expected to be the same as the numerical values of the corresponding parameters given in table 1 for the elastic scattering of  $^6\text{Li} + ^{28}\text{Si}$  at 22.8 MeV.

As in the analysis of the elastic scattering data, the

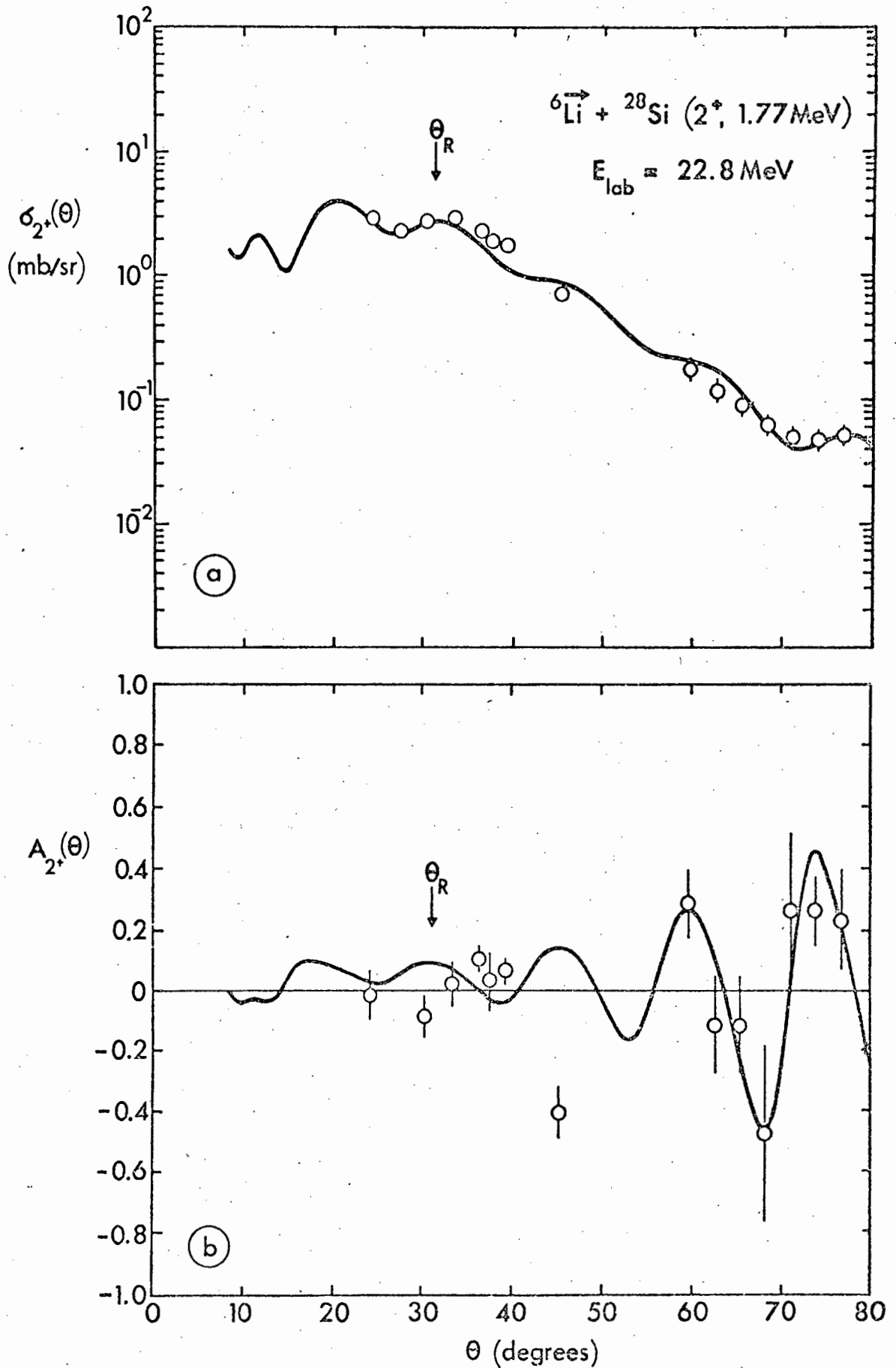


Fig. 8. Angular distribution (a) and vector analyzing power (b) for the inelastic scattering of  ${}^6\vec{\text{Li}} + {}^{28}\text{Si}$  at  $E_{\text{lab}} = 22.8\text{MeV}$  with excitation of the 1.77 MeV  $2^+$  state of  ${}^{28}\text{Si}$ . The solid curves are calculated using the closed formalism with parameters given in Table 2. The data are from ref.<sup>11</sup>).

**TABLE 2:** Parameters of the analysis of the data on the inelastic scattering of  ${}^6\text{Li} + {}^{28}\text{Si}$  at  $E_{\text{lab}} = 22.8$  MeV with excitation of the 1.77 MeV  $2^+$  state in  ${}^{28}\text{Si}$ .

n	$\xi$	$\theta_R$ (deg)	$\Lambda$	$\Delta$	$\alpha$	$\Lambda_s$	$\Delta_s$	$\kappa_r$	$\kappa_i$	$r_0$ (fm)	$r'_0$ (fm)	d (fm)
3.49	0.17	31.4	12.4	1.3	0.4	11.8	0.43	0.090	0.235	1.63	2.61	0.61

Deformation parameters:

$\beta_2$ (C)	$\delta_2$ (C) (fm)	$\beta_2$ (N)	$\delta_2$ (N) (fm)	B(E2) ( $e^2b^2$ )
0.290	1.10	0.074	0.59	0.0195

$l$ -space parameters  $\Lambda$  and  $\Delta$  may be reduced, by means of eqs. (7.1) and (7.2), to the geometrical parameters  $r_0$ ,  $r'_0$  and  $d$ . The numerical values of these geometrical parameters, given in table 2, agree favourably with the numerical values of the corresponding parameters given in table 1 for the elastic scattering of  ${}^6\bar{\text{Li}} + {}^{28}\text{Si}$  at 22.8 MeV. Also given in table 2 are the deformation lengths  $\delta_L^{(N)}$  and  $\delta_L^{(C)}$  and the corresponding deformation parameters  $\beta_L^{(N)}$  and  $\beta_L^{(C)}$ , defined by eqs. (3.8) and (3.9), the adiabaticity parameter  $\xi$ , the average Sommerfeld parameter  $n$ , defined by eq. (5.6), and the reduced EL transition probability  $B(EL)$  defined by

$$B(EL) = \left[ \frac{3}{4\pi} \beta_L^{(C)} z_2 e R_C^L \right]^2. \quad (7.3)$$

Referring to fig. 8, it was found that the amplitudes for Coulomb excitation are only of significance in fitting the first two data points of the inelastic cross section. The vector analyzing power data up to  $40^\circ$  could not be reproduced anyway. It is for these reasons that we used the approximate formula (5.9) to evaluate the Coulomb integrals  $I_{LM}(\vartheta, \xi)$  instead of using the tabulated values of ref.<sup>22</sup>). In view of this, the numerical value of  $B(E2)$ , given in table 2, can be regarded as being in satisfactory agreement with the experimental value  $0.0317 \pm 0.0017$  given in ref.<sup>36</sup>).

The data on the inelastic cross section over the whole angular range and the data on the vector analyzing power beyond  $50^\circ$  were reproduced satisfactorily. Since it was found that the amplitudes for nuclear excitation dominate the

amplitudes for Coulomb excitation beyond about  $30^\circ$ , the discussion in subsection 6.4 is applicable to the inelastic cross section and the vector analyzing power over this angular range. Accordingly, the oscillations, at least beyond  $40^\circ$ , in the theoretical curves shown in fig. 8, are attributed to Fraunhofer diffraction.

A comparison between fig. 6 and fig. 8 shows that the Fraunhofer oscillations in the elastic cross section ratio and vector analyzing power are approximately  $180^\circ$  out of phase with the corresponding oscillations in the inelastic cross section and vector analyzing power respectively. This is in agreement with the extended Blair phase rule discussed in subsection 6.4.

8. SUMMARY

The purpose of this thesis has been to develop a closed S-matrix formalism for the vector and tensor polarization in elastic and inelastic scattering of strongly absorbed particles of general spin  $s$  by spin-zero target nuclei, and to apply this formalism in an analysis of recent experimental data.

From this analysis the following conclusions can be drawn:

- i) Both scattering and polarization of strongly absorbed particles are predominantly diffractive, and for the relatively light systems studied here are mainly of Fraunhofer type; only the heaviest system ( ${}^6\text{Li} + {}^{58}\text{Ni}$ ) shows the characteristics of Fresnel diffraction.
- ii) The spin-orbit interaction of both  ${}^3\text{He}$  and  ${}^6\text{Li}$  has a significant imaginary part.
- iii) The critical angular momentum  $\Lambda_s$  (hence the radius) of the spin-orbit interaction is consistently smaller than  $\Lambda$  of the central part.
- iv) The  $l$ -space width  $\Delta_s$  (hence the diffuseness) of the spin-orbit phase is abnormally small compared with the central width  $\Delta$ , in agreement with optical model findings.
- v) All of these properties are shared by  ${}^3\text{He}$  and  ${}^6\text{Li}$ , indicating a close similarity between the spin-orbit interaction of light and heavy ions.

APPENDIX ITHE ELASTIC SCATTERING AMPLITUDE, TREATING THE  
SPIN-ORBIT COUPLING IN DISTORTED-WAVE-BORN APPROXIMATION

Using the Gell-Mann-Goldberger transformation<sup>37)</sup>, the transition operator may be written

$$T(\hat{k}_f, \hat{k}_i) = T_0(\hat{k}_f, \hat{k}_i) + \Delta T(\hat{k}_f, \hat{k}_i) , \quad (\text{I.1})$$

where

$$\Delta T(\hat{k}_f, \hat{k}_i) = \langle \Psi_0^{(-)}(\mathbf{k}_f, \mathbf{r}) | H' | \Psi_0^{(+)}(\mathbf{k}_i, \mathbf{r}) \rangle , \quad (\text{I.2})$$

$$H' = \sum_{\mathbf{k}} u_{\mathbf{k}}(r) \sum_{\mathbf{q}} (-1)^q S_{\mathbf{k}\mathbf{q}} R_{\mathbf{k}-\mathbf{q}}(\hat{\mathbf{r}}) . \quad (\text{I.3})$$

Here the subscript 0 denotes operators or wave functions corresponding to no spin-orbit coupling. The form of  $H'$  is taken from ref.<sup>38)</sup>, where  $S_{\mathbf{k}}$  and  $R_{\mathbf{k}}$  are spherical tensors of rank  $k$  in the spin-space of the projectile and co-ordinate space respectively, so that  $T$ ,  $T_0$  and  $\Delta T$  are operators on the projectile spin.

Without spin-orbit coupling, eq. (2.10) may be written

$$\Psi_0^{(\pm)}(\mathbf{k}, \mathbf{r}) = \frac{4\pi}{kr} \sum_{\ell m} \psi_{\ell}^{(\pm)}(k, r) i^{\ell} Y_{\ell m}(\hat{\mathbf{r}}) Y_{\ell m}^*(\hat{\mathbf{k}}) . \quad (\text{I.4})$$

Substituting eqs. (I.3) and (I.4) into eq. (I.2), we have

$$\Delta T(\hat{k}_f, \hat{k}_i) = \left(\frac{4\pi}{k}\right)^2 \sum_{\ell_f m_f} \sum_{\ell_i m_i} \sum_{kq} (-1)^q i^{\ell_i - \ell_f} Y_{\ell_f m_f}(\hat{k}_f) Y_{\ell_i m_i}^*(\hat{k}_i) \times$$

$$\left[ \int_0^\infty dr \psi_{\ell_f}^{(-)*}(k, r) \psi_k(r) \psi_{\ell_i}^{(+)}(k, r) \right] \left[ \int d\hat{r} Y_{\ell_f m_f}^*(\hat{r}) R_{k-q}(\hat{r}) Y_{\ell_i m_i}(\hat{r}) \right] S_{kq} . \quad (\text{I.5})$$

The scattering amplitude

$$A(\hat{k}_f, \hat{k}_i) = \frac{\mu}{2\pi\hbar^2} T(\hat{k}_f, \hat{k}_i) \quad (\text{I.6})$$

may therefore be written in the form

$$A(\theta) = A_0(\theta) + \sum_{k \neq 0} \sum_q (-1)^q A_{k-q}(\theta) S_{kq} , \quad (\text{I.7})$$

where  $\sin(\theta) = |\hat{k}_i \times \hat{k}_f|$ . The density operator for the spin of the scattered projectiles, when the incident beam is unpolarized, is given by

$$\rho(\theta) = \frac{1}{2S+1} A(\theta) A^\dagger(\theta) . \quad (\text{I.8})$$

Substituting eq. (I.7) into eq. (I.8) and keeping only the leading terms of the form  $A_0(\theta) A_{ij}(\theta)$ , we have

$$(2S+1)\rho(\theta) \approx |A_0(\theta)|^2 + A_0(\theta) \sum'_{kq} (-1)^q A_{k-q}^*(\theta) S_{kq}^\dagger$$

$$+ A_0^*(\theta) \sum'_{kq} (-1)^q A_{k-q}(\theta) S_{kq}$$

$$= |A_0(\theta)|^2 + \sum'_{kq} \left\{ A_0(\theta) A_{k-q}^*(\theta) + (-1)^q A_0^*(\theta) A_{k-q}(\theta) \right\} S_{kq} , \quad (\text{I.9})$$

where  $\Sigma'$  denotes summation over all values of  $k \neq 0$ .

Equation (I.9) amounts to an expansion of the density operator  $\rho(\theta)$  in terms of the spin-tensor components  $S_{kq}$ . The coefficient of  $S_{kq}$  is therefore proportional to the polarization term of rank  $k$  and magnetic quantum number  $q$ . (In the case of the scattering of a vector polarized beam of projectiles, the coefficient of  $S_{kq}$  would be proportional to the component  $T_{kq}$  of the analyzing power.) Referring back to eq. (I.5) we see that the coefficient of  $S_{kq}$  in eq. (I.9) comes from the term  $(k,q)$  in eq. (I.3), so that to first order in DWBA, we have a one-to-one correspondence between the type of spin-orbit coupling term in the optical potential, and the type of polarization it causes.

## APPENDIX II

PROOF OF THE IDENTITY  $h_{kq}(\theta) = 0$  FOR  $q$  ODD†

The general formula for the amplitude for elastic scattering of spin- $s$  projectiles by spin-0 targets, with tensor spin-orbit coupling, is given by<sup>14)</sup>

$$A(\nu_f, \nu_i; \theta) = -i \frac{2\pi}{k} \sum_{jM} \sum_{l_f m_f} \sum_{l_i m_i} \langle l_f m_f s \nu_f | jM \rangle \langle l_i m_i s \nu_i | jM \rangle \\ \times i^{l_i - l_f} Y_{l_f m_f}(\hat{k}_f) Y_{l_i m_i}^*(\hat{k}_i) S_{l_f l_i}^j \quad (\theta \neq 0) \quad (\text{II.1})$$

where  $\sin(\theta) = |\hat{k}_i \times \hat{k}_f|$ . From eqs. (II.1), (2.47) and (2.50) we have

$$h_{kq}(\theta) = \frac{(2\kappa+1)^{\frac{1}{2}}}{2s+1} \left(\frac{2\pi}{k}\right)^2 \sum_{\nu_f \nu_i \tau} \langle s \kappa \nu_f q | s \nu_i \tau \rangle \\ \sum_{jM} \sum_{l_f m_f} \sum_{l_i m_i} \langle l_f m_f s \nu_f | jM \rangle \langle l_i m_i s \tau | jM \rangle i^{l_i - l_f} Y_{l_f m_f}(\hat{k}_f) Y_{l_i m_i}^*(\hat{k}_i) S_{l_f l_i}^j \\ \sum_{j'M'} \sum_{l_f' m_f'} \sum_{l_i' m_i'} \langle l_f' m_f' s \nu_i | j'M' \rangle \langle l_i' m_i' s \tau | j'M' \rangle i^{l_f' - l_i'} Y_{l_f' m_f'}(\hat{k}_f) Y_{l_i' m_i'}^*(\hat{k}_i) S_{l_f' l_i'}^{j' *} \\ (\theta \neq 0) \quad (\text{II.2})$$

Since, by our choice of co-ordinate system (2.35),  $\hat{z} \perp \hat{k}_i$  and  $\hat{z} \perp \hat{k}_f$ , the terms under the summation signs are zero unless  $l_f + m_f$ ,  $l_i + m_i$ ,  $l_f' + m_f'$  and  $l_i' + m_i'$  are even.

† This result has been proved for  $\kappa = 1$  and 2 (ref. 38)), and, with  $\underline{l} \cdot \underline{s}$  coupling, for all values of  $\kappa$  (ref. 39)).

Now, provided parity is conserved, we also have (see page 455 of ref.<sup>14</sup>)  $S_{\ell\ell'}^j \neq 0$  only if  $\ell - \ell'$  is even. This implies that the only nonzero terms on the right hand side of eq. (II.2) are those with  $m_f + m_i$  and  $m_f' + m_i'$  even. From the Clebsch-Gordon coefficients this implies that the only nonzero terms are those with  $v_f + \tau$  and  $v_i + \tau$  and hence also  $v_i - v_f = q$  even.

APPENDIX IIIDERIVATION OF THE FORMULA (3.28)

Using eq. (2.5) we obtain

$$\begin{aligned}
 I &\equiv \int d\hat{r} \psi_{j_f l_f s}^{M_f \dagger}(\hat{r}) Y_{LM}^*(\hat{r}) \psi_{j_i l_i s}^{M_i}(\hat{r}) \\
 &= \sum_{m_f \nu_f} \sum_{m_i \nu_i} \langle l_f s m_f \nu_f | j_f M_f \rangle \langle l_i s m_i \nu_i | j_i M_i \rangle \delta_{\nu_f \nu_i} \int d\hat{r} Y_{l_f m_f}^*(\hat{r}) Y_{LM}^*(\hat{r}) Y_{l_i m_i}(\hat{r}) \\
 &= \sum_{m_f m_i \nu_i} \langle l_f s m_f \nu_i | j_f M_f \rangle \langle l_i s m_i \nu_i | j_i M_i \rangle \frac{\hat{l}_f \hat{L} \hat{l}_i}{(4\pi)^{\frac{1}{2}}} \begin{pmatrix} l_f & L & l_i \\ 0 & 0 & 0 \end{pmatrix} \begin{pmatrix} l_f & L & l_i \\ m_f & M & -m_i \end{pmatrix} (-1)^{m_i} \\
 &= \sum_{m_f m_i \nu_i} \langle l_f s m_f \nu_i | j_f M_f \rangle \langle l_i s m_i \nu_i | j_i M_i \rangle \frac{\hat{l}_f \hat{L}}{(4\pi)^{\frac{1}{2}} \hat{l}_i} \\
 &\quad \times \langle l_f L 0 0 | l_i 0 \rangle \langle l_f L m_f M | l_i m_i \rangle, \tag{III.1}
 \end{aligned}$$

where we have used the notation  $\hat{x} = (2x+1)^{\frac{1}{2}}$ . In view of eqs. (3.25) and (3.26), and from the assumption that  $s \ll L_f, L_i$ , we have  $m_f, m_i, M_f, M_i, \nu_f, \nu_i$  and  $M \ll L_f, L_i$  so that we may use the approximation<sup>15)</sup> (c.f. eqs. (2.29) and (2.30)),

$$\langle l s m \nu | j M \rangle \approx d_{\nu j-l}^s(\frac{1}{2}\pi). \tag{III.2}$$

Equation (III.1) then becomes

$$I = \sum_{\nu_i} d_{\nu_i j_f - l_f}^s \left(\frac{1}{2}\pi\right) d_{\nu_i j_i - l_i}^s \left(\frac{1}{2}\pi\right) \frac{\hat{l}_f \hat{l}_i}{(4\pi)^{\frac{1}{2}} \hat{l}_i} \\ \times d_{0 l_i - l_f}^L \left(\frac{1}{2}\pi\right) d_{M l_i - l_f}^L \left(\frac{1}{2}\pi\right) \delta_{M_f M_i - M} . \quad (\text{III.3})$$

Writing  $j_f = l_f + \tau_f$  and  $j_i = l_i + \tau_i$ , eq. (III.3) becomes

$$I = \delta_{M_f M_i - M} \delta_{\tau_f \tau_i} \frac{\hat{l}_f \hat{l}_i}{(4\pi)^{\frac{1}{2}} \hat{l}_i} d_{0 l_i - l_f}^L \left(\frac{1}{2}\pi\right) d_{M l_i - l_f}^L \left(\frac{1}{2}\pi\right) . \quad (\text{III.4})$$

APPENDIX IVMOTIVATION FOR THE PARAMETERIZATION (6.7) OF  $\delta_s(\lambda)$ 

From eqs. (4.9) and (4.14), we have

$$\delta_c^{(N)}(\lambda) = -\frac{\mu}{\hbar^2} \int_{\frac{\lambda}{k}}^{\infty} dr \frac{r [\text{Re } U_c^{(N)}(\lambda)]}{[k^2 r^2 - \lambda^2]^{\frac{1}{2}}} \quad (\text{IV.1})$$

If we take

$$\text{Re } U_c^{(N)}(r) = -V_0 \left[ 1 + \exp\left(\frac{r-R}{d}\right) \right]^{-1} \equiv -V_0 f(r), \quad (\text{IV.2})$$

we then have

$$\begin{aligned} \delta_c^{(N)}(\lambda) &= \frac{\mu V_0}{\hbar^2} \int_{\frac{\lambda}{k}}^{\infty} dr \frac{r f(r)}{(k^2 r^2 - \lambda^2)^{\frac{1}{2}}} \\ &= -\frac{\mu V_0}{\hbar^2 k^2} \int_{\frac{\lambda}{k}}^{\infty} dr f'(r) (k^2 r^2 - \lambda^2)^{\frac{1}{2}}, \end{aligned} \quad (\text{IV.3})$$

so that

$$\frac{d \delta_c^{(N)}(\lambda)}{d\lambda} = \frac{\lambda \mu V_0}{\hbar^2 k^2} \int_{\frac{\lambda}{k}}^{\infty} dr \frac{f'(r)}{(k^2 r^2 - \lambda^2)^{\frac{1}{2}}} \quad (\text{IV.4})$$

Now if we take the Thomas-Fermi form for  $U_s(r)$ , namely

$$U_s(r) = \frac{U_0}{r} \frac{d}{dr} \left[ 1 + \exp\left(\frac{r-R}{d}\right) \right]^{-1} = \frac{U_0}{r} f'(r), \quad (\text{IV.5})$$

and substitute this into eq. (4.10), we have

$$\delta_s(\lambda) = -\frac{\lambda \mu u_0}{\hbar^2} \int_{\frac{\lambda}{k}}^{\infty} dr \frac{f'(r)}{(k^2 r^2 - \lambda^2)^{\frac{1}{2}}}, \quad (\text{IV.6})$$

hence by comparison with eq. (IV.4), and using eq. (6.3), we have

$$\delta_s(\lambda) = -\frac{u_0 k^2}{V_0} \frac{d\delta_c^{(N)}(\lambda)}{d\lambda} = \frac{u_0 k^2 \alpha}{2V_0} \frac{d}{d\lambda} [1 + \exp(\frac{\Lambda - \lambda}{\Delta})]^{-1}. \quad (\text{IV.7})$$

This parameterized form was considered in ref.<sup>40</sup>).

In the high-energy approximation we have  $\Lambda = kR$  and  $\Delta = kd$ , where  $R$  and  $d$  are the radius and diffuseness of the function  $f(r)$ . If we had chosen a spin-orbit potential of the form (IV.5) but with radius  $R_s$  and diffuseness  $d_s$ , we would have, in place of eq. (IV.7),

$$\delta_s(\lambda) = \beta \frac{d}{d\lambda} [1 + \exp(\frac{\Lambda_s - \lambda}{\Delta_s})]^{-1}, \quad (\text{IV.8})$$

where  $\Lambda_s = kR_s$ ,  $\Delta_s = kd_s$  and  $\beta$  is a constant.

APPENDIX VEVALUATION OF THE FUNCTION  $\mathfrak{F}(\Delta z)$ 

Substituting eqs. (4.29) and (6.9) into eq. (4.31) gives

$$\mathfrak{F}(\Delta z) = \frac{1}{\Delta} \int_{-\infty}^{\infty} d\lambda [1 + \exp(\frac{\lambda - \Lambda}{\Delta} - i\alpha)]^{-2} \exp[\frac{\lambda - \Lambda}{\Delta} - i\alpha + i(\lambda - \Lambda)z] \quad (V.1)$$

Let  $\mu = \frac{\lambda - \Lambda}{\Delta}$ ; therefore

$$\begin{aligned} \mathfrak{F}(\Delta z) &= \int_{-\infty}^{\infty} d\mu [1 + \exp(-\mu - i\alpha)]^{-2} \exp[-\mu - i\alpha + i\Delta z \mu] \\ &= \int_{-\infty}^{\infty} d\mu \exp(i\Delta z \mu) \frac{d}{d\mu} [1 + \exp(-\mu - i\alpha)]^{-1} \\ &= -i\Delta z \lim_{\epsilon \rightarrow 0^+} \int_{-\infty}^{\infty} d\mu [1 + \exp(-\mu - i\alpha)]^{-1} \exp(i\Delta z \mu - \epsilon \mu) \quad (V.2) \end{aligned}$$

We evaluate the right hand side of eq. (V.2) for  $z > 0$ . For  $z < 0$  the final result is the same. We first evaluate

$$I_{\epsilon}(z) = \int_{\Gamma} d\mu f(\epsilon, z; \mu) \quad , \quad (V.3)$$

where

$$f(\epsilon, z; \mu) = [1 + \exp(-\mu - i\alpha)]^{-1} \exp(i\Delta z \mu - \epsilon \mu) \quad (V.4)$$

and the contour of integration  $\Gamma$  is shown in fig. 9.

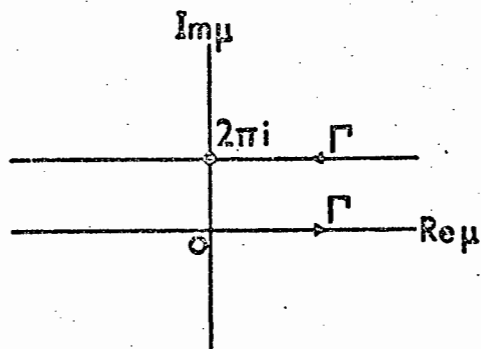


Fig. 9. Contour of integration  $\Gamma$  for the integrals (V.3) and (VI.4).

Recall from subsection 3.1 that we restrict  $\alpha$  to the interval  $(-\frac{1}{2}\pi, \frac{1}{2}\pi)$ . This implies that the singularity of the function  $f(\varepsilon, z; \mu)$  inside the contour  $\Gamma$  is at the point  $\mu_\alpha = (\pi - \alpha)i$ . Now

$$\operatorname{Res}_{\mu=\mu_\alpha} [f(\varepsilon, z; \mu)] = \exp[-(\Delta z + i\varepsilon)(\pi - \alpha)] , \quad (\text{V.5})$$

so that

$$I_\varepsilon(z) = i2\pi \exp[-(\Delta z + i\varepsilon)(\pi - \alpha)] . \quad (\text{V.6})$$

We also have

$$I_\varepsilon(z) = \int_{-\infty}^{\infty} d\mu f(\varepsilon, z; \mu) - \int_{-\infty}^{\infty} d\mu f(\varepsilon, z, \mu + i2\pi) . \quad (\text{V.7})$$

Since  $f(o, z; \mu + i2\pi) = \exp(-2\pi\Delta z) f(o, z; \mu)$  we have from eqs. (V.2), (V.6) and (V.7) in the limit as  $\varepsilon \rightarrow 0$ ,

$$\frac{d}{dz} [1 - \exp(-2\pi\Delta z)] \mathfrak{J}(\Delta z) = i2\pi \exp[-\Delta z(\pi - \alpha)] , \quad (V.8)$$

i.e.

$$\mathfrak{J}(\Delta z) = \frac{\pi\Delta z}{\sinh(\pi\Delta z)} e^{\alpha\Delta z} . \quad (V.9)$$

APPENDIX VIEVALUATION AND ASYMPTOTIC FORM OF THE FUNCTION  $G(z)$ 

Substituting eqs. (6.7) and (6.9) into eq. (4.68) gives

$$G(z) = 2\kappa \int_{-\infty}^{\infty} d\lambda \left[1 + \exp\left(\frac{\Lambda - \lambda}{\Delta} - i\alpha\right)\right]^{-1} \left[1 + \exp\left(\frac{\Lambda_S - \lambda}{\Delta_S}\right)\right]^{-2} \\ \times \exp\left[\frac{\Lambda_S - \lambda}{\Delta_S} + i(\lambda - \bar{\lambda})z\right]. \quad (\text{VI.1})$$

Let  $\Delta = q\Delta_S$ ,  $(\Lambda - \Lambda_S)/\Delta_S = \gamma$  and  $\mu = (\lambda - \Lambda)/\Delta$ ; therefore

$$G(z) = 2\kappa\Delta \exp[i(\Lambda - \bar{\Lambda})z - \gamma] \int_{-\infty}^{\infty} d\mu g(\mu; z), \quad (\text{VI.2})$$

where

$$g(\mu, z) = \left[1 + \exp(-\mu - i\alpha)\right]^{-1} \left[1 + \exp(-\gamma - q\mu)\right]^{-2} \exp[(-q + i\Delta z)\mu]. \quad (\text{VI.3})$$

We evaluate the right hand side of eq. (VI.2) for  $z > 0$  and  $q$  integer. For  $z < 0$  the result is the same. We first evaluate

$$I(z) = \int_{\Gamma} d\mu g(\mu; z), \quad (\text{VI.4})$$

where the contour of integration  $\Gamma$  is shown in fig. 9.

Since  $|\alpha| < \frac{1}{2}\pi$ , the singularities of  $g(\mu, z)$  inside the contour  $\Gamma$  are at the points

$$\mu_\alpha = (\pi - \alpha)i \quad (\text{VI.5})$$

$$\mu_\gamma^{(n)} = \frac{1}{q} [-\gamma + i\pi(2n-1)] \quad n = 1, 2 \dots q, \quad (\text{VI.6})$$

so that

$$I(z) = i2\pi \left\{ \text{Res}_{\mu=\mu_\alpha} [g(\mu; z)] + \sum_{n=1}^q \text{Res}_{\mu=\mu_\gamma^{(n)}} [g(\mu; z)] \right\}, \quad (\text{VI.7})$$

where

$$\text{Res}_{\mu=\mu_\alpha} [g(\mu; z)] = \frac{\exp[(-q+i\Delta z)\mu_\alpha]}{[1+\exp(-\gamma-q\mu_\alpha)]^2}, \quad (\text{VI.8})$$

$$\begin{aligned} \text{Res}_{\mu=\mu_\gamma^{(n)}} [g(\mu; z)] &= \frac{1}{q^2} \frac{\exp[(-q+i\Delta z)\mu_\gamma^{(n)}]}{[1+\exp(-\mu_\gamma^{(n)}-i\alpha)]^2} \\ &\times \left\{ i\Delta z + (1+i\Delta z)\exp(-\mu_\gamma^{(n)}-i\alpha) \right\}. \end{aligned} \quad (\text{VI.9})$$

We also have

$$\begin{aligned} I(z) &= \int_{-\infty}^{\infty} d\mu g(\mu; z) - \int_{-\infty}^{\infty} d\mu g(\mu+i2\pi; z) \\ &= [1 - \exp(-2\pi\Delta z)] \int_{-\infty}^{\infty} d\mu g(\mu; z). \end{aligned} \quad (\text{VI.10})$$

Equations (VI.2), (VI.7) and (VI.10) give the final result

$$G(z) = \frac{i4\pi\kappa\Delta}{1 - \exp(-2\pi\Delta z)} \exp[i(\lambda - \bar{\lambda})z - \gamma] \\ \times \left\{ \text{Res}_{\mu=\mu_\alpha} [g(\mu; z)] + \sum_{n=1}^q \text{Res}_{\mu=\mu_\gamma^{(n)}} [g(\mu; z)] \right\}. \quad (\text{VI.11})$$

We now write down the leading terms for  $z < 0$  and for  $z > 0$ .

For  $z < 0$  and  $\gamma > 1$ , we have

$$\text{Sup}_n \left\{ \text{Res}_{\mu=\mu_\gamma^{(n)}} [g(\mu; z)] \right\} = \text{Res}_{\mu=\mu_\gamma^{(q)}} [g(\mu; z)] \quad (\text{VI.12})$$

$$\sim -i \frac{\Delta z}{q^2} \frac{\exp(\gamma - 2\pi\Delta z + \frac{\pi\Delta z}{q} - i \frac{\gamma\Delta z}{q})}{1 + \exp(\frac{\gamma}{q} + i \frac{\pi}{q} - i\alpha)}. \quad (\text{VI.13})$$

For  $z > 0$  and  $\gamma > 1$ , we have

$$\text{Sup}_n \left\{ \text{Res}_{\mu=\mu_\gamma^{(n)}} [g(\mu; z)] \right\} = \text{Res}_{\mu=\mu_\gamma^{(1)}} [g(\mu; z)] \quad (\text{VI.14})$$

$$\sim -i \frac{\Delta z}{q} \frac{\exp(\gamma - \frac{\pi\Delta z}{q} - i \frac{\gamma\Delta z}{q})}{1 + \exp(\frac{\gamma}{q} - i \frac{\pi}{q} - i\alpha)}. \quad (\text{VI.15})$$

Provided  $q > 1$ , the leading terms in the braces  $\{ \}$  on the right hand side of eq. (VI.11) is given, for  $z < 0$ , by (VI.13) and for  $z > 0$ , by (VI.15). We therefore finally have, for  $|\pi\Delta z| > 1$ ,

$$G(z) \underset{z < 0}{\sim} \frac{2\pi\kappa\Delta^2 z}{q^2 \sinh(\pi\Delta z)} \frac{\exp[-\pi\Delta z(1 - \frac{1}{q}) + iz(\lambda - \bar{\lambda} - \frac{\gamma\Delta}{q})]}{1 + \exp(\frac{\gamma}{q} + i \frac{\pi}{q} - i\alpha)}, \quad (\text{VI.16})$$

$$G(z) \underset{z>0}{\sim} \frac{2\pi\kappa\Delta^2 z}{q^2 \sinh(\pi\Delta z)} \frac{\exp[\pi\Delta z(1-\frac{1}{q}) + iz(\Lambda - \bar{\Lambda} - \frac{\gamma\Delta}{q})]}{1 + \exp(\frac{\gamma}{q} - i\frac{\pi}{q} - i\alpha)} \quad (\text{VI.17})$$

under the conditions  $\gamma > 1$ ,  $q$  integer and greater than unity,  
 where  $\gamma = (\Lambda - \Lambda_s)/\Delta_s$  and  $q = \Delta/\Delta_s$ .

REFERENCES

1. J.S. Blair, Phys. Rev. 95 (1954) 1218
2. W.E. Frahn and R.H. Venter, Ann. of Phys. 24 (1963) 243;  
R.H. Venter, Ann. of Phys. 25 (1963) 405
3. W.E. Frahn and R.H. Venter, Ann. of Phys. 27 (1964) 135;  
R.H. Venter and W.E. Frahn, Ann. of Phys. 27 (1964) 385
4. W.E. Frahn and G. Wiechers, Nucl. Phys. 74 (1965) 65
5. F.J.W. Hahne, Ph.D. thesis, University of Cape Town  
(1967); Nucl. Phys. A106 (1968) 660
6. W.E. Frahn, in Heavy ion high spin states and nuclear  
structure (I.A.E.A., Vienna, 1975) p. 157
7. W.E. Frahn, Nucl. Phys. A272 (1976) 413
8. W.E. Frahn and D.H.E. Gross, Ann. of Phys. 101 (1976) 520
9. K. Kauffmann, Z. Physik A282 (1977) 163
10. W. Weiss, P. Egelhof, K.D. Hildenbrand, D. Kassen,  
M. Makowska-Rzeszutko, D. Fick, H. Ebinghaus, E. Steffens,  
A. Amakawa and K.I. Kubo, Phys. Lett. 61B (1976) 237
11. D. Fick, private communication
12. Nuclear Structure Group, Univ. of Birmingham, Report No.  
76-05, 1976, and J.B.A. England, private communication

13. W.E. Frahn, in Fundamentals in nuclear theory (I.A.E.A., Vienna, 1967) p. 3
14. R.G. Newton, Scattering theory of waves and particles (McGraw-Hill, New York, 1966)
15. P.J. Brussaard and H.A. Tolhoek, Physica 23 (1957) 955
16. Proc. Third Int. Symp. on polarization phenomena in nuclear reactions, Madison, 1970, ed. H.H. Barschall and W. Haeberli, p. xxv
17. A. Messiah, Quantum mechanics Vol. 2 (North-Holland, Amsterdam, 1961)
18. N. Austern, Direct nuclear reaction theories (Wiley, New York, 1970) section 5.3
19. M.P. Fricke, R.M. Drisko, R.H. Bassel, E.E. Gross, B.J. Morton and A. Zucker, Phys. Rev. Lett. 16 (1966) 746
20. N.J. Sopkovich, Nuovo Cim. 26 (1962) 186; K. Gottfried and J.D. Jackson, Nuovo Cim. 34 (1964) 735
21. A. Messiah, Quantum mechanics Vol. 1 (North-Holland, Amsterdam, 1961) appendix B, section 5
22. K. Alder, A. Bohr, T. Huus, B. Mottelson and A. Winther, Rev. Mod. Phys. 28 (1956) 432
23. N. Austern and J.S. Blair, Ann. of Phys. 33 (1965) 15
24. F.J.W. Hahne, Nucl. Phys. A104 (1967) 545

25. J.A. McIntyre, K.H. Wang and L.C. Becker, Phys. Rev. 117 (1960) 1337
26. M.D. Cohler, N.M. Clarke, C.J. Webb, R.J. Griffiths, S. Roman and O. Karban, J. Phys. G (Nucl. Phys.) 2 (1976) 151
27. S. Roman, A.K. Basak, J.B.A. England, O. Karban, G.C. Morrison and J.M. Nelson, Nucl. Phys. A284 (1977) 365
28. S. Roman, Proc. Fourth Int. Symp. on polarization phenomena in nuclear reactions, Zurich, 1975, ed. W. Grüebler and V. König, p. 255
29. T.E.O. Ericson, Preludes in theoretical physics (North-Holland, Amsterdam, 1965) p. 321
30. J.S. Blair, Phys. Rev. 115 (1959) 928
31. R.A. Hardekopf, L.R. Veaser and P.W. Keaton Jr., Phys. Rev. Lett. 35 (1975) 1623
32. D. Kassen, Ph.D. thesis, Heidelberg University, 1977, unpublished
33. R.J. Griffiths, M.D. Cohler and N.M. Clarke, King's College, University of London 1975, unpublished (private communication by J.B.A. England)
34. J.W. Luetzelschwab and J.C. Hafele, Phys. Rev. 180 (1969) 1023
35. D. Fick, private communication

36. O. Häusser, T.K. Alexander, D. Pelte, B.W. Hooton and H.C. Evans, Phys. Rev. Lett. 23 (1969) 320
37. M. Gell-Mann, M.L. Goldberger, Phys. Rev. 91 (1953) 398
38. G.R. Satchler, Nucl. Phys. 21 (1960) 116
39. G.R. Satchler, Nucl. Phys. 55 (1964) 1
40. W.E. Frahn, "Polarization in elastic heavy ion scattering", informal report, Max-Planck Institute for Nuclear Physics, Heidelberg, 1975